University of California
Los Angeles

Computational Complexity and Decidability of Tileability

A dissertation submitted in partial satisfaction
of the requirements for the degree
Doctor of Philosophy in Mathematics

by

Jed Chang-Chun Yang

2013

Abstract of the Dissertation

Computational Complexity and Decidability of Tileability

by

Jed Chang-Chun Yang

Doctor of Philosophy in Mathematics

University of California, Los Angeles, 2013

Professor Igor Pak, Chair

For finite polyomino regions, tileability by a pair of rectangles is NP-complete for all but trivial cases yet can be solved in quadratic time for simply connected regions. Through a series of reductions and improvements, we construct a set of 117 rectangles for which the tileability of simply connected regions is NP-complete.

Tiling by dominoes in the plane is a matching problem, and thus can be solved in polynomial time. While the decision problem remains polynomial in higher dimensions, we prove that the counting problem becomes #P-complete. We also establish NP- and #P-completeness results for another generalization of domino tilings to higher dimensions.

We show that tileability of cofinite regions is undecidable, even for some fixed set of tiles, but present an algorithm for solving the case where all tiles are rectangular. We also show that whether a finite region can be enlarged by tiles such that the resulting region becomes tileable is also undecidable. Moreover, the existence of a tileable rectangle by a set of polyominoes is also shown to be undecidable.

It is not surprising that tiles can emulate other computational systems such as Turing machines and cellular automata. Some of these connections and consequences are explored and outlined. In particular, there are conjectures in the theory of cellular automata that, if proved, could lead to improvements of results in the theory of tilings.

The dissertation of Jed Chang-Chun Yang is approved.

Bruce L. Rothschild

Amit Sahai

Benjamin Sudakov

Igor Pak, Committee Chair

University of California, Los Angeles

2013

To the Author

Table of Contents

List of Figures

List of Tables

Acknowledgments

I must first thank my doctoral advisor, Igor Pak, without whom I would never have completed my degree. He not only proposed many research problems, but also patiently listened to my thoughts every week and encouraged my progress. Beyond fruitful mathematical discussions, his guidance in general regarding a career in mathematics has also been invaluable. Besides being an incredible and knowledgeable mathematician, he is also a kind person who cares about his students. Moreover, he shares my sense of humour, making our meetings that much more enjoyable.

Chapter 2 is a version of [PY11], co-authored with my advisor, who is partially supported by the NSF and BSF grants. We are grateful to Alex Fink, Jeff Lagarias, Leonid Levin, Cris Moore, Günter Rote, and Damien Woods for helpful conversations at various stages of that project, some of which inspired further work detailed in the following chapter. We also thank the anonymous referees for attentive reading and useful comments on previous versions of this paper. Chapter 4 is a version of [PY12], also co-authored with my advisor. We are very grateful to Cris Moore for helpful conversations; in particular, Theorem 4.1.1 arose as a question in our discussions. Chapter 5 is a version of [Yan12]. I am grateful to my advisor Igor Pak for proposing these problems, helpful conversations, reading this paper, and providing invaluable feedback. My work is supported by the NSF under Grant No. DGE-0707424.

In addition to my advisor, I would like to mention a few professors. I thank Richard M. Wilson, who introduced me to combinatorics during my undergraduate studies at Caltech. He guided me in two summers of research under Caltech's SURF (Summer Undergraduate Research Fellowship) program, without which I would have had no prior research experience when starting my graduate career. One of the summers resulted in [Yan10]. Cris Moore, an expert in tilings, among many other subjects, attended my Advancement to Candidacy exam and asked interesting questions that inspired more research. I thank my doctoral committee members, who read and approved my dissertation. Paul Balmer's lectures, where I learned the art of commutative diagrams (see Section 7.2), were so enjoyable that I took six algebra

courses with him, which is numerically co-maximal with the number of courses I took from my advisor.

The atmosphere and camaraderie amongst graduate students at UCLA are also to be praised. Many of us encouraged one another when studying for qualifying exams. Beren Sanders once said, "The beauty of quals, Jed, is that it is not a zero-sum game. We could all pass." And that we did. I especially want to thank Athipat Thamrongthanyalak, my officemate and friend. We must have eaten over a hundred meals together. Siddhartha Kanungo had encouraged me with his superb work ethics, wisdom from life experiences, and was my trainer and coach for all three departmental table tennis tournaments, where I won silver once and bronze twice, losing to professors Kefeng Liu, Christoph Thiele, and exchange student Alfonso, respectively, while remaining undefeated amongst graduate students. I have known Joshua $\mathbb{Z}$ahl since our Caltech days, and together we have played violin duets, travelled to conferences, and shared many meals at Enzo's Pizzeria. Stedman Wilson, my advisor's first student at UCLA, and I have shared "uncountably many conversations about mathematics, the universe, and life (in that order)." I am grateful to have a colleague who shares my love of music and my (and our advisor's) sense of humour. After our success in harmonizing and serenading *You Are My Sunshine* at a conference in Wyoming, he invited me to the annual *Messiah* sing-along at his church, an experience so enjoyable that I attended again even in his absence.

Outside of my colleagues at UCLA, I would like to thank my two *de facto* best friends. Since I am a mathematician, I will use numbers to justify this unofficial designation. During my graduate career, I have talked on the phone for about 600 hours, roughly 60% of which is divided fairly evenly between my parents and these two friends. The next friend is responsible for about 3%, and the subsequent 9 friends account for 6% in aggregate. With the sharpness of this threshold, it seems fitting to thank them by name. Caleb E. Ng and I attended Caltech together, though we were merely acquaintances there. After graduation, we started talking a lot more, despite never living in the same city concurrently. Throughout our graduate careers, we often encouraged one another to continue despite setbacks. I would not be here

today if not for our phone conversations several times a week. Indeed, in the last five years, we have talked for over 140 hours. Stephanie C. Chan has also been a very faithful friend. Although she has only talked to me on the phone for about 64% as much as Caleb, this is more than four times as much as the length with my next friend, and she made up for it by visiting me at least 30 times and allowing me to visit her a similar amount. We served the Lord together in various capacities, and have faithfully prayed for one another through our ups and downs.

One of the main reasons I chose to pursue my PhD at UCLA was because of the desire to continue meeting at the Alhambra Christian Fellowship, which I attended during my four years at Caltech. There are too many individuals here that would be worth mentioning. Due to space constraints, I will only name a few. Jonah Chang, a fellow UCLA graduate student in the Department of Chemistry, was the only one who visited me regularly besides Stephanie. He didn't mind eating the same mapo tofu and broccoli I repetitively cooked for him. We would have some fellowship and sing hymns in two-part harmony. During my Caltech days, Hou-En and June Han, my "parents," drove me to ACF twice a week and took care of me in general. After my move to UCLA, Steve and Tammy Lu continued the good work and looked after me: we have shared plenty of meals together, and I would sometimes visit them late at night to borrow DVDs. I am thankful for having them in my life, and for their kindness in opening up their home for prayer meetings week after week. Throughout my time here, I have had the opportunity to provide rides to eight UCLA students regularly. Even if this was a burden at times, overall I have been blessed by getting to know these younger ones. Among them, Hannah Chan had frequently offered to drive (my car) so as to lessen my burden. When I started my project on domino tilings in three dimensions, it was helpful to have LEGO bricks to help visualize my ideas (see Figure 4.17). I borrowed an ample supply from Cether Deng (and family).

I would, of course, like to thank my parents, Wei-Pang and Chien-Ling C. Yang, for their unconditional support. They taught me rudimentary arithmetic (*e.g.*, a *youtiao* is \$3 and a *shaobing* is \$5; given \$20 to buy two *youtiao* and one *shaobing*, how much money will be

left?) by age 2, and solving simple systems of linear equations (*e.g.*, between chickens and rabbits, there are 5 heads and 14 legs, how many of each are there?) by age 3. We had a big white board in our dining room, and while I was in elementary school, mathematics was always a dish served at dinner. While my mother cooked, my father would teach me math, and we would continue discussing throughout dinner. Sometimes we could not figure out a problem after dinner, and would simply give up and leave it on the board. We would return later and find it already solved by my mother. Besides teaching me mathematics, they also taught me many valuable life lessons: *e.g.*, "aim for the second best," "put in 20% effort to achieve 80%," and "study less and play more." These maxims, which are the opposite of traditional Chinese teachings, nurtured me into the person I am today. I also thank my sister, Jung Chang-Hsiung Yang, for always being there for me. In my entire life up to this point, she has never let me down even once. She gives me a hug whenever I am tired or need encouragement. She never argues, but is always willing to listen. I cannot imagine my life without her.

Finally, I offer up thanksgiving to Jesus Christ, who not only is my Saviour but also my Lord. "And we know that all things work together for good to them that love God, to them who are the called according to his purpose." My mathematical abilities, self-discipline, and work ethic—traits that were indispensable to my success—are all from Him. Even the environment and circumstances about me have been sovereignly arranged by His hands. "All the way my Saviour leads me, what have I to ask beside?" Indeed, my graduate work, yea, even my life would have been impossible without His loving support and guidance. I owe my all to Him.

Vita

2008	Bachelor of Science with Honor, Mathematics, California Institute of Technology, Pasadena, CA, USA
2008–2010	Chancellor's Fellowship, University of California, Los Angeles, CA, USA
2010	Master of Arts, Mathematics, University of California, Los Angeles, CA, USA
2010–2013	NSF GRFP Graduate Research Fellow, National Science Foundation, USA

CHAPTER 1

Introduction

We consider tilings on the integer lattice, where *tiles* are finitely many closed unit squares glued together along edges. A *tiling* is a collection of translated copies of tiles that are pairwise disjoint in their interior. The tiled *region* is the union of the tiles in the tiling.

1.1 Tiling simply connected regions with rectangles

Tiling finite regions in the plane with a pair of horizontal and vertical bars is NP-complete [BNRR95], as long as one bar has length at least 3. On the other hand, for any pair of two rectangles, there is a quadratic time algorithm (in the area of the region) for deciding the tileability of simply connected regions by these two rectangles [Rém05]. This is in sharp contrast to the fact that even tileability by bars of length 3 is NP-complete for regions which have holes, and may suggest that simple connectivity plays a crucial role in the complexity of finite tilings.

One very natural question to ask is whether the quadratic time algorithm for simply connected regions extends to the case for more rectangles. In Chapter 2, we construct a finite set $\mathbf{R}$ of rectangles such that tileability of simply connected regions with $\mathbf{R}$ is NP-complete. We perform this construction in two steps. First, we create a set of tiles whose corresponding tileability question for simply connected regions is NP-complete (Lemma 2.3.2). This is done using a reduction from a variant of the boolean satisfiability problem known as Cubic Monotone 1-in-3 SAT. We then prove a general reduction lemma (Lemma 2.3.3) that creates a set $\mathbf{R}$ of rectangles from a set $\mathbf{T}$ of tiles and provide a corresponding transformation

of the regions so that tileability of the given region by **T** is equivalent to the tileability of the transformed region with **R**. Combining the two results, we get a set of at most 10^6 rectangular tiles whose tileability problem for simply connected regions is NP-complete (Theorem 2.1.1). Along the way, we also show that the associated counting problem is #P-complete (Theorem 2.1.2).

Chapter 2 consists of material in [PY11] and the sketch of (iii)⇒(ii) in the proof of Lemma 2.3.1, which is taken from the appendix of [Yan12].

After [PY11] was written, the bound of 10^6 is subsequently reduced to 117 by a series of ideas that build on top of each other. The first is a simplification of the tiles based on a suggestion by Günter Rote, which reduces the number to at most 20808. The second is inspired by a question from Alex Fink and improves the general bound in the reduction lemma. This leads to a set of at most 353 rectangles such that the corresponding tileability problem for simply connected regions is NP-complete. Finally, some ad-hoc optimizations lead to the promised bound of 117 rectangles. These improvements are detailed in Chapter 3 and have not appeared elsewhere.

1.2 The complexity of generalized domino tilings

As mentioned above, for tilings by a horizontal and a vertical bar in the plane, tileability is known to be NP-complete in general, except when both bars have length two ("dominoes"). Tiling by dominoes is a matching problem and thus can be solved in polynomial time. While computing the number of matchings is classically #P-complete [Val79b], the number of domino tilings in the plane can be computed in polynomial time (see *e.g.* [Ken04, LP09]).

In Chapter 4, we consider two higher-dimensional analogues of these problems. One way to think of a domino is a pair of adjacent hypercubes. Tiling with these dominoes, even in higher dimensions, correspond to matching problems, and thus can still be solved in polynomial time. However, the counting problem is #P-complete and remains so even when considering only contractible regions (Theorem 4.1.4).

We also consider *slabs*, halves of hypercubes of side length 2, which are also dominoes in the plane. For this generalization, we are able to prove both NP-completeness and #P-completeness for tiling by slabs. Similarly, these results hold for contractible regions alone as well.

The proofs involve embedding the problem of counting perfect matchings in cubic bipartite graphs (which is #P-complete) and 1-IN-3 SAT (which is NP-complete and #P-complete) as higher-dimensional domino and slab tilings, respectively. We then modify the regions constructed in these reductions to obtain contractibility without introducing new tilings. One of the goals is to show that even though simply connected regions are much simpler to tile in the plane, as seen in the examples mentioned above, simple connectivity (and even contractibility) do not play major roles in tilings of higher dimensions. Indeed, methods such as *augmentation* (see Subsection 4.8.5) are readily available.

Chapter 4 is a copy of [PY12].

1.3 Rectangular tileability and complementary tileability are undecidable

Considering decidability for infinite problems is as natural as computational complexity for finite problems. One such question is whether a given set of tiles can tile *some* rectangular region. Even though the tiling is finite, the size of the smallest such witness might grow without bound. Indeed, it is shown in Chapter 5 that this is the case, and the existence of a tileable rectangle is undecidable. This is proved by embedding the undecidable POST CORRESPONDENCE PROBLEM. Moreover, the result holds even if the number of tiles is bounded to be at most 19. The problem is decidable if we are limited to a single tile (with translated copies). However, it is unknown what happens for a single tile and its isometric copies.

Another way to obtain undecidability is to tile infinite regions. It is known that tileability of the infinite plane is undecidable with the set of tiles as the input [Ber66]. One could reverse

the question by fixing the set of tiles while varying the infinite region. To phrase the infinite region as a finite input, one could consider tiling of cofinite regions or tiling infinite regions with periodic boundaries. These are considered in sections 5.4 and 5.5, respectively, and are indeed undecidable.

Tileability of a finite region is a finite problem, and signed tileability is well understood by algebraic methods (see [Pak00]). Therefore it may be of interest that *augmentability* of finite regions, an intermediate concept between tileability and signed tileability, is undecidable. This is demonstrated in Section 5.6.

The material in Chapter 5 appears in [Yan12] with minor additions as promised in the paper. In particular, the proofs of Lemma 5.5.1 and Theorem 5.5.2 have been expanded, and the theorem and its proof in Subsection 5.7.7 are newly added.

1.4 Turing machines, cellular automata, and related conjectures

Proofs in Chapter 5 frequently call upon the emulation of Turing machines by tiles. This classical technique is outlined in Chapter 6, followed by an application to demonstrate the (computational) power of tiles from a philosophical standpoint.

In the same vein, emulation of cellular automata by tiles is described in Chapter 7. A more involved construction shows that tiles can be emulated by cellular automata as well. By using a suitably strong form of universality of cellular automata, the number of rectangles needed in Chapter 2 can be decreased. Indeed, some corollaries of open conjectures regarding cellular automata are sketched. In particular, if a specific cellular automaton is shown to be (intrinsically) universal, then the number of rectangles needed in Theorem 2.1.1 is reduced to 51.

Finally, in Chapter 8, two number theoretic conjectures are stated. If solved, these would lead to more improvements on the number of rectangles. In particular, if the claims are proved, the bound for the number of rectangles is further reduced to 8. That is, one

would obtain a set of 8 rectangles such that the corresponding tileability of simply connected regions is NP-complete.

Except for the paragraph before Lemma 6.1.1, which is adapted from the appendix of [Yan12], the remainder of Chapters 6, 7, and 8 are newly written.

CHAPTER 2

Tiling simply connected regions with rectangles

In [BNRR95], it was shown that tiling of general regions with two rectangles is NP-complete, except for a few trivial special cases. In a different direction, Rémila [Rém05] showed that for simply connected regions by two rectangles, the tileability can be solved in quadratic time (in the area). We prove that there is a finite set of at most 10^6 rectangles for which the tileability problem of simply connected regions is NP-complete, closing the gap between positive and negative results in the field. We also prove that counting such rectangular tilings is #P-complete, a first result of this kind.

2.1 Introduction

The study of *finite tilings* is a classical subject of interest in both theoretical and recreational literature [Gol65, GS87]. In the *tileability problem*, a finite set of tiles $\mathbf{T}$ is fixed, and a region is an input. This problem is known to be polynomial in some cases, and NP-complete in others (see [Pak03]). Over the years, the hardness results were successively simplified (in statement, not in proof), with both sets of tiles and the regions becoming more restrictive. This chapter is a new step in this direction.

In [BNRR95], it was shown that tiling of general regions with two bars is NP-complete, except for the case of dominoes. In a different direction, Rémila [Rém05] (building on the ideas in [KK92, Thu90]), showed that for *simply connected regions* and two rectangles, the tileability can be solved in quadratic time (in the area). The following theorem closes the gap between these polynomial and NP-complete results.

Theorem 2.1.1 (Main Theorem) *There exists a finite set* $\mathbf{R}$ *of at most* 10^6 *rectangular tiles, such that the tileability problem of simply connected regions with* $\mathbf{R}$ *is* NP*-complete.*

Our proof of the Main Theorem is split into two parts. In the first part, we use the language of *Wang tiles* to reduce the Cubic Monotone 1-in-3 SAT problem, known to be NP-complete, to the $\mathbf{T}$-tileability of simply connected regions with Wang tiles. In the second part, we reduce Wang tileability to tileability with rectangular tiles. Both our reductions are *parsimonious* and are used to prove that counting the number of tilings of simply connected regions is also hard, via reduction from 2SAT.

Theorem 2.1.2 *There exists a finite set* $\mathbf{R}$ *of at most* 10^6 *rectangular tiles, such that counting the number of tilings of simply connected regions with* $\mathbf{R}$ *is* #P*-complete.*

Although #P-completeness is known for tilings of general regions with right tromino and square tetromino [MR01], nothing was known for tilings with rectangles. We refer to Section 2.7 for the history of the problem, references, and further remarks.

2.2 Definitions and basic results

2.2.1 Polyomino tiles

Consider the integer lattice $\mathbb{Z}^2$ as a union of closed unit squares with pairwise disjoint interiors. A *region* is a finite union of such unit squares such that the interior is connected. A (*polyomino*) *tile* is a finite simply connected region.

A *tileset* $\mathbf{T}$ is a collection of tiles. Given a region Γ and a tileset $\mathbf{T}$, a $\mathbf{T}$*-tiling* of Γ is a union of translated copies of tiles from $\mathbf{T}$ with pairwise disjoint interiors covering Γ. If a region admits a $\mathbf{T}$-tiling then it is $\mathbf{T}$*-tileable*. We may simply say *tiling* and *tileable* when $\mathbf{T}$ is understood. Consider the following decision problems regarding tileability:

SIMPLY CONNECTED TILEABILITY

Instance: Simply connected region Γ, finite tileset $\mathbf{T}$.

Decide: Whether Γ is $\mathbf{T}$-tileable?

SIMPLY CONNECTED $\mathbf{T}$-TILEABILITY

Instance: Simply connected region Γ.

Decide: Whether Γ is $\mathbf{T}$-tileable?

An input region can be given by the (finite) union of the squares it contain. The following is one of the early NP-completeness results [GJ79].

Theorem 2.2.1 *If both region Γ and tileset $\mathbf{T}$ are part of the input,* SIMPLY CONNECTED TILEABILITY *is* NP*-complete in the plane.*

For the rest of the chapter, we will focus on finding a fixed $\mathbf{T}$ such that SIMPLY CONNECTED $\mathbf{T}$-TILEABILITY is NP-complete. The following result is an extension of Theorem 2.2.1.

Theorem 2.2.2 *There exists a set $\mathbf{T}$ of 23 tiles, such that* SIMPLY CONNECTED $\mathbf{T}$-TILEABILITY *is* NP*-complete.*

The proof follows an explicit construction of Wang tiles (see below). While we do not use Theorem 2.2.2, it is of independent interest, and the intermediate results in its proof provide a key step towards the proof of the Main Theorem. The history behind this theorem and its potential generalizations is outlined in Subsection 2.7.1.

2.2.2 Wang tiles

The *edges* of a polyomino tile are the unit-length edges on the boundary. Given a set of colors and a polyomino tile τ, a *generalized Wang tile* is an assignment of colors to the edges of τ. A generalized Wang tile of a unit square is also called a *Wang square*. The region Γ we are trying to tile will also have specified colors on its boundary. A region is (*Wang*) *tileable*

if there is a tiling where incident edges have the same color, including on the boundary of the region (see Figure 2.1). If a tileset consists of (generalized) Wang tiles, tileability always mean Wang tileability.

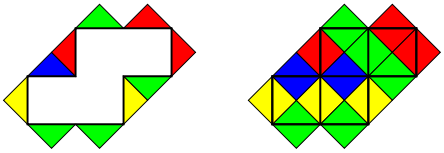

Figure 2.1: A colored region (left) and a Wang tiling (right). Colored edges are drawn as triangles for visibility.

2.2.3 Relational Wang tiles

Let us consider a more general setting. A set of *relational Wang tiles* is a collection $\mathbf{W}$ of squares and the following data. The vertical (respectively horizontal) *Wang relation* $V_{\mathbf{W}}(\tau, \tau')$ (respectively $H_{\mathbf{W}}(\tau, \tau')$) specify that $\tau' \in \mathbf{W}$ is allowed to be placed immediately below (respectively to the right of) $\tau \in \mathbf{W}$. We suppress the subscripts when it can be understood from context. The *boundary tiles* of a region Γ is a map from the exterior edges of Γ to the tiles $\mathbf{W}$. By abuse of language, we define the notion of tiling in this context: a $\mathbf{W}$-*tiling* of a region Γ is a map $\pi : \Gamma \to W$ such that tiles placed next to each other satisfy the Wang relations. Whenever a tile is adjacent to an exterior edge, we check the Wang relations as if the boundary tile corresponding to the edge is on the other side of the edge.

2.2.4 Complexity

Throughout the chapter we consider many tiling problems that are NP-complete. All these problems are trivially in NP. Indeed, given a description of a tiling, one could simply check if it is in fact a tiling. To prove NP-hardness, we reduce a known NP-complete problem to the problem in question. We refer to [GJ79, Pap94] for definitions and details.

We will embed Cubic Monotone 1-in-3 SAT as a tiling problem. Let $X = \{x_1, \ldots, x_n\}$ be a set of boolean variables. A (*monotone* 1-*in*-3) *clause* C is a set of three variables. A (*cubic monotone* 1-*in*-3) *expression* E is a finite collection $\mathcal{C}$ of monotone 1-in-3 clauses, where each variable $x_i \in X$ occurs three times. We say such E is (1-*in*-3) *satisfiable* if there is an assignment of boolean values $\{0, 1\}$ to the variables $x_i \in X$ such that each clause in E contains precisely one variable receiving 1 (and thus two variables receiving 0).

Cubic Monotone 1-in-3 SAT

Instance: Set X of variables, cubic monotone expression E.

Decide: Whether E is 1-in-3 satisfiable?

The following result was shown by Gonzalez in the language of exact covers:

Theorem 2.2.3 ([Gon85]) Cubic Monotone 1-in-3 SAT *is* NP*-complete.*[1]

We will reduce Cubic Monotone 1-in-3 SAT to a tiling problem Simply Connected **T**-Tileability for some fixed **T**.

2.2.5 Counting problems

Throughout the chapter we consider natural counting problems corresponding to the decision problems. For example, instead of asking whether satisfying assignments exist, we ask *how many* satisfying assignments there are. Similarly, for tileability, we count the number of tilings. If in the proof of NP-completeness, the corresponding reductions give a bijection between the sets of solutions, we call such reduction *parsimonious*.

Parsimonious reductions have the additional benefit of proving counting results using the same reduction. The class #P consists of the counting problems associated with decisions problems in NP. A counting problem is #P-complete if it is in #P and every #P question

[1] Given an expression E, we can associate a bipartite graph G with vertex set $X \sqcup \mathcal{C}$, where a variable $x \in X$ is adjacent to a clause $C \in \mathcal{C}$ if $x \in C$. Moore and Robson showed something stronger in [MR01], that this problem is NP-complete even if we require the associated graph to be planar. They did this by reducing from Planar 1-in-3 SAT, which is NP-complete [Lar93, MR08]. However, we do not need to use the planar version.

can be reduced to it. Thus, if there is a parsimonious reduction from problem Q_1 to Q_2, then if Q_1 is #P-complete, then so is Q_2. We refer to [Val79b] (see also [Pap94]) for definitions and details on #P complexity class.

One main goal is to reduce Cubic Monotone 1-in-3 SAT to a tiling problem Simply Connected $\mathbf{T}$-Tileability for some fixed $\mathbf{T}$. This reduction will turn out to be parsimonious, hence the number of satisfying assignments of a given instance of the satisfiability problem can be calculated by counting the number of tilings of the transformed instance.

However, it is not known whether the associated counting problem #Cubic Monotone 1-in-3 SAT is #P-complete. To get the #P-completeness result in Theorem 2.1.2, we will modify the reduction to use 2SAT instead, whose associated counting problem #2SAT is #P-complete.

2.3 Reduction lemmas

2.3.1 Basic reductions

In this section we consider five classes of Tileability problems. Let $\mathcal{T}$ be a collection of tiles and $\mathcal{R}$ be a collection of regions. A decision problem in $(\mathcal{T}, \mathcal{R})$-Tileability consists of a *fixed* tileset $\mathbf{T} \subset \mathcal{T}$, receives some $\Gamma \in \mathcal{R}$ as input, and outputs whether Γ is $\mathbf{T}$-tileable.

We say $(\mathcal{T}, \mathcal{R})$-Tileability is *linear time reducible* to $(\mathcal{T}', \mathcal{R}')$-Tileability if for any finite tileset $\mathbf{T} \subset \mathcal{T}$, there exists a finite tileset $\mathbf{T}' \subset \mathcal{T}'$ and a *reduction map* $f : \mathcal{R} \to \mathcal{R}'$ that is computable in linear time (in the complexity of $\Gamma \in \mathcal{R}$), such that $\Gamma \in \mathcal{R}$ is $\mathbf{T}$-tileable if and only if $f(\Gamma)$ is $\mathbf{T}'$-tileable.[2] If, moreover, that $(\mathcal{T}', \mathcal{R}')$-Tileability is linear time reducible to $(\mathcal{T}, \mathcal{R})$-Tileability, then they are *linear time equivalent*. Note that the transformation of the tilesets need not be efficient nor bijective.

For instance, if $\mathcal{T}$ is the collection of all rectangular tiles and $\mathcal{R}$ consists of simply connected regions, then $(\mathcal{T}, \mathcal{R})$-Tileability is a class of problems regarding tiling simply

[2]Recall that the tiles in the input are given as collections of unit squares.

connected regions with rectangular tiles. To simplify the notation, we drop the prefix in $(\mathcal{T}, \mathcal{R})$-TILEABILITY when the sets $\mathcal{T}$ and $\mathcal{R}$ are understood.

Lemma 2.3.1 (Tileability Equivalence Lemma) *The following classes of* SIMPLY CONNECTED TILEABILITY *problems are linear time equivalent:*

(i) TILEABILITY *with a fixed set of rectangular tiles.*

(ii) TILEABILITY *with a fixed set of polyomino tiles.*

(iii) TILEABILITY *with a fixed set of generalized Wang tiles.*

(iv) TILEABILITY *with a fixed set of Wang squares.*

(v) TILEABILITY *with a fixed set of relational Wang tiles.*

Moreover, the size of the tileset can be preserved in the reductions between (ii) *and* (iii).

Proof. The reductions (i)⇒(ii)⇔(iii)⇒(iv)⇒(v) are elementary and given below. The reduction (v)⇒(i) is stated separately as Lemma 2.3.3 and proved in the next section.

We may consider a rectangular tile as a polyomino tile, which in turn is a monochromatic generalized Wang tile. Therefore the reductions (i)⇒(ii)⇒(iii) are immediate, where each reduction map is simply the identity.

(iii)⇒(iv). Given a set of generalized Wang tiles, color each interior edge with a new color not used anywhere else, and consider each square as a separate Wang square (see Figure 2.2). These tiles are forced to reassemble themselves as the original generalized Wang tiles. The reduction map is again the identity.

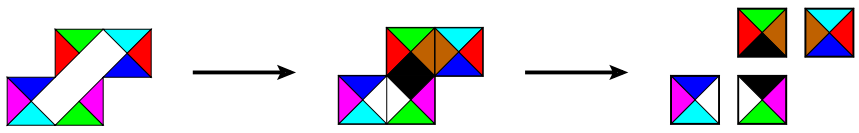

Figure 2.2: From generalized Wang tiles to Wang squares.

(iv)⇒(v). It is obvious how to define the Wang relations to mimic the colored Wang tiles without increasing the number of tiles. To encode the boundary conditions, we may need to introduce less than 4χ tiles, where χ is the number of colors permitted on the boundary. Indeed, to specify a color c on the top boundary, we need to choose an (arbitrary) tile whose bottom color is c. If no such tile exists, we must add a new tile to do so. If we do not involve the new tile in any Wang relations in the other directions, then it will never be used in the actual tiling, and thus will not affect tileability. We do the same for the other three directions.

The final reduction (v)⇒(i) is more difficult and is the content of Lemma 2.3.3 and proved in a later section.

To preserve the number of tiles in (iii)⇒(ii), scale the generalized Wang tile and replace each colored edge by an appropriate rectilinear zig-zag curve to encode the matching rules.

An explicit construction can be found in [Gol70]. We reproduce it here since we do need to investigate *some* construction more closely in Chapter 5. The *corner zig-zags* are made slightly more complicated than the original for clarity.

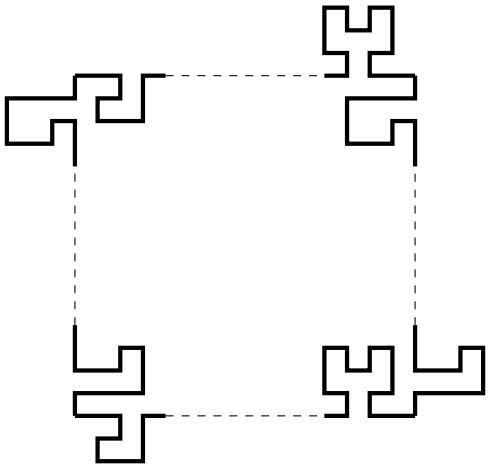

Figure 2.3: Geometric encoding of a Wang square as a polyomino.

Suppose there are m edge colors used, and let $r > 1 + \log_2 m$. The dashed lines in Figure 2.3 are of length r. Each edge color corresponds to a binary number with at most

r digits. These digits are used to modify the dashed line segments. A digit 0 makes no modification, while a digit 1 adds a square outward in the corresponding position on the bottom and right, and removes a square inward along the top and left.

The zig-zags on the corners force these tiles to align in a (dilated) square lattice grid. Note that even if rotations and reflections are allowed, the corner zig-zags moreover force all the tiles to have the same orientation. Thus we *could* in fact allow all isometries when tiling by polyominoes. This fact is used in the proof of Corollary 5.3.4. When these polyominoes are adjacent, the series of one-square modifications on the touching boundaries enforce the color matching rules. This construction clearly works for tiling finite or cofinite regions instead of the plane as well. □

2.3.2 Two main reductions

Lemma 2.3.2 (First Reduction Lemma) *There exists a set* $\mathbf{T}$ *of at most* 23 *generalized Wang tiles with total area* 133 *and using* 9 *colors such that* Simply Connected $\mathbf{T}$-Tileability *is* NP*-complete. Moreover, this will be achieved by a parsimonious reduction from* Cubic Monotone 1-in-3 SAT.

Lemma 2.3.3 (Second Reduction Lemma) *For a set* $\mathbf{W}$ *of at most* k *Wang squares with* c *(boundary) colors, there exists a set* $\mathbf{R}$ *of at most* $8(k+4c)^2$ *rectangular tiles with the following property. Given a simply connected colored region* Γ*, there is a simply connected region* Γ' *such that* Γ *is* $\mathbf{W}$*-tileable if and only if* Γ' *is* $\mathbf{R}$*-tileable. Moreover, this reduction is parsimonious and can be computed in linear time.*

We may transform the set of 23 generalized Wang tiles afforded by Lemma 2.3.2, according to the procedure outlined in (iii)⇒(ii) of Lemma 2.3.1, in order to obtain Theorem 2.2.2 using 23 polyomino tiles. Similarly, using the transformation of Lemma 2.3.3, we conclude the result for rectangular tiles in Theorem 2.1.1 (see Subsection 2.6.1). Theorem 2.1.2 can be shown by modifying the proof of Lemma 2.3.2 to achieve a parsimonious reduction from, say, 2SAT, whose associated counting problem is #P-complete (see Subsection 2.6.2).

2.4 Proof of the First Reduction Lemma (Lemma 2.3.2)

2.4.1 General setup

The goal of this section is to construct a set of generalized Wang tiles that could be used to solve Cubic Monotone 1-in-3 SAT. Each expression will be encoded as a colored rectangular boundary. Tiles corresponding to variables and clauses will appear on the left and right sides of the region, respectively. The variable tiles will "transmit" its state (0 or 1) through "wires" to the clause tiles; each clause tile will "check" if precisely one out of three signals it receives is 1. The path of the transmissions will be regulated by placing "crossover tiles" that allow signals to crossover at specific locations. The positioning of such tiles will be enforced by using a combination of "control tiles" that follow instructions encoded on the boundary. Empty spaces will be filled by "filler tiles."

2.4.2 Tileset T

Let **T** be a tileset with the 7 small tiles shown in Figure 2.4 and the 3 big tiles in Figure 2.5. Some horizontal edges are colored by their labels; all unlabeled edges are colored by 0, which is omitted in the figures for clarity, but acts as any other ordinary color.

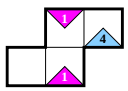

(a) left tile L

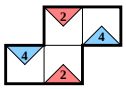

(b) weak tile W

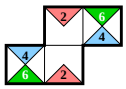

(c) strong tile S

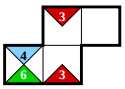

(d) right tile R

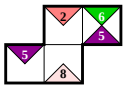

(e) bottom tile B

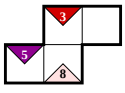

(f) corner tile K

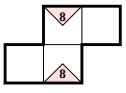

(g) filler tile F

Figure 2.4: Tiles in tileset **T**.

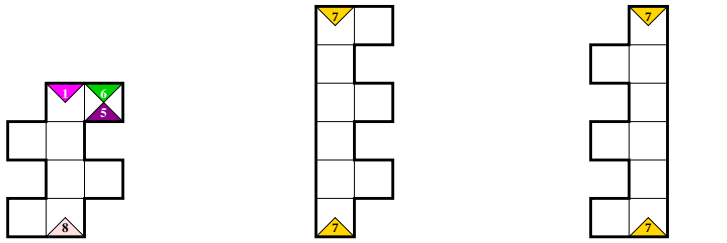

(a) crossover tile X (b) variable tile V (c) clause tile C

Figure 2.5: More tiles in $\mathbf{T}$.

2.4.3 Tileset $\mathbf{T}'$

Recall that the vertical edges of our tiles in $\mathbf{T}$ are all colored with 0. Form $\mathbf{T}'$ by recoloring the vertical edges of tiles in $\mathbf{T}$ as follows. Given each small tile $\tau \in \mathbf{T}$ in Figure 2.4, we introduce a variant by coloring all its vertical edges with 1. The color of the vertical edges is called the *parity* of τ. Include both this variant and the original in $\mathbf{T}'$.

Given a rectangular array of these tiles, the parities are consistent across each row and are independent across the columns. Intuitively, these tiles act as wires that can transmit data (parity of the tile) horizontally across the region.

We continue defining $\mathbf{T}'$. We add three new versions of the crossover tile X as in Figure 2.6a. Intuitively, this allows the data transmissions to *crossover*. We also add a variant of the variable tile V, as in Figure 2.6b, where all the right vertical edges are colored with 1. The parity of the variable tile corresponds to the truth value assigned to that variable. Finally, we *replace* the clause tile C by the three shown in Figure 2.6c, where each tile has one out of three pairs of left vertical edges colored with 1. Thus $\mathbf{T}'$ consists of 23 tiles.

We will place the variable tiles on the left and the clause tiles on the right. It remains to send the data from the variables to the correct clauses. We achieve this by specifying boundary colors to force crossover tiles to appear at the desired locations.

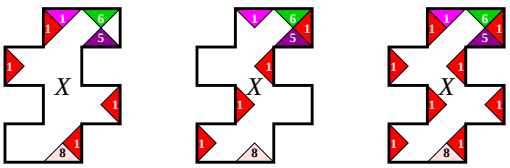

(a) crossover tile X

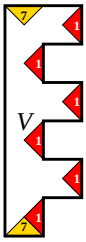

(b) variable tile

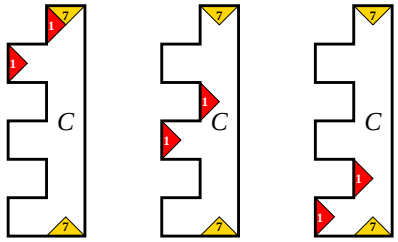

(c) clause tile

Figure 2.6: Variations of tiles in **T**.

2.4.4 Reduction construction

Our goal is to embed the decision problem Cubic Monotone 1-in-3 SAT as a tiling problem. Given a cubic monotone 1-in-3 SAT expression E with variables $X = \{x_1, \ldots, x_n\}$ and clauses $\mathcal{C} = \{C_1, \ldots, C_n\}$, consider it as a permutation $\sigma = \sigma_E \in S_{3n}$ in the symmetric group on $3n$ letters as follows. Think of σ as a bijection from the ordered multiset $X' = \{x_1, x_1, x_1, x_2, \ldots, x_n\}$ to the ordered multiset $\mathcal{C}' = \{C_1, C_1, C_1, C_2, \ldots, C_n\}$, where each variable and each clause is listed three times. For each $x_i \in C_j$, we have $\sigma(x_i) = C_j$ once. Now identify each multiset with $[3n] = \{1, 2, \ldots, 3n\}$ to get σ as a permutation in S_{3n}. Let $s_i = (i, i+1)$ be an adjacent transposition for $i \in [3n-1]$. Write $\sigma = s_{i_1} s_{i_2} \ldots s_{i_d}$ as a product of adjacent transpositions, with $d = O(n^2)$.[3]

Let c_k be the color sequence $01(02)^{k-1}63$. Define a rectangular region $\Gamma = \Gamma_E$ as follows. The height of Γ is $6n$ and the vertical edges are colored with 0. The width is the length of the color sequence $7c_{i_1}c_{i_2}\ldots c_{i_d}07$, which is used as the top boundary. The bottom boundary is $7(08)^t07$ with the same length as the top boundary. The following result demonstrates the ability to place the crossover tile X at arbitrary depth of a large rectangular region.

[3]For illustration purposes, it is often convenient to encode the product of adjacent transpositions using *wiring diagrams*, as shown in Figures 2.7a and 2.8a.

Sublemma 2.4.1 *The region* Γ *admits a unique* $\mathbf{T}$*-tiling.*

Proof. The left and right sides are forced to be filled with variable and clause tiles, respectively. Now consider the section in between.

For $k \geq 1$ and $\ell \geq 0$, consider a row of tiles $LW^kS^\ell R$ (meaning an L tile followed by a W tiles k times, an S tile ℓ times, and ending with an R tile). The bottom color sequence is $01(02)^k(62)^\ell 63$. One easily checks that the unique way to tile the next row is with $LW^{k-1}S^{\ell+1}R$.

If $k = 0$, we get the case where we have a row $LS^\ell R$ with bottom color sequence $01(62)^\ell 63$. The unique way to tile the next row is with $XB^\ell K$.

The section below will be filled by filler tiles F. Thus every section below c_i is filled uniquely, with the crossover tile X occupying rows i and $i+1$ in the first column. □

The above proof is illustrated with two examples in the next subsection.

Corollary 2.4.2 *The expression* E *is satisfiable if and only if* Γ_E *is* $\mathbf{T}'$*-tileable. Moreover, the reduction is parsimonious, that is, the number of tilings of* Γ_E *is the number of satisfying assignments for* E*.*

The corollary follows immediately from the construction given above, and concludes the proof of Lemma 2.3.2.

2.4.5 Examples of the tiling construction

In Figure 2.7 we show how to place a crossover tile in a special case, corresponding to expression $\{(x, y, x), (x, y, y)\}$. We illustrate the crossings with a *wiring diagram* and then give a complete Wang tiling. In Figure 2.8 below we give a bigger example of the wiring diagram and the unique Wang tiling, corresponding to expression $\{(x, y, x), (x, y, z), (y, z, z)\}$.

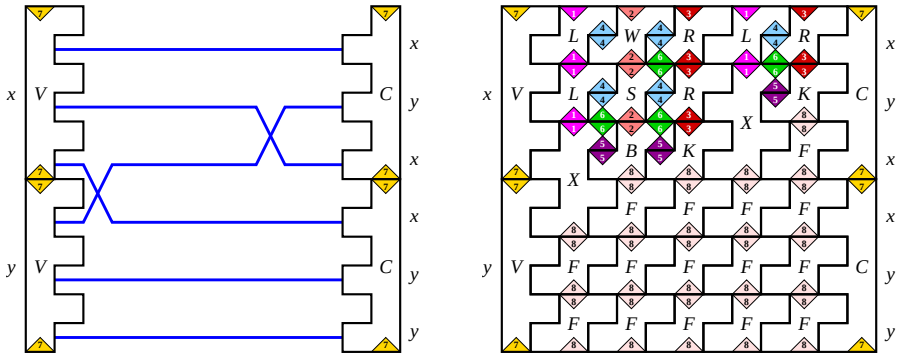

(a) Wiring diagram (b) Unique tiling

Figure 2.7: A small example of how to place crossover tiles.

2.5 Proof of the Second Reduction Lemma (Lemma 2.3.3)

2.5.1 Basics

In this section, we provide a further connection between Wang tiles and rectangular tiles (by making a reduction from the latter to the former). Recall that by Lemma 2.3.1, we can replace generalized Wang tiles with relational Wang tiles.

Without loss of generality, we may assume that the Wang relations are irreflexive, that is, there is no tile τ such that $H(\tau, \tau)$ or $V(\tau, \tau)$. Indeed, suppose $\mathbf{W}$ is a set of Wang tiles. Let $\mathbf{W}' = \{\tau_i : i \in \{0, 1\},\ \tau \in \mathbf{W}\}$ be a doubled set of tiles. Define its horizontal Wang relation as follows. For $\tau, \tau' \in \mathbf{W}$ and $i, j \in \{0, 1\}$, let $H_{\mathbf{W}'}(\tau_i, \tau'_j)$ if and only if $H_{\mathbf{W}}(\tau, \tau')$ and $i \neq j$. Its vertical Wang relation is defined analogously. It is clear that the Wang relations of $\mathbf{W}'$ are irreflexive. Moreover, a $\mathbf{W}$-tiling can be made into a $\mathbf{W}'$-tiling by adding subscripts to the tiles in a checkerboard fashion, while the reverse can be done by ignoring the subscripts. Of course, the same transformation is done on the boundary tiles as well. Clearly this does not affect tileability nor the number of such tilings.

From now on, assume we are given a fixed set $\mathbf{W}$ of relational Wang tiles whose relations H and V are irreflexive. Our goal is to produce a fixed set $\mathbf{R}$ of rectangular tiles with the following property: Given any simply connected region Γ with specified boundary tiles, we

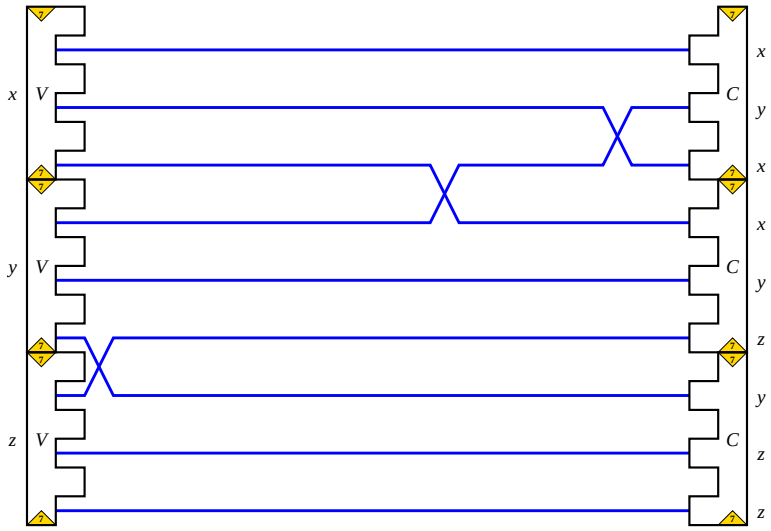

(a) Wiring diagram

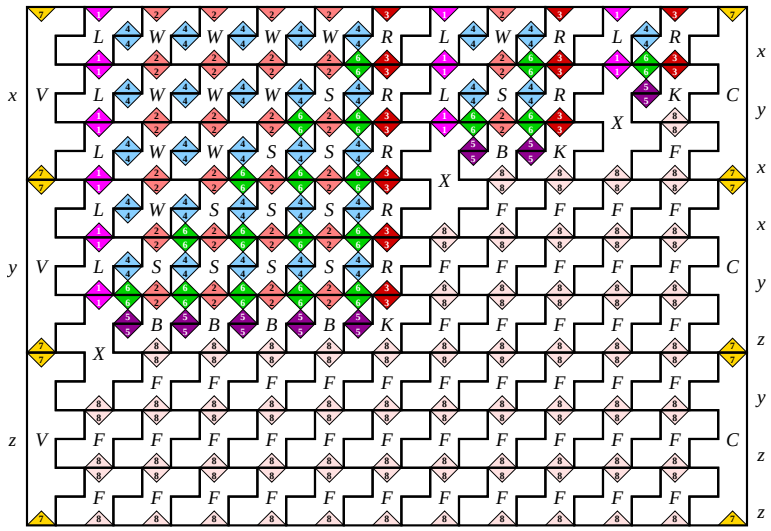

(b) Unique tiling

Figure 2.8: A bigger example of the unique base tiling.

can produce (in linear time) a simply connected region Γ' such that Γ is **W**-tileable if and only if Γ' is **R**-tileable. Moreover, the number of **W**-tilings of Γ will be the same as the number of **R**-tilings of Γ'.

For simplicity, we first consider the case where we are given an $r \times c$ rectangular region Γ with specified boundary tiles.

2.5.2 Expansion

From this point on, we only consider tiling using rectangular tiles. Fix M and e to be positive integers. Given a region Γ_0, we obtain an (M, e)-*expansion* Γ by scaling Γ_0 by a factor of M and then *perturb* it by moving each corner vertex of the boundary curve of the region Γ, at most e in each direction, such that Γ is still a region (with rectilinear edges). Recall that a (rectangular) tile is just a simply connected region, thus the notion of (M, e)-expansion of a tile is defined. A tileset $\mathbf{T}$ is an (M, e)-*expansion* of a tileset $\mathbf{T}_0$ if each $\tau \in \mathbf{T}$ is an (M, e)-expansion of some $\tau_0 \in \mathbf{T}_0$.

A tiling π of a region Γ is an (M, e)-*expansion* of a tiling π_0 of some region Γ_0 if it can be obtained by dilating by a factor of M, and then perturbing the tiles and the region by at most e as above. Note that after scaling, each tile may grow or shrink in each dimension by at most $2e$, and can *shift* around from its starting point by at most e.

Given a tileset $\mathbf{T}_0$ and an (M, e)-expansion $\mathbf{T}$, a region Γ *respects the expansion* if there is a unique region Γ_0 such that any $\mathbf{T}$-tiling of Γ is an (M, e)-expansion of a $\mathbf{T}_0$-tiling of Γ_0.

Intuitively, we will choose $M > 100e$, say, and carefully perturb only a few tiles, so that when consider tilings of regions respecting the expansion, we can essentially predict what the new tiling can be based on the original tiling.

2.5.3 Rectangular tiles $\mathbf{R}_0$ and the region $\Gamma_0(r, c)$

Consider the following tileset:

$$\mathbf{R}_0 = \{f = R(34, 11),\ w = R(31, 14),\ s = R(10, 10),\ h = R(11, 31),\ v = R(14, 34)\},$$

where $R(a, b)$ denotes a rectangle of height a and width b (see Figure 2.9). For a rectangle t, write $\mathbf{ht}\, t$ and $\mathbf{wd}\, t$ for its height and width, respectively.

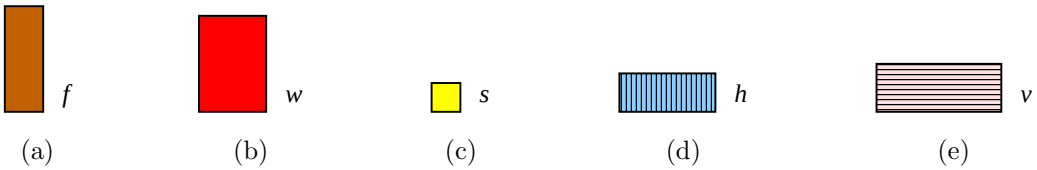

Figure 2.9: Rectangular tiles $\mathbf{R}_0$: (a) fixed rectangle f, (b) fixed rectangle w, (c) flexible square s, (d) flexible rectangle h, and (e) flexible rectangle v.

Now consider the region $\Gamma_0(r, c)$ defined as follows (see Figure 2.10). On each vertical side, there are r *protrusions* of height $\mathbf{ht}\, h$ and width $\mathbf{wd}\, s$, separated by height $\mathbf{ht}\, f$. On each horizontal side, there are c *cavities* of width $\mathbf{wd}\, v$ and height $\mathbf{ht}\, s$, separated by width $\mathbf{wd}\, f$.

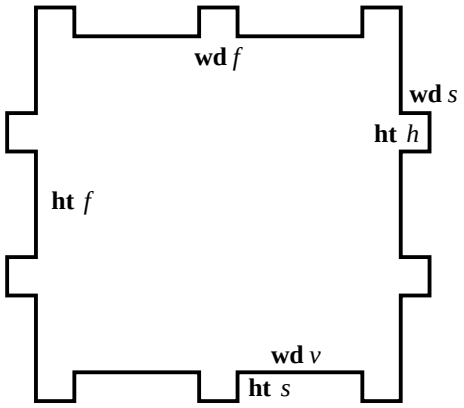

Figure 2.10: Boundary region $\Gamma_0(2, 2)$.

Sublemma 2.5.1 *The unique* $\mathbf{R}_0$*-tiling of* $\Gamma_0(r, c)$ *consists of* r *rows and* c *columns of the* w *tile.*

Proof. Fix natural numbers $a = 10$ and $b = 1$. The tiles introduced above can now be written as $f = R(3a + 4b, a + b)$, $w = R(3a + b, a + 4b)$, $s = R(a, a)$, $h = R(a + b, 3a + b)$, and $v = R(a + 4b, 3a + 4b)$.

We begin with a few definitions. A horizontal (vertical) segment of a region is called *bounded* if the region extends downward (to the right) on both sides of the segment. For $t \in \{v, h\}$, a *pair* (t, s) is the configuration of placing the tile s above or below t, aligned on the left. The *orientation* of the pair is positive (negative) if s is placed below (above). Similarly, for $t \in \{w, f\}$, a pair (t, s) is obtained by placing s to the left or right of t, aligned on top. The orientation is positive (negative) if s is placed to the right (left). A bounded segment is *tiled by a tile* (*pair*) if in all tilings, the tile (pair) is adjacent to the segment.

We will tile the region $\Gamma_0(r, c)$ in steps, as indicated by the numbers labeled on Figure 2.11. Note that since $a > b$, each bounded horizontal segment of width $\mathbf{wd}\, f$ on the top border must be tiled by f tiles, labeled 1. Similarly on the left, the bounded vertical segments of height $\mathbf{ht}\, h$ must be tiled by h tiles, labeled 2. This creates a bounded vertical segment of height $\mathbf{ht}\, v + \mathbf{ht}\, s$ on the top left corner; since $a > 3b$, it is tiled by the pair (v, s), labeled 3. Since $a > 4b$, it is obvious that it needs to be positively oriented, to avoid a hole of width $\mathbf{wd}\, v - \mathbf{wd}\, s$ and height $\mathbf{ht}\, s$, which cannot be filled.

Note that since $a > 3b$, this creates a new bounded horizontal segment of width $\mathbf{wd}\, w + \mathbf{wd}\, s$, which is tiled by the pair (w, s), labeled 4. If w is on the left, it will create a bounded horizontal segment of width $\mathbf{wd}\, f + \mathbf{wd}\, s$ to its left. Otherwise, if w is on the right, several s will be forced to appear on the left and still create the same bounded segment. Therefore, the (w, s) pair creates the bounded segment, regardless of how it is oriented.

Since $a > 3b$, this bounded horizontal segment of width $\mathbf{wd}\, f + \mathbf{wd}\, s$ is again tiled by an (f, s) pair, labeled 5. Like the (v, s) pair above, since $a > 4b$, this needs to be positively oriented. This creates the bounded vertical segment of height $\mathbf{ht}\, v + \mathbf{ht}\, s$, tiled by a pair (v, s), labeled 6, as above. In either orientation, it bounds the vertical segment of height $\mathbf{ht}\, w$ above, concluding that the (w, s) pair (labeled 4) we placed above needs to be positively oriented. Furthermore, this bounds the vertical segment of height $\mathbf{ht}\, h + \mathbf{ht}\, s$, again tiled

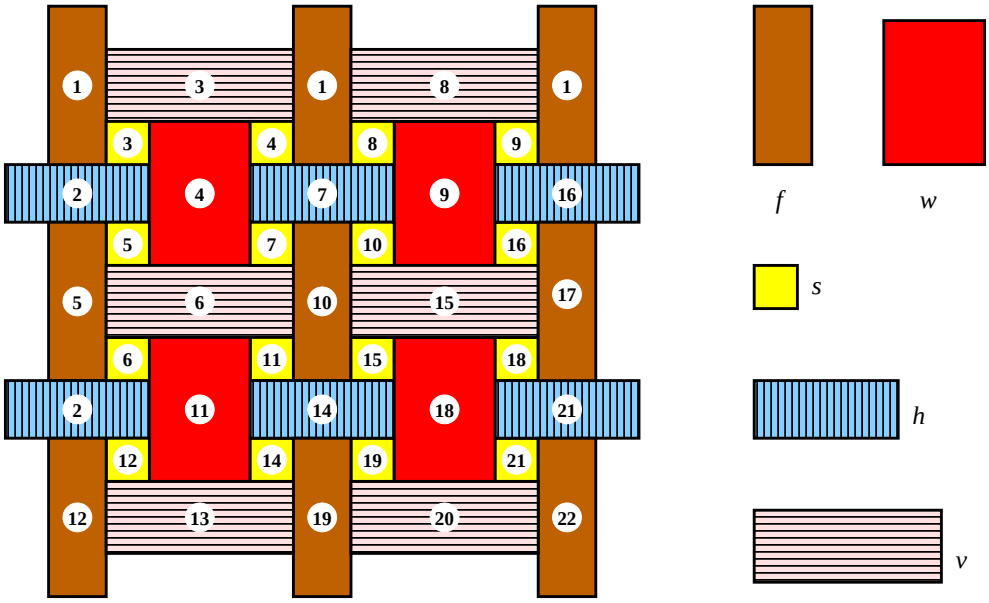

Figure 2.11: Unique base tiling labeled by order.

by the pair (h, s), labeled 7. As before, in either orientation, we have a bounded vertical segment of height $\mathbf{ht}\, v + \mathbf{ht}\, s$, which necessarily needs to be tiled by the positively oriented pair (v, s), labeled 8. This creates a bounded horizontal segment of width $\mathbf{wd}\, w + \mathbf{wd}\, s$.

We continue in like manner, working our way on the anti-diagonal from top right to bottom left. Each time we place the pair (w, s), forcing the adjacent pair (h, s) placed in the previous stage to be positively oriented. Then we place (f, s), forcing the adjacent (v, s) to be positively oriented as well. This procedure repeats with (w, s) and (f, s) in an alternating fashion. The last (f, s) will be placed in positive orientation and creates a bounded vertical segment of height $\mathbf{ht}\, v + \mathbf{ht}\, s$.

Similarly, we work from bottom left to top right on the next anti-diagonal. We alternate between placing (v, s) and (h, s) pairs, positively orienting the (w, s) and (f, s) pairs in the previous stage, respectively. This continues until the entire region is filled. □

2.5.4 Expansion R of $\mathbf{R}_0$

We will now define a clever set of perturbed expansion tiles that will correspond to the relational Wang tiles. Only the tiles s, h, and v will have perturbations. Let $\mathbf{W} = \{\tau_1, \ldots, \tau_n\}$ be the fixed set of relational Wang tiles with irreflexive horizontal and vertical Wang relations H and V, respectively. Fix $e = 5^n$ and $M = 100e$ for the remainder of the section. Let $\mathbf{R}$ be an (M, e)-expansion of $\mathbf{R}_0$ as follows:

For $t \in \{s, h, v\}$, let $t(a, b)$ be the scaled version of t with height and width increased by a and b, respectively. Imagine that the h and v tiles can stretch horizontally and vertically, respectively, and the s tiles can stretch in both directions. Then the w tiles, having no perturbations, will only shift around a little (by at most e). The f tiles will stay fixed, enforcing the global structure. See Figure 2.12. A w tile will be shifted to the right and down by 5^i to *represent* the Wang tile τ_i. To restrict the shifts to only those sizes, we replace s with the appropriate perturbed versions. Namely, for each i, introduce four tiles with perturbations $s(\pm 5^i, \pm 5^i)$, where all four combinations of signs are included. To enforce the Wang relations, for each $\tau_i, \tau_j \in \mathbf{W}$ such that $V(\tau_i, \tau_j)$ or $H(\tau_i, \tau_j)$, we introduce the perturbation $v(5^j - 5^i, 0)$ or $h(0, 5^j - 5^i)$, respectively. This is the set $\mathbf{R}$ we will use.

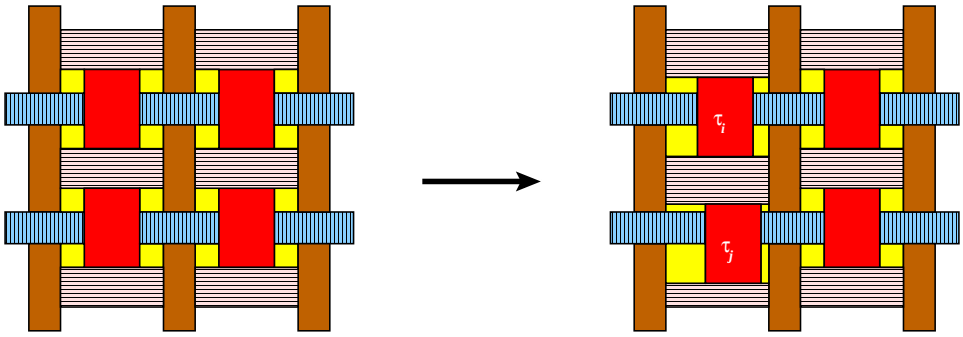

Figure 2.12: Shifting an expansion of the unique tiling to represent Wang tiles.

2.5.5 Rectangular tiling

Obtain an (M, e)-expansion $\Gamma(r, c)$ of $\Gamma_0(r, c)$ by scaling with a factor of M and then perturbing it as follows. Recall that there are r protrusions on each vertical side and c cavities on each horizontal side. Each protrusion or cavity corresponds to a boundary tile of Γ in a natural way. Perturb the protrusion or cavity to the right or down, respectively, by 5^i units if it corresponds to τ_i.

Sublemma 2.5.2 *The (M, e)-expansion $\Gamma(r, c)$ of $\Gamma_0(r, c)$ respects the expansion $\mathbf{R}$ of $\mathbf{R}_0$.*

Proof. Recall the argument in the proof of Sublemma 2.5.1. As the inequalities are all satisfied, the f tiles are fixed and force the perturbations to stay local. The w tiles have two degrees of freedom. They can move $\pm 5^i$ in each direction, as regulated by the s tiles. Now note that the inequalities in the proof of Sublemma 2.5.1 are preserved. We leave the (easy) details to the reader. □

We now return to the proof of Lemma 2.3.3. It is clear that given a Wang $\mathbf{W}$-tiling of the rectangle Γ with boundary, we will get an $\mathbf{R}$-tiling of $\Gamma(r, c)$. Indeed, simply take the unique tiling of $\Gamma_0(r, c)$ as afforded by Sublemma 2.5.1, scale by a factor of M, and then shift each w tile to the right and down by 5^i if it represents τ_i, and adjust the other tiles in the obvious way.

Conversely, if we are given an $\mathbf{R}$-tiling of $\Gamma(r, c)$, we wish to recover the $\mathbf{W}$-tiling of Γ. This is achieved using the following two sublemmas, both of which are clear when all numbers are considered in base 5; we omit the (easy) details.

Sublemma 2.5.3 *The equation $5^i - 5^j = 5^k + 5^\ell$ does not admit a solution in $\mathbb{N}$.*

Therefore each w tile will shift to the right and down (as opposed to shifting left or up), and hence indeed represents a Wang tile τ_i for some i.

Sublemma 2.5.4 *The equation $5^i - 5^j = 5^k - 5^\ell$ does not admit solutions in $\mathbb{N}$ except if $i = j$ or $i = k$.*

If a w tile representing τ_j is to the right of a w tile representing τ_i, then $h(0, 5^j - 5^i)$ must be in $\mathbf{R}$. By the sublemma above, the differences $5^j - 5^i$ are all distinct (recall that the Wang relations are irreflexive, so $i = j$ does not happen), therefore we must have had $H(\tau_i, \tau_j)$ as part of the Wang relation. Similarly for the vertical Wang relation V. So by reading off the associated tile τ_i from the shifts of each w tile, we get a Wang $\mathbf{W}$-tiling of Γ.

This completes the construction of $\Gamma_0(r, c)$ for the case when Γ is a rectangle. For the general case, when Γ is a simply connected region, the proof follows verbatim after replacing $\Gamma(r, c)$ and $\Gamma_0(r, c)$ by appropriate regions.

It remains to get the upper bound estimates on the number of rectangles involved in the construction. Suppose we are given a set of k Wang squares using c colors (on the boundary). By Lemma 2.3.1 we can equivalently consider a set of less than $k + 4c$ relational Wang tiles. To satisfy irreflexivity, we might need to double the set of tiles, resulting in $n = |\mathbf{W}| < 2(k + 4c)$ tiles. When making $\mathbf{R}$, we will have one each of f and w tiles. There will be $4n$ perturbed s tiles and at most n^2 perturbed h and v tiles each. In total,

$$|\mathbf{R}| \leq 2n^2 + 4n + 2 = 2(n + 1)^2 \leq 8(k + 4c)^2.$$

This concludes the proof of Lemma 2.3.3.

2.6 Proof of theorems

2.6.1 Proof of Theorem 2.1.1

In the proof of Lemma 2.3.2 in Section 2.4, we constructed the set $\mathbf{W}$ of 23 generalized Wang tiles using 9 colors, such that Simply Connected $\mathbf{W}$-Tileability is NP-complete. It remains to count the total number of rectangles we obtain from the series of reduction constructions.

First, compute the number of Wang squares given by the transformation in Lemma 2.3.1. Observe that the total area of tiles in $\mathbf{W}$ is $9 \cdot 5 + 8 \cdot 4 + 4 \cdot 14 = 133$. Therefore we can break them into 133 Wang squares by adding $133 - 23$ more colors. But as these colors do

not appear on the boundary, they need not be counted. Hence, in Lemma 2.3.3, we can take $k = 133$ and $c = 9$, thus giving us at most 10^6 rectangles. □

2.6.2 Proof of Theorem 2.1.2

First, note that the reduction in the proof of Theorem 2.1.1 is parsimonious. However, there seems to be no #P-completeness result for the #Cubic Monotone 1-in-3 SAT problem. This is easy to fix by making a similar reduction from the 2SAT problem, whose associated counting problem is #P-complete (see [Val79b]).

An instance of 2SAT is a set of variables and a collection of clauses. Each clause is a disjunction of two literals, where each literal is either a variable or a negated variable. The problem is to decide whether there is a satisfying assignment such that each clause has at least one true literal. We modify the proof of Lemma 2.3.2 to obtain a parsimonious reduction from 2SAT. By replacing the two variations of the variable tile by the ones shown in Figure 2.13a, we may set up unnegated and negated copies of a single variable. Indeed, with a sequence of $5(26)^{r-1}36(26)^{s-1}4$ as colors on the left vertical edge, we create a list of $r + s$ variables, where the last s are negated. By replacing the three variants of the clause tile by the three obvious candidates in Figure 2.13b, we force each clause to be satisfied.

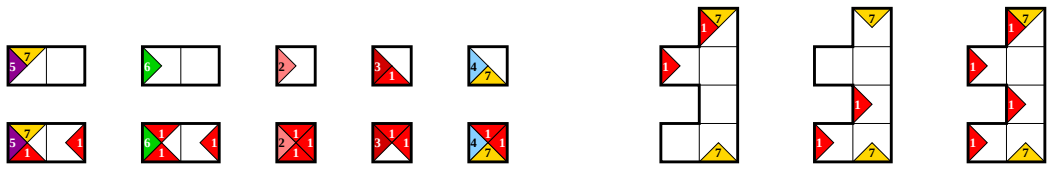

(a) tiles for variables (b) clause tiles

Figure 2.13: Tiles for 2SAT.

Note that the modified tileset has a smaller total area, and has the same number of colors used on the boundary. Therefore as in the proof of Theorem 2.1.1, we apply Lemma 2.3.3 to conclude that 10^6 rectangles suffice. □

2.7 Final remarks and open problems

2.7.1

Theorem 2.2.1 was only announced in [GJ79], referencing an unpublished preprint. Of course, now we have much stronger results.

A version of Lemma 2.3.2 was first announced in Levin's original 1973 short note on NP-completeness [Lev73], but the proof has never been published.[4] Although we were unable to find in the literature an explicit construction for either Lemma 2.3.2 or, equivalently, of Theorem 2.2.2, we do not claim this result as ours, since it became a folklore decades ago. We include the proof for completeness, and since we need an explicit construction. An alternative proof is outlined in Subsection 2.7.2 below.

Let us mention that using [Oll09], the number of tiles in Theorem 2.2.2 can be reduced to 11, but this reduction has no effect on the number of tiles in the main theorems. Indeed, Theorem 2.2.2 is an immediate corollary of Lemma 2.3.2, which is the one needed in the proof of main theorems 2.1.1 and 2.1.2.

2.7.2

Our proof of Lemma 2.3.2 is completely elementary and yields explicit bounds (see also Subsection 2.7.1). Let us sketch an alternate proof of the lemma, using a non-deterministic *universal Turing machine* (UTM). It was suggested to us by Cris Moore.

Fix some non-deterministic universal Turing machine $\mathfrak{M}$. Given two finite tape configurations and a natural number t (in unary), it is NP-complete to decide whether $\mathfrak{M}$ transforms the first tape configuration to the second with t steps of computation. Fix a finite set $\mathbf{W}$ of Wang tiles that simulate the space-time computation diagram of $\mathfrak{M}$ (see Section 6.1). Encode the given tape configurations as the top and bottom boundaries of a rectangular region with height t. This region is tileable by $\mathbf{W}$ if and only if $\mathfrak{M}$ transforms the first

[4] Leonid Levin, personal communication.

tape configuration to the second in precisely t steps. The details are straightforward (see *e.g.* [LP97, §7]).

Note that this method also proves the counting result. Indeed, one can devise a UTM so that there is a bijective correspondence between the accepting paths of the UTM and of the Turing machine it is simulating.

We do not know if this approach leads to improvements in the number of Wang tiles in the lemma, as this would depend on the smallest UTM. Given an m-state n-symbol Turing machine with k instructions, the standard construction of Wang tiles to simulate such a Turing machine yields more than $nm + n + k$ tiles. As a perspective, among the smallest known UTMs, this minimum is achieved by Rogozhin's 4-state 6-symbol machine with 22 instructions, which already yields more than 52 tiles [Rog96] (see also [NW09]). Unless a substantial progress is made in finding small UTMs, our elementary proof still gives better bounds.

Indeed, the proof of Lemma 2.3.2 constructs a set of 23 generalized Wang tiles (133 Wang squares). However, it is possible to decrease these numbers by elementary means. After this chapter (as a paper) was written, incremental improvements have led to a set of 117 rectangles. The details are in the next chapter.

2.7.3

In the tiling literature, the original theoretical emphasis was on tileability of the plane, the decidability and aperiodicity. The problem was often stated in the equivalent language of Wang tiles [Ber66, Rob71, Wan65]. Unfortunately, there does not seem to be any standard treatment of the *finite Wang tiling* problems. Although some equivalences in the Lemma 2.3.1 are routine, such as the reduction in Figure 2.2, others seem to be new. We present full proofs for completeness.

2.7.4

Historically, finite tilings were a backwater of the tiling theory, with coloring arguments being the only real tool [Gol65]. On a negative (complexity) side, originally, the tileability problem was studied for general regions, where the tiles were part of the input. The NP-completeness of this most general problem is given in [GJ79, §GP13]. When the set of tiles is fixed, NP-completeness was shown for general regions and various fixed small sets of tiles (see [MR01] and [BNRR95] building on the earlier unpublished work by Robson).

On the positive side, papers of Thurston [Thu90] and Conway & Lagarias [CL90] introduced the *height function* and the *tiling group* interrelated approaches. The key underlying idea is the use of combinatorial group theory applied to the boundary word of the *simply connected regions*, so the tilings become *Van Kampen diagrams* of the corresponding tiling group. This approach allowed numerous applications to perfect matchings [Cha96], tile invariants [Kor04, MP02, Rei03], tileability [She02], various local move connectivity results [KP04, Rém98], classical geometric problems [Ken96], applications to colorings and mixing time [LRS01], *etc.* More relevant to this chapter, the breakthrough result by C. and R. Kenyon [KK92] proved that tileability with bars of simply connected (s.c.) regions can be decided in polynomial time. This result was further extended to all pairs of rectangles by Rémila in [Rém05], and by Korn [Kor04] to an infinite family of *generalized dominoes*. Our Main Theorem puts an end to the hopes that these results can be extended to larger sets of rectangles.

Note also that having s.c. regions gives a speed-up for polynomial problems. For example, domino tileability is a special case of perfect matching, solvable in quadratic time on all planar bipartite graphs [LP09]. However, Thurston's algorithm is linear time (in the area), for all s.c. regions (see [Cha96, Thu90]).

2.7.5

We conjecture that in the Main Theorem (Theorem 2.1.1), the number of rectangles can be reduced down to 3, thus matching the lower bound (Rémila's tileability algorithm for the case of two rectangles). As a minor supporting evidence in favor of this conjecture, let us mention that the proofs in [KK92, Rém05] are crucially based on *local move connectivity*, which fails for three general rectangles. In the absence of algebraic methods, there seem to be no other (positive) approach to tileability.

2.7.6

This result of Main Theorem can be contrasted with a large body of positive results on tiling rectangular regions with a fixed set of rectangles.

Theorem 2.7.1 ("Tiling rectangles with rectangles" Theorem [LMP05]) *For every finite set* $\mathbf{R}$ *of rectangular tiles, the tileability problem of an* $[M \times N]$ *rectangle can be decided in* $O(\log M + \log N)$ *time.*

Note that Theorem 2.7.1 has linear time complexity for the rectangular regions written *in binary*. This result is based on the pioneer results by Barnes [Bar82a, Bar82b] applying commutative algebra, the *finite basis theorem* [DK75] (see also [Rei05]), and the *transfer matrix method* (see *e.g.* [Sta97, Ch. 4]).

It seems, tilings of rectangles have additional structure, which general regions do not have. See *e.g.* [BSST40, CGG$^+$82, Rob82] for assorted results on the subject. On the other hand, when the tiles are part of the input, deciding tileability can be NP-hard, and the proof can be used to show that counting tilings is #P-hard. Note that the results in [LMP05] only discuss tileability, not counting. It would be interesting to obtain general results on the local move connectivity and hardness of counting results for tilings of rectangular regions with rectangles.

2.7.7

Although counting perfect matchings in general graphs is #P-complete, for the grid graphs a *Pfaffian formula* gives a count for the number of domino tilings for any (not necessarily simply connected) region; this formula can be applied in polynomial time [LP09] (see also [Ken04]). In a different direction, Moore and Robson [MR01] conjecture that already for two bars, the problem is #P-complete for general regions. They note that the corresponding reductions in [BNRR95, MR01] are not parsimonious. Thus, until now, the #P-completeness was open for any finite set of rectangular tiles, even for general regions.

We make a stronger conjecture that for every tileset $\mathbf{T}$ of two bars $[1 \times k]$ and $[\ell \times 1]$, where $k, \ell \geq 2$, $(k, \ell) \neq (2, 2)$, the counting of tilings by $\mathbf{T}$ of simply connected regions is #P-complete. In particular, the number 10^6 in Theorem 2.1.2 can be decreased to 2. There is no direct evidence in favor of this, except that the general combinatorial counting problems tend to be #P-complete unless there is a special algebraic formula counting them. Furthermore, when it comes to tile counting, there seem to be no direct benefit of simple connectivity of the regions, so such result is likely to be equally hard as for general regions. We refer to [Jer03] for the introduction and references.

2.7.8

By a simple modification of the Wang tiles, we can also get a parsimonious reduction from SAT. For that, first, we can introduce wire splitters and the NOT gate. By doing so, we remove the "cubic" and "monotone" constraints, respectively. These would play the same role as crossover tiles, and require a separate color on the boundary for each. This would also increase the set of tiles by introducing new variants for the V and L tiles as well. We omit the details.

We can then introduce the AND gate in a similar fashion, again with a new control color on the top and new versions of the V, C and L tiles. This gives the embedding of SAT.

This reduction is parsimonious in the same way as the reduction in Theorem 2.1.2, which implies that the associated counting problem is also #P-complete.

Let us compute the total number of rectangles necessary for this construction. First, this would increase the number of Wang tiles from 23 to no more than $23 \cdot 8$. Then, the same argument as above gives the 10^8 bound in the number of rectangular tiles. We omit the (easy) calculation and details.

2.7.9

The reductions in this chapter can be used to prove *uniqueness* results on tileability with rectangles, i.e. whether there exists a unique tiling of a region with a given set of rectangular tiles. In [BNRR95], the problem was completely resolved in the case of two bars. An even simpler solution follows from [KK92] in this case. Since all tilings are local move connected, taking the "minimal tiling" constructed by the algorithm in [KK92] and trying all potential moves gives an easy polynomial time test. More generally, Rémila [Rém05] showed that for two general rectangles one can go from one to another with certain non-local moves which are easy to describe. Again, since he produces the "minimal tiling," his algorithm can be used to decide unique tileability with two rectangles.

Now, our approach, via reduction from the general SAT problem (see above) shows that for a certain finite set of rectangles, uniqueness of tilings of a simply connected region is as hard as UNIQUE SAT, which is co-NP-hard and has been extensively studied [BG82, VV86]. This seems to be the first result of this type.

2.7.10

Although Theorem 2.7.1 extends directly to bricks in higher dimensions [LMP05], this is an exception rather than the rule. In fact, in Chapter 4, we show that almost no other positive tileability results extend to higher dimensions, even Thurston's algorithm mentioned above.

CHAPTER 3

Reducing the number of rectangles

In the previous chapter, we established that a bound of 10^6 suffices to find a *fixed* set of rectangles $\mathbf{R}$ such that the tileability problem of simply connected regions with $\mathbf{R}$ is NP-complete. In this chapter, we will incrementally reduce this number by incorporating various ideas. Obvious places of attack include optimizing the Wang tileset construction in Lemma 2.3.2 and the bound in the Second Reduction Lemma (Lemma 2.3.3).

3.1 Improving the Wang tileset

The generalized Wang tileset $\mathbf{W}_{15}$ consists of V_i, L_i, R_i, and F_i, for $i \in \{0,1\}$, X_{ij} for $i,j \in \{0,1\}$, and C_i for $i \in \{1,2,3\}$ (see Figure 3.1, where $\delta_{i,j}$ is the Kronecker delta, 1 if $i = j$ and 0 otherwise). When referring to a tile, we may suppress the subscript for notational convenience.

Note that a color sequence of $\ell o^k r$ on the top boundary will conjure a crossover tile X to appear in row $k+1$ below the color ℓ. Using these, we can follow the same general setup as before to embed a cubic monotone 1-in-3 SAT expression. Indeed, create a rectangular region of height $3n$, where n is the number of variables. Color the left, right, and bottom boundaries by ℓ, r, and o, respectively.

This means that there will be n variable tiles on the left, each either V_0 or V_1, denoting whether the variable is false or true, respectively. The L, R, F tiles all transmit data horizontally, as before. The X tiles will appear at predefined locations, causing the signals to crossover. Finally, the n clause tiles C on the right will check 1-in-3 satisfaction.

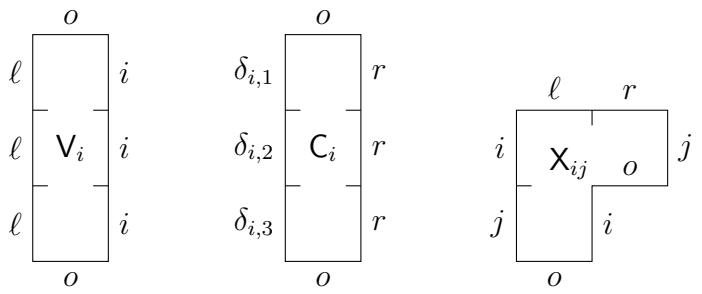

(a) Tile V_i. (b) Tile C_i. (c) Tile X_{ij}.

(d) Tile L_i. (e) Tile F_i. (f) Tile R_i.

Figure 3.1: Tiles for constructing $\mathbf{W}_{15}$.

This proves the following lemma, improving the previous construction of 23 generalized Wang tiles.

Lemma 3.1.1 *There exists a set* $\mathbf{W}_{15}$ *of at most* 15 *generalized Wang tiles such that* Simply Connected **T**-Tileability *is* NP*-complete.*

This directly leads to an improvement of Theorem 2.1.1.

Theorem 3.1.2 *There exists a finite set* $\mathbf{R}_{15}$ *of at most* 20808 *rectangular tiles, such that the tileability problem of simply connected regions with* $\mathbf{R}_{15}$ *is* NP*-complete.*

Proof. The total area of $\mathbf{W}_{15}$ is $3 \cdot 9 + 2 \cdot 2 + 1 \cdot 4 = 35$, thus we may take $k = 35$ (the number of Wang squares) and $c = 4$ (the number of *boundary* colors) in Lemma 2.3.3 to get a set $\mathbf{R}_{15}$ of at most 20808 rectangular tiles. □

3.2 Improving the Second Reduction Lemma

What follows is a second version of the Second Reduction Lemma (Lemma 2.3.3).

Lemma 3.2.1 (Second Second Reduction Lemma) *For a set* $\mathbf{W}$ *of at most* k *Wang squares with* c *colors, there exists a set* $\mathbf{R}$ *of at most* $2k + 8\min\{k, c^2\} + 3$ *rectangular tiles with the following property. Given a simply connected colored region* Γ*, there is a simply connected region* Γ' *such that* Γ *is* $\mathbf{W}$*-tileable if and only if* Γ' *is* $\mathbf{R}$*-tileable. Moreover, this reduction is parsimonious and can be computed in linear time.*

In particular, this gives a linear bound $10k + 3$, which is a big improvement over the previous quadratic bound $8(k + 4c)^2$. Note that here c is the number of colors, not just the boundary colors as in the original Second Reduction Lemma 2.3.3. Another distinction is that the Wang tiles here are not relational.

Proof. First assume that each Wang tile does not have monochromatic parallel edge pairs, and follow the proof of the original Second Reduction Lemma and take the same $\mathbf{R}_0$ as constructed in Section 2.5. Let $\mathbf{R}'$ be a different (M, e)-expansion of $\mathbf{R}_0$ as follows:

The tiles f, h, and v will have no perturbations. Suppose the Wang tiles have colors $\{1, 2, \ldots, c\}$. For each Wang tile with colors N, E, S, W on the north, east, south, and west sides, respectively, denoted $\tau(W, \frac{N}{S}, E)$, introduce a perturbed w tile $w(5^S - 5^N, 5^E - 5^W)$. Furthermore, introduce four perturbed s tiles $s(-5^N, 5^W)$, $s(-5^N, -5^E)$, $s(5^S, 5^W)$, and $s(5^S, -5^E)$. This finishes the construction.

Instead of having a single w tile shift 5^i to the right and down to indicate tile τ_i, we shift the h and v tiles 5^i to the right and down, respectively, to indicate color i on the edge of the two adjacent Wang tiles. Given a colored $[r \times c]$ rectangular region, let $\Gamma(r, c)$ be an (M, e)-expansion of $\Gamma_0(r, c)$, obtained by perturbing the protrusions and the cavities corresponding to color i on the boundary by 5^i to the right and down, respectively (cf. Section 2.5).

It is easy to see that if we are given a Wang tiling, we can place all the h and v tiles by shifting them the appropriate amounts from the base tiling, and then filling in the w and s tiles, which are, by construction, available to fill the gaps precisely.

Conversely, if there is a rectangular tiling, Sublemma 2.5.3 implies that the h and v will always shift to the right or down only, thus enabling us to color the edges of a Wang tiling of the rectangular boundary given. Sublemma 2.5.4 implies that the Wang tiles and the w tiles are in bijective correspondence, hence the Wang tiling obtained above by coloring edges is indeed a tiling by Wang tiles.

Note that for this argument, a Wang tile cannot have monochromatic parallel edge pairs. This is analogous to the irreflexivity requirement of the relational Wang tiles. To ensure this, one can double the set of tiles as follows: replace a Wang tile $\tau(W, \frac{N}{S}, E)$ by tiles $\tau(W, \frac{N}{S'}, E')$ and $\tau(W', \frac{N'}{S}, E)$.

Let us count the number of tiles created. We have the three fixed tiles f, h, and v. For each Wang tile in the doubled set of size $2k$, we create a w tile and four perturbed versions of s. Some of the s tiles may be the same, thus we get an upperbound of $8k$. On the other hand, for the s tiles involving north and west colors, there are at most $2c^2$ of them, one from each type of the doubled tiles. Similarly for the other three corners, thus yielding a bound of $8c^2$ instead. Combining these gives the desired $2k + 8\min\{k, c^2\} + 3$ bound. □

Corollary 3.2.2 *There exists a finite set $\mathbf{R}_f$ of at most 353 rectangular tiles, such that the tileability problem of simply connected regions with $\mathbf{R}_f$ is* NP*-complete.*

Proof. Starting with the generalized Wang tiles $\mathbf{W}_{15}$ constructed in Lemma 3.1.1, we break them into $k = 35$ Wang squares. The number of colors far exceed $\sqrt{35}$, thus we use the $10k + 3$ bound from the second Second Reduction Lemma to obtain a set of at most 353 rectangles. □

3.3 Ad-hoc optimizations

The procedures of the Second Reduction Lemmas work on general sets of Wang tiles. However, we need only apply to a specific set. Let us consider this carefully to further reduce the number of rectangles needed.

One obvious waste is the general bound, where we estimate the number of tiles given the construction. At the end, we will carefully count exactly how many rectangles we obtain. Recall that for the original Second Reduction Lemma, the Wang tiles must be irreflexive—no tile is allowed adjacent to itself. To ensure this, we had to double the number of tiles. Similarly, in the second Second Reduction Lemma, the Wang tiles cannot have monochromatic parallel edge pairs. We also doubled the number of tiles to satisfy this requirement. In what follows, we will modify the set of tiles slightly by hand so no doubling is needed. This will increase the number of tiles, but not as much as doubling.

Lemma 3.3.1 *There exists a set* $\mathbf{W}_a$ *of at most* 33 *Wang squares, without monochromatic parallel edge pairs, such that* Simply Connected **T**-Tileability *is* NP*-complete.*

Proof. Please refer to Figure 3.2 for the modifications of the L, F, X, and C tiles from $\mathbf{W}_{15}$.

Recall that the setup is for tiles to transmit truth values horizontally from left to right. We invert the truth values at each column, so the L and the F tile do not have monochromatic pairs of vertical edges. For easy reading of the truth values of variables, we may use a rectangle with even width, so the clause tiles will get as input truth values that have been inverted even number of times (*i.e.*, not at all). The truth inversion setup solves the problem for the two X_{ii} tiles having monochromatic vertical pairs for the bottom squares, but shifts the problem to the other two X_{ij} tiles, namely, when $i \neq j$. Thus we make those tiles $[2 \times 2]$ squares with the obvious fourth tile. Namely, the right color of the fourth tile is the same as the left color of the tile in the top left. To match with what follows, the bottom color of the fourth tile will be ℓ instead of the expected o.

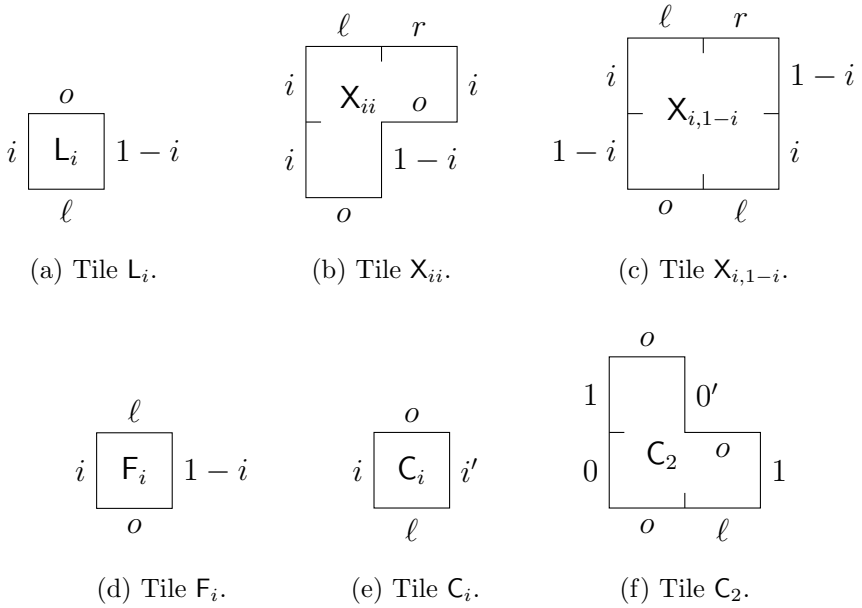

(a) Tile L_i. (b) Tile X_{ii}. (c) Tile $\mathsf{X}_{i,1-i}$.

(d) Tile F_i. (e) Tile C_i. (f) Tile C_2.

Figure 3.2: Tiles for constructing $\mathbf{W}_a$.

As for horizontal edges, the L and the F tiles are the only ones presenting problems. We replace the top of L by color o and similarly replace the top of F by color ℓ. Now L and F will occur as alternating sequences in each column. Imagine placing a crossover X tile where we want it to occur, and putting R tiles diagonally on top of it. We can then fill in the region above and below with L and F tiles. The top and bottom edges will be alternating sequence of o and ℓ colors. They will start as the same sequence if the number of variables is even, and opposite otherwise. To place a crossover tile with its top in row k, we change one of the ℓ on the top boundary to r, and change the k^{th} color to its left from ℓ to o if k is even, and o to ℓ if k is odd.

We have removed the need for doubling, yielding a set of $4 \cdot 2 + 3 \cdot 7 + 2 \cdot 2 + 1 \cdot 4 = 37$ Wang squares, much better than 35 tiles doubled to 70. We now apply one last ad-hoc trick to reduce this number further.

Replace the C tiles (accounting for $3 \cdot 3$ of the area) with the tiles C_i, $i \in \{0, 1\}$, and C_2 that contribute only 5 to the area.

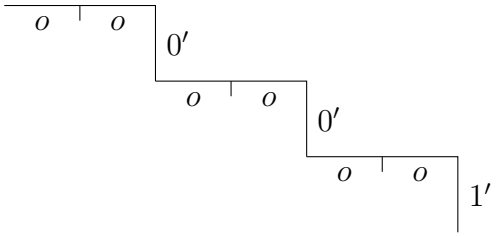

Figure 3.3: Right boundary to be used with the $\mathbf{W}_a$ tiles.

To use these tiles instead, we replace the right boundary of the rectangle by n copies of the boundary shown in Figure 3.3. We then extend the bottom boundary of the rectangle to reach the end of this staircase boundary, using the colors ℓ and o depending on the parity of how many squares are above. Namely, the sequence $\ldots \ell^2 o^2 \ell^2 o^2 \ell^2$, comprising of an alternating sequence of ℓ^2 and o^2, *ending* with ℓ^2 on the right.

We will start with a rectangle of even width, so as to have the same parity between the second vertical edge (the right edge of a variable tile) and the penultimate vertical edge (the left edge of the right-most square) in each row. If the penultimate edge has color i while the color of the last vertical edge is i', then tile C_i fits there. Otherwise, C_2 allows shuffling a 1 signal down a row, provided that the next row carries a 0 signal. In such a manner, every three rows will check 1-in-3 satisfaction, as desired.

The space below such a clause region will not be disturbed, and will simply be filled with L and F tiles. This results in the desired construction of $\mathbf{W}_a$ with 33 Wang squares. □

We now explicitly count how many rectangles we get when applying the second Second Reduction Lemma to this carefully constructed tileset $\mathbf{W}_a$.

Theorem 3.3.2 *There exists a finite set* $\mathbf{R}_a$ *of* 117 *rectangular tiles, such that the tileability problem of simply connected regions with* $\mathbf{R}_a$ *is* NP*-complete.*

Proof. Recall that besides the three tiles (f, h, and v) that do not have perturbations, we create five types of tiles, listed below in the first column of Table 3.1. We count the number of *new* rectangles created due to the introduction of $\mathsf{L}, \mathsf{F}, \ldots, \mathsf{C}$ tiles, in that order. For

example, the top and left edges of the left tile of R_i are colored the same as that of F_i, thus the $s(-5^N, 5^W)$ entry for R is 2 instead of 4. We also note that when breaking X_{ij}, $i \neq j$, into four Wang squares each, we may color the internal horizontal edge on the right as o, then the top right corner tile of X_{ij}, $i \neq j$, is the same as the one for X_{jj}. That is, we may use the same color for the top internal vertical edge for these as to shave the number of tiles from 33 down to 31.

	L	F	R	V	X	C	Σ
$w(5^S - 5^N, 5^E - 5^W)$	2	2	4	6	12	5	31
$s(-5^N, 5^W)$	2	2	2	5	8	2	21
$s(-5^N, -5^E)$	2	2	4	4	6	1	19
$s(5^S, 5^W)$	2	2	4	5	8	2	23
$s(5^S, -5^E)$	2	2	2	5	6	4	20
Σ	10	10	16	24	40	14	114

Table 3.1: Number of tiles in $\mathbf{R}_a$ of each type.

The row and column labeled Σ gives the row and column sums, respectively. Using these ad-hoc methods, we have constructed a set of $114 + 3 = 117$ rectangles, as desired. □

CHAPTER 4

The complexity of generalized domino tilings

Tiling planar regions with dominoes is a classical problem in which the decision and counting problems are polynomial. We prove a variety of hardness results (both NP- and #P-completeness) for different generalizations of dominoes in three and higher dimensions.

4.1 Introduction

The study of *domino tilings* is incredibly rich in its history, applications, and connections to other fields. A geometric version of the *perfect matching* problem in grid graphs, the problem is a special case of a general study of tilings of finite regions, with its own set of problems and generalization directions, very different from graph theory. In this chapter we study the decision and the counting problems for the tilings of a given region. Both problems have a large literature and long history in combinatorics and computational complexity, as well as in the recreational literature, but much of the work concentrated on tilings in the plane. Significantly less is known in three and higher dimensions, where much of the intuition and many tools specific to two dimensions break down.

To summarize the results of this chapter in one sentence, we show that the classical domino tiling problems become computationally hard already in three dimension, even when the topology of regions is restricted. This further underscores the fundamental difficulty of obtaining even the most basic (positive) tiling results in higher dimensions. We should mention that dimension three is critically important for applications ranging from enumer-

ative combinatorics to probability, to statistical physics, and to solid-state chemistry (see *e.g.* [KRS96, Ken04, LP09, dT08]).

The (single tile) *tileability problem* can be stated as follows. Given a tile T, decide whether a region $\Gamma \subset \mathbb{R}^d$ is tileable with copies of T (rotations and reflections are allowed). When T is a domino $[2 \times 1]$, the tileability problem can be solved in polynomial time, via the reduction to perfect matching [LP09], and the result generalizes to any $d \geq 2$. On the other hand, when T is a bar $[3 \times 1]$, the tileability problem is NP-complete [BNRR95] in the plane.

Our first result is on the tileability with a brick $T = [2 \times 2 \times 1]$, which we call a *slab*. Viewed as half-cubes, slabs can be thought of as a natural generalization of 2-dimensional dominoes.

Theorem 4.1.1 *Tileability of* 3*-dimensional regions with slabs is* NP*-complete.*

Now, when the region $\Gamma \subset \mathbb{R}^2$ is simply connected (s.c.), the tileability problem is simpler in many cases. For example, when T is a domino, the s.c. tileability problem can be solved in linear time in the area $|\Gamma|$, while quadratic for general regions [Thu90] (see also [Cha96]). Moreover, when T is any rectangle, the s.c. tileability problem is polynomial [Rém05] (see also [KK92]), as opposed to NP-complete for general regions. Interestingly, this phenomenon does not extend to higher dimensions.

Theorem 4.1.2 *Tileability of* contractible 3*-dimensional regions with slabs is* NP*-complete.*

For the definition of contractible regions in higher dimension, generalizing s.c. regions in the plane, see Section 4.2. Note that in the plane, finding a tile such that the tileability problem of simply connected regions is NP-complete remains an open problem (see Section 4.8).

The next set of results concerns *counting problems*: given Γ, compute the number of tilings of Γ with copies of tile T (again, rotations and reflections are allowed). It is well known that in the plane, the number of domino tilings of Γ can be computed in polynomial time (see *e.g.* [Ken04, LP09]). This is perhaps surprising, since computing the number of

perfect matchings is classically #P-complete [Val79b]. The following result is one of the historically first applications of #P-completeness.

Theorem 4.1.3 (Valiant [Val79a]) *Number of domino tilings of* 3*-dimensional regions is* #P*-complete.*

Let us note that Valiant's result is strongly related, but slightly different (see Subsection 4.8.4). We re-prove Valiant's theorem both for completeness and as a stepping stone towards stronger results. The proof uses a reduction from the perfect matching problem in cubic bipartite graphs. This construction allows us to prove the following far-reaching extension of Theorem 4.1.3.

Theorem 4.1.4 *Number of domino tilings of* contractible 3*-dimensional regions is* #P*-complete.*

We conclude with the following counting version of theorems 4.1.1 and 4.1.2. This is obtained essentially for free by using the same construction as in the proof of the theorems.

Theorem 4.1.5 *Number of slab tilings of* 3*-dimensional regions is* #P*-complete. Moreover, the result holds when considering only contractible regions.*

Much of the rest of the chapter consists of proofs of these results. In Section 4.7, we present generalizations to dimensions $d \geq 4$. We conclude with final remarks and open problems in Section 4.8, where we also continue a historical discussion of these and related tiling results.

4.2 Definitions and basic results

Consider $\mathbb{Z}^3$ as the union of closed unit cubes in $\mathbb{R}^3$ centered at the integer lattice points. We will suggestively refer to the elements of $\mathbb{Z}^3$ as *cubes*. A *region* Γ is a finite subset of $\mathbb{Z}^3$, and is naturally identified with $\overline{\Gamma} \subset \mathbb{R}^3$, the union of the corresponding closed unit cubes. We say that a region $\Gamma \subset \mathbb{Z}^3$ is *contractible* if $\overline{\Gamma} \subset \mathbb{R}^3$ is contractible and has contractible interior.

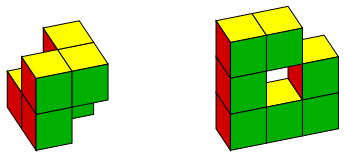

Figure 4.1: Examples of non-contractible regions of $\mathbb{Z}^3$.

Neither of the requirements is redundant. For example, the set on the left in Figure 4.1 consisting of six closed cubes is contractible but its interior is not, since the center becomes a hole. The region on the right with seven closed cubes is not contractible but its interior is. We wish to be strict and consider these as non-contractible.

Let T be a *tile*, which is simply a contractible region. A *T-tiling* of a region Γ is a partition of Γ into pairwise disjoint (as subsets of $\mathbb{Z}^3$) isomorphic copies of T. Here we allow T to be rotated and reflected—though all the tiles we will consider are bricks, which have mirror symmetries. When the tile T is understood, we simply call it a tiling. This leads us to the following two decision problems:

T-Tileability

Instance: A region Γ.

Decide: Does the region Γ admit a T-tiling?

Contractible T-Tileability

Instance: A contractible region Γ.

Decide: Does the region Γ admit a T-tiling?

To analyze the complexities of these problems, we will follow the usual line of attack by embedding known problems as tiling problems. As such, let us define two more decision problems we will use. A graph is *cubic* if each vertex has degree 3. A *perfect matching* is a collection of pairwise-disjoint edges that cover all the vertices.

Cubic Bipartite Perfect Matching

Instance: A cubic bipartite graph G.

Decide: Does the graph G admit a perfect matching?

Suppose we are given a set of boolean variables. A *literal* is a variable or the negation thereof. A 3-*SAT expression* $\mathcal{C}$ is a conjunction of clauses, each a disjunction of three literals. We will write $\mathcal{C} = \{C_1, \ldots, C_t\}$ as a set of triples C_i of literals, where the negation of a variable v is denoted $\overline{v}$. An assignment of boolean values to the variables is 1-*in*-3 *satisfying* if each clause C_i has precisely one true literal. This leads to the following natural decision problem:

1-IN-3 SAT

Instance: A 3-SAT expression $\mathcal{C}$.

Decide: Does the expression $\mathcal{C}$ admit a 1-in-3 satisfying assignment?

For each decision problem, we also have an associated counting problem, where we count the number of witnesses. In particular, for the problems above, we need to count the number of tilings, perfect matchings, and satisfying assignments, respectively. By abuse of language, we say a decision problem is #P-complete if its associated counting problem is #P-complete. We reduce the tiling problems from the following two well-known problems.

Theorem 4.2.1 ([DL92]) CUBIC BIPARTITE PERFECT MATCHING *is* #P-*complete.*

Theorem 4.2.2 ([Sch78, CH96]) 1-IN-3 SAT *is* NP-*complete and* #P-*complete.*

For convenience and without loss of generality, we will assume that each variable v_k appears unnegated somewhere in the boolean expression. Indeed, if a variable occurs only negated, we may simply replace it by its negation. If v_k does not occur, add the clause $(v_k, \overline{v}_k, f)$, where f is a new variable. The number of satisfying assignments is obviously preserved.

4.3 Proof of Theorem 4.1.3

4.3.1 Reduction construction

We will reduce the counting of perfect matchings in cubic bipartite graphs to the counting of tilings with dominoes. Given a cubic bipartite graph, we want to create a region, such that the number of tilings of the region is the number of perfect matchings of the given graph.

Given two cubes $u, v \in \mathbb{Z}^3$, a *wire* is a sequence of distinct cubes $u = c_1, c_2, \ldots, c_t = v$ in $\mathbb{Z}^3$, such that c_i and c_j are adjacent if and only if $|i - j| = 1$. We call c_1 and c_t the *endpoints* of the wire, $\{c_2, \ldots, c_{t-1}\}$ the *interior*, and t the *length*. A collection of wires is *proper* if no wires intersect the interior of other wires, and any two cubes in the union of the wires are adjacent if and only if they are consecutive elements in (precisely) one such wire.

Let G be a connected graph. We will create a region $\Gamma \subset \mathbb{Z}^3$ representing this graph G as follows. Let $f : V(G) \to \mathbb{Z}^3$ be an injective map, and identify each vertex with its image. For each edge $uv \in E(G)$, we connect $f(u)$ and $f(v)$ by a wire, which is identified with the edge. Let Γ be the union of these wires (and thus contains the vertices). If the collection of the wires is proper, we call Γ a *lattice drawing* of G.

Color the space $\chi : \mathbb{Z}^3 \to \mathbb{Z}_2$ in a checkerboard fashion, and call $\chi(x, y, z) = x + y + z \pmod 2$ the *parity* of $(x, y, z) \in \mathbb{Z}^3$.

Lemma 4.3.1 *Every connected simple graph G with maximum degree at most 6 has a lattice drawing. Moreover, if G is bipartite, it can be drawn with each edge having endpoints of opposite parity.*

Proof. It is obvious that if we pick f so that the images are sufficiently spaced out, we can connect the vertices with proper wires. The maximum degree condition is due to the limitation that a cube has only 6 neighbors. The second part of the lemma is immediate. □

4.3.2 Proof of correctness

Fix a lattice drawing Γ constructed above, and consider a tiling by dominoes. The neighborhood of a vertex is shown in Figure 4.2. The solid blue square represents the vertex, with three emanating wires representing its incident edges.

Consider a wire corresponding to some edge. Since the collection of wires is proper, there are no other cubes adjacent to the interior of this wire. Thus in any domino tiling, the dominoes must tile the wire along its length. Since the endpoints have opposite parity, this wire has even number of cubes. Hence either it is partitioned into dominoes under the tiling,

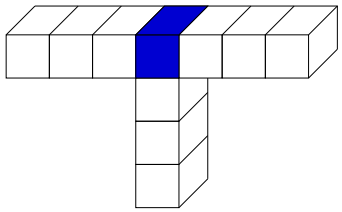

Figure 4.2: A vertex with three incident wires.

or the dominoes it contains are all in its interior, in which case its endpoints are covered by dominoes that are contained in other wires.

Lemma 4.3.2 *If M is the collection of edges in Γ that are partitioned into dominoes, then M is a perfect matching of G.*

Proof. Pick a vertex and consider the domino covering it: that domino is contained in precisely one of the incident edges. Thus for every vertex precisely one incident edge is in M, implying that M is a perfect matching. □

We just extracted a perfect matching of G from a tiling of Γ. Notice that this map is bijective, that is, every perfect matching induces a unique tiling. Indeed, for each edge in the matching, tile the corresponding wires by dominoes covering the endpoints, then finish the tiling in the obvious manner. This means that the number of tilings is exactly the number of perfect matchings, concluding the proof of Theorem 4.1.3.

4.4 Proof of Theorem 4.1.4

4.4.1 Reduction construction

The main idea is to create a large contractible "plate" that admits a unique domino tiling, and then place the construction from the proof of Theorem 4.1.3 adjacent to this plate, while being careful as to not introduce new tilings for the plate. Given a region Γ, a subregion $S \subset \Gamma$ is called *frozen* if it is tiled the same way in all possible tilings of Γ.

We will call the $z = k$ plane *Layer* k. The entire construction of Γ will lie in four layers, from Layer -1 to Layer 2. When considering cubes on a layer, we will employ the usual convention of referring to the $+x$, $-x$, $+y$, $-y$ directions as right, left, above, and below. When referring to an adjacent cube in a different layer, we will specify the layer specifically, as to avoid confusion.

Let us start with a *plate* that lies in Layer 0, which is a region whose columns have even lengths and are offset with each other, causing *jagged* borders. It is obvious that it

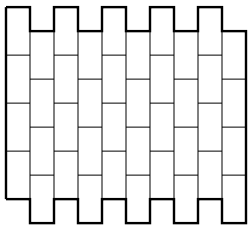

Figure 4.3: A plate with a unique tiling.

admits a unique tiling, which is shown in Figure 4.3. We will modify this plate carefully as to introduce only local changes in the tilings while preserving the unique global tiling.

Suppose we are given a cubic bipartite graph G with bipartition A and B. We will place the vertices in A on the left side of a plate, and vertices in B on the right side. Now we must connect the corresponding vertices with wires. We can achieve the desired connections by interchanging adjacent wires in steps. Indeed, think of the correspondence as a permutation and write it as a product of transpositions. The resulting schematic is known as a *wiring diagram*. These wires will, for the most part, stay in Layer 1. In between each pair of wires, we will add a *tension line*. We then modify the region locally with a *crossover* X*-gadget* at each location indicated in the wiring diagram.

As an example, we see the general picture in Figure 4.4. There is a big plate, with offset columns causing jagged borders on the top and bottom of the region, indicated by the short dashes. There are four vertices, each one with three wires coming out of it, indicated by the

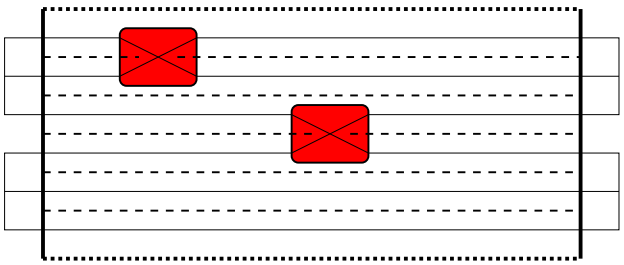

Figure 4.4: Overview of the layout.

solid lines. The tension lines between the wires are indicated by the long dashed lines. The red boxes are the X-gadgets.

The wire and the tension line are shown in Figure 4.5. The schematic is drawn in

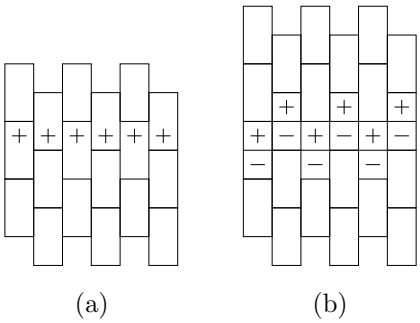

Figure 4.5: A wire (left) and a tension line (right).

Layer 0. The unique tiling of the frozen region in Layer 0 is shown: dominoes that are entirely in this layer are drawn as 2×1 rectangles in the plane. When a $+$ (resp. $-$) sign is present, it means the region includes the adjacent cube in Layer $+1$ (resp. -1).

Here we show half of a vertex V-gadget in Figure 4.6a. A single square in the schematic denotes that the cube in Layer 0 is always tiled with a domino sticking out to Layer 1 or -1. The symbol $\pm$ signifies that the adjacent cubes in both Layers ± 1 are included. The blue circle is the center of the V-gadget, and needs to satisfy positional parity as defined in the proof of the previous theorem. Besides some isolated cubes, Layer 1 contains the wires. Notice that there are three wires coming out of the center of the V-gadget. The third wire that is not drawn completely in the figure should mirror the other wire in the obvious way,

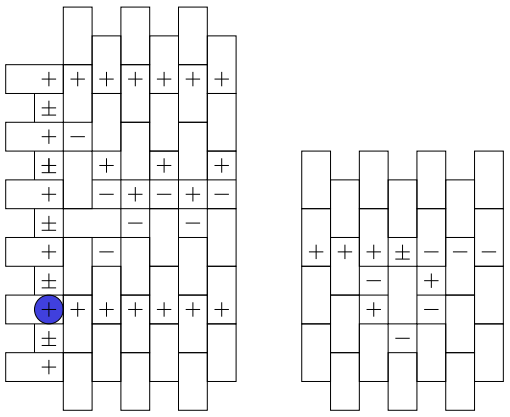

(a) (b)

Figure 4.6: Half of a vertex V-gadget (left) and a hole H-gadget (right).

including the initialization of the tension line. The wires (sequences of +) extend towards the right. Between each pair, we have a tension line (the sequence of jagged + and −). Notice that we can easily make the V-gadgets taller as to have more separation between the wires and tension lines exiting to the right. This will be used to align all these things together correctly. We use the mirror image when putting the V-gadget on the right side of the plate. Between pairs of V-gadgets, we also add tension lines running horizontally across the entire plate.

To make the crossover X-gadget, we combine the hole H-gadget (Figure 4.6b) and the splitter Y-gadget (Figure 4.7). We use the same schematic convention as above in these figures. Here the symbol $\oplus$ denotes that there is a cube in Layer 1, but not in Layer 0. Similarly, symbol $\boxplus$ signifies the inclusion of the cubes on Layers 1 and 2 (in addition to Layer 0). First use the H-gadget to guide the lower wire to Layer -1, and use the Y-gadget to merge and align them together. Then we reverse the process using a rotated copy of the splitter, as to make the wires crossover each other. Finally, bring the wire back to Layer 1 with another H-gadget. This completes the construction of the crossover X-gadget.

It is clear that the X-gadget takes two wires on the left, separated by a tension line, and outputs two wires on the right, again separated by a tension line. Notice that in the construction of the X-gadget, we could make the output wires further away from each other,

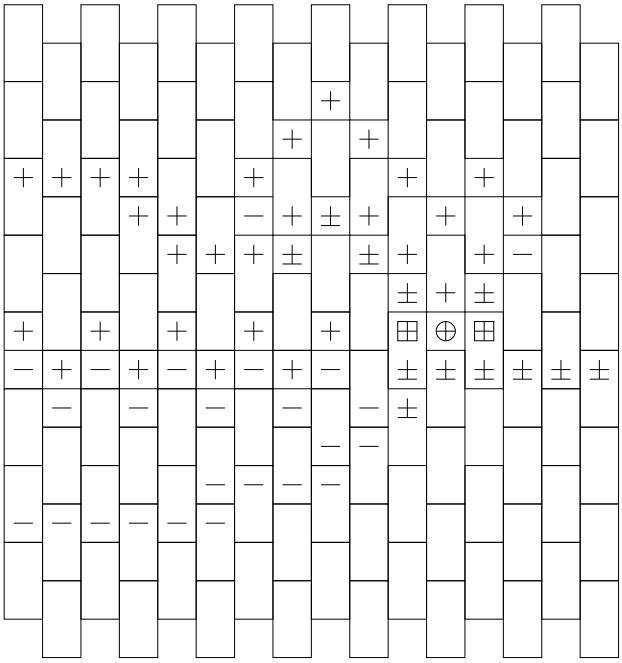

Figure 4.7: A splitter Y-gadget.

which is also the case for the V-gadget, as mentioned above. As such, we could align all these wires and tension lines so they feed into each other perfectly across the entire construction. Thus using X-gadgets, we are able to correctly connect the wires coming from V-gadgets. This complete the construction of the region, which we shall call Γ.

4.4.2 Proof of correctness

It remains to check that Γ is contractible, and its domino tilings are in bijection with perfect matchings in graph G.

Lemma 4.4.1 *The region Γ is contractible.*

Proof. Consider Layer 0. It has a hole for each Y-gadget. However, the adjacent cube in Layer 1 is present, and is contained in a 3×3 region. Furthermore, the adjacent cube in Layer -1 is not present. As such, filling in the hole in Layer 0 does not alter contractibility.

Now that there are no holes in Layer 0, we may deformation retract everything in other layers to Layer 0, and then contract it to a point. □

It remains to find a frozen subregion $\Gamma' \subset \Gamma$ such that $\Gamma_0 = \Gamma \backslash \Gamma'$ is a lattice drawing of the given graph. Let us start with $\Gamma' = \varnothing$ (thus $\Gamma_0 = \Gamma$) and alter Γ' inductively. A cube in a region is *isolated* if it has precisely one neighbor (out of the six adjacent possibilities). Notice that an isolated cube must be tiled by a domino covering its unique neighbor. We will *remove* the isolated cubes of Γ_0 by moving them from Γ_0 to Γ'. We repeat this process inductively until there are no more isolated cubes.

Lemma 4.4.2 *At any step,* Γ' *is a frozen subregion of* Γ*. When the process finishes,* Γ_0 *is a lattice drawing of the given graph.*

Proof. It follows immediately by construction that Γ' is frozen. The rest of this proof is devoted to the second part of the lemma.

Let us perform another induction on the number of X-gadgets. For the base case, suppose we did not have any X-gadgets. That is, we start with the boring cubic graph where disjoint pairs of vertices are joined by three edges each.

Consider each V-gadget. After the first step, everything in Layers 0 and -1 on the two left-most columns in Figure 4.6a are removed, leaving the wire in Layer 1. The tension lines are all removed as well. It is clear that in the next step, the remaining horizontal domino will also be removed, along with the domino above it.

Thus after two steps, what we are left with in Layer 0 is a collection of disconnected plates, each of which has a wire across it horizontally in Layer 1. These wires protrude to the left and right.

Each of these plates have jagged columns thanks to the initial boundary and the tension lines. As such, in each step, the top- and bottom-most cubes are isolated, hence removed with their neighbors, creating another jagged boundary. This process continues until all cubes in Layer 0 are removed, including the ones adjacent to the wire in Layer 1. Note that

half of the cubes adjacent to said wire are removed from above, and the other from below. Thus it is important that both sides were jagged, which is the motivation for introducing the tension lines. We are left with the lattice drawing of the aforementioned contrived cubic graph.

Now for the inductive step, suppose we add an extra X-gadget. We want to show that the global situation is not altered, and that the local situation is what we wanted. Indeed, the X-gadget consists of two H-gadgets and two Y-gadgets. Having analyzed the V-gadget, one should be able to inspect the H-gadget construction in Figure 4.6b, and easily see that after finitely many steps, we will be left with the wires in Layers ± 1, plus the connecting cube between them in Layer 0.

The Y-gadget is a bit more complicated, but can be carefully analyzed in the same manner. Indeed, after the first step, all the cubes in Layer -1 are removed except for the wire. Similarly, the Layers 1 and 2 cubes for $\boxplus$ are removed, so are all the cubes in Layer 1, save the wire. As for Layer 0, we get a small island of six vertical dominoes in the middle, and a giant plate with enough tension lines such that a similar inductive removal process as above will remove it completely. Hence we are left with precisely the wires, thus completing the proof of the lemma. □

4.5 Proof of Theorem 4.1.1 and the first part of Theorem 4.1.5

4.5.1 Reduction construction

Here we reduce 1-IN-3 SAT to a tiling problem. The reduction will be parsimonious, thus proving both NP-completeness and #P-completeness.

Consider a sequence of cubes in the $z = 0$ plane, where two cubes are adjacent if and only if they are consecutive elements in the sequence (this is called a wire in the proof of Theorem 4.1.3). Consider the sequence as a region and duplicate it also in the $z = 1$ plane. We now call a *wire* the union of these two copies. In a wire, a pair of adjacent cubes, one with

$z = 0$ and one with $z = 1$, is called a *cube pair*. In any tiling by slabs, each cube pair must be covered by the same slab. If we translate the wire to the $z = k$ and the $z = k + 1$ planes, we say the wire *lives* in the $z = k$ *biplane*. Color the biplane $\chi(x, y, z) = x + y \pmod 2$ in a checkerboard fashion, ignoring the z-coordinate. We call the color of a cube (pair) its *parity*, which can be *even* or *odd*. Similarly, we may rotate and consider wires living in $x = k$ or $y = k$ biplanes. In those cases, the biplane coloring would ignore the x- or the y-coordinate, respectively. Notice that a cube $(x, y, z) \in \mathbb{Z}^3$ might have different parities depending on the biplane being considered. However, each cube pair lives in a unique biplane: thus the parity of a cube pair is unambiguous. When we draw diagrams consisting of wires in each biplane, we simply draw the two-dimensional regions used to form the wires.

The variable V-gadget, shown in Figure 4.8, is made by removing two diagonal cubes of a $2 \times 2 \times 2$ region, and then attaching six wires. Notice that the wires come in pairs, and

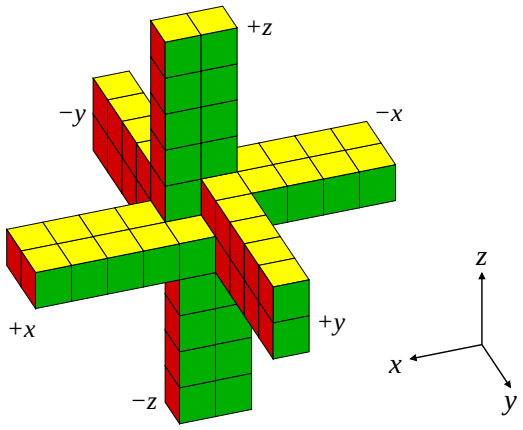

Figure 4.8: A variable V-gadget, with six wires coming out of it.

each pair lives in a biplane. We label the wires with their initial coordinate directions. Each wire has an endpoint in the V-gadget, called the *variable endpoint*; the other one is called the *free endpoint*. We now describe where to place the V-gadgets and how to join these free endpoints together.

Suppose we are given a 3-SAT expression $\mathcal{C} = \{C_1, \ldots, C_t\}$ on the variable set $X = \{v_1, v_2, \ldots, v_n\}$, where each clause $C_i = (c_{i1}, c_{i2}, c_{i3})$ consists of three literals, each either a variable v_k or a negation $\overline{v}_k$, for some $k \in [n] = \{1, \ldots, n\}$. We now construct a region Γ.

If c_{ij} is v_k or its negation $\overline{v}_k$, place a V-gadget at $(10k, 10(3i + j), 0)$. That is, the wires live in the $x = 10k$, $y = 10(3i + j)$, and $z = 0$ biplanes, respectively. Moreover, the variable endpoint of each wire has odd parity with respect to the coloring of the biplane in which the wire lives.

Consider the $x = 10k$ plane for each $k \in [n]$, which is drawn schematically in Figure 4.9. Notice that all the $\pm z$ wires corresponding to the variable v_k are on this biplane. For each

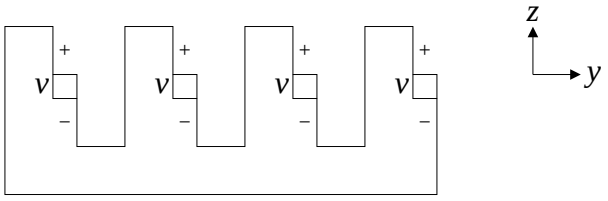

Figure 4.9: Synchronization of variables: This is a diagram in some $x = 10k$ (bi)plane. The squares represent the V-gadgets and the lines represent the wires.

V-gadget, we will bend the $+z$ wire to the left and down as shown. We link up the first wire with the last, and also the remaining adjacent pairs.

Figure 4.10 shows a clause C-gadget, which is simply a joining of three wires. The parity

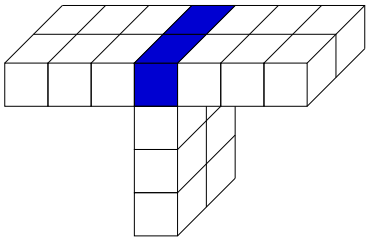

Figure 4.10: A clause C-gadget, where three wires meet.

of the gadget is the parity of the blue cube pair at the center where the three wires meet.

Now let us work in the $z = 0$ biplane, schematically shown in Figure 4.11. For each

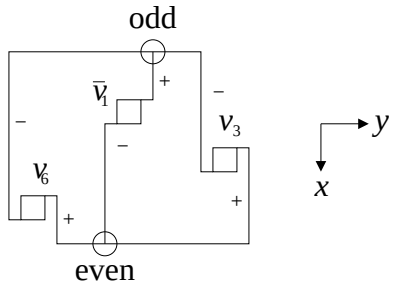

Figure 4.11: Diagram in the $z = 0$ (bi)plane. The circles, where the lines meet, indicate the C-gadgets, which are at two different parities.

clause, there are three corresponding V-gadgets. From each V-gadget, take the $+y$ (resp. $-y$) wire if the corresponding variable appears in the clause unnegated (resp. negated). Extend these three wires to $x = 10(n + 1)$ and join them together at a C-gadget with even parity. Similarly, extend the three remaining $\pm y$ wires to $x = -10$ and join together at a C-gadget with odd parity. We call these the even and odd C-gadgets corresponding to each clause, respectively.

Finally, for each V-gadget, let us join the remaining $+x$ wire and the $-x$ wire together to form a loop.

Lemma 4.5.1 *The wires can be joined together such that no cubes are adjacent unless they are in fact adjacent cubes from a single wire.*

Proof. As the V-gadgets are sufficiently spaced out, it is very obvious that we can make the wires avoid each other, besides when they meet at the V- and C-gadgets. □

This finishes the construction.

4.5.2 Proof of correctness

Fix a region Γ constructed above from a 3-SAT expression $\mathcal{C}$. It remains to show that the tilings of Γ and the 1-in-3 satisfying assignments of $\mathcal{C}$ are in bijective correspondence.

First, consider a tiling of Γ. We say that the *phase* of an endpoint of a wire is *positive* if the wire contains the tile that covers that endpoint, and *negative* otherwise.

Lemma 4.5.2 *A wire of even length has the same phase at both endpoints, while a wire of odd length has opposite phases at its two endpoints.*

Proof. As in the proof of Theorem 4.1.3, the slabs must line up along the length of the wire, since the various wires do not intersect or come near each other (except at the endpoints). □

The following is immediate by observing the way slabs can come together to tile the V-gadget:

Lemma 4.5.3 *There are two ways to tile each* V*-gadget locally. In either tiling, the three $+$ wires have the same phase at their variable endpoints, and the three $-$ wires have the opposite phase at their variable endpoints as the $+$ wires.*

Let the *phase* of the V-gadget be the common phase of the $+$ wires at their variable endpoints.

Lemma 4.5.4 *The* V*-gadgets corresponding to v_k (or its negation $\overline{v}_k$) all have the same phase.*

Proof. Consider two adjacent V-gadgets in the construction shown in Figure 4.9. Suppose the gadget on the left has positive phase (the opposite situation is similar). Then by Lemma 4.5.3, its $-z$ wire has negative phase at the variable end. This wire is linked with the $+z$ wire of the gadget on the right. Since both endpoints have odd parity, the wire has odd length, thus by Lemma 4.5.2, the variable endpoint of the $+z$ wire of the gadget on the right (hence the gadget) has positive phase. □

This allows us to assign a truth value to the variable v_k:

Lemma 4.5.5 *Let the boolean assignment of v_k be the common phase of the* V*-gadgets corresponding to v_k. This defines a* 1*-in-*3 *satisfying assignment.*

Proof. Fix a clause (c_1, c_2, c_3) and consider the corresponding even C-gadget. There are three wires connecting the corresponding V-gadgets to the center of the C-gadget. The variable endpoints of the wires have odd parity, and the free endpoints are all at the center of the C-gadget, which has even parity. As such, the wires have even lengths; thus by Lemma 4.5.2, each wire has the same phase on both its endpoints.

The center of the C-gadget is tiled by some slab, which is contained in precisely one of its three wires. Without loss of generality, suppose only the wire corresponding to c_1 is of positive phase (at both of its endpoints). Recall that the phase of a V-gadget is the phase of its + wires at their variable endpoints. If $c_i = v_k$ is an unnegated variable, then the $+y$ wire was used, and thus v_k (and hence c_i) is positive if and only if $i = 1$. On the other hand, if $c_i = \overline{v}_k$ is a negated variable, then the $-y$ wire was used. Thus v_k is *negative* if and only if $i = 1$, but then c_i is again positive if and only if $i = 1$. □

This shows that the assignment is indeed 1-in-3 satisfying. We thus have a map from the tilings of Γ to the satisfying assignments of $\mathcal{C}$.

For the inverse, suppose we have a 1-in-3 satisfying assignment. Simply tile each V-gadget according to the assignment in the obvious way. It only remain to tile the wires. However, by construction, once we choose the phase of a V-gadget, the tiling of all six wires emanating from that region is forced.

The $\pm z$ wires fit together because the phases of the V-gadgets are consistently assigned, in accordance to the truth value of the variable in the given satisfying assignment.

Recall that for each V-gadget, its $+x$ and $-x$ wires form a loop. Since the two endpoints both have odd parity, the length of the wire is odd. By Lemma 4.5.2, the two endpoints have opposite phases in a tiling, which is precisely what the V-gadget would produce as in Lemma 4.5.3.

It is obvious that the $\pm y$ wires fill up the even C-gadgets perfectly because the boolean assignment was 1-in-3 satisfying. For the odd C-gadgets, notice that since we take the leftover wires, precisely one of the three is *negative* at its variable endpoint. However, since we join

them at a cube pair with odd parity, the wires are of odd lengths, thus precisely one of the three is positive on the free endpoint at the C-gadget, as needed.

This establishes the desired bijective correspondence, and implies that the construction is indeed a parsimonious reduction from 1-IN-3 SAT to the slab tiling problem, concluding the proof of Theorem 4.1.1. Note that this also implies that the associated counting problem is #P-complete, yielding the first part of Theorem 4.1.5; in the next section we prove a stronger result.

4.6 Proof of Theorem 4.1.2 and the second part of Theorem 4.1.5

4.6.1 Reduction construction

Given a region Γ_0 as constructed from the previous section, we will enlarge it to a contractible region $\Gamma \supset \Gamma_0$, such that $\Gamma' = \Gamma \backslash \Gamma_0$ is a frozen subregion of Γ.

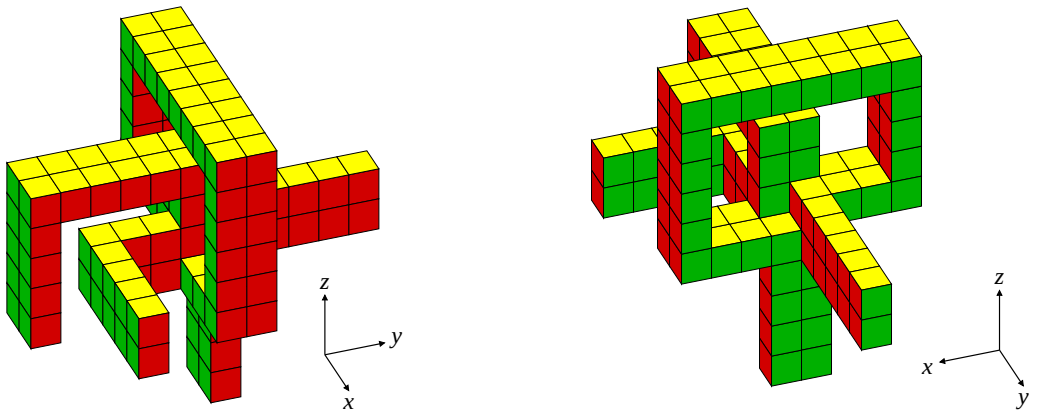

Figure 4.12: A variable V-gadget, shown in two perspectives.

First we modify the variable V-gadget. The following description is relative to a V-gadget placed at $(0, 0, 0)$. We must make these adjustments to each V-gadget used. Recall that in the proof of Theorem 4.1.1, each $+z$ wire was bent as in Figure 4.9. Let us make this precise by making it bend towards the $-y$ direction when it hits $z = 3$, and bend towards $-z$ when it hits $y = -5$ (see Figure 4.12). We define a region X, shown in Fig-

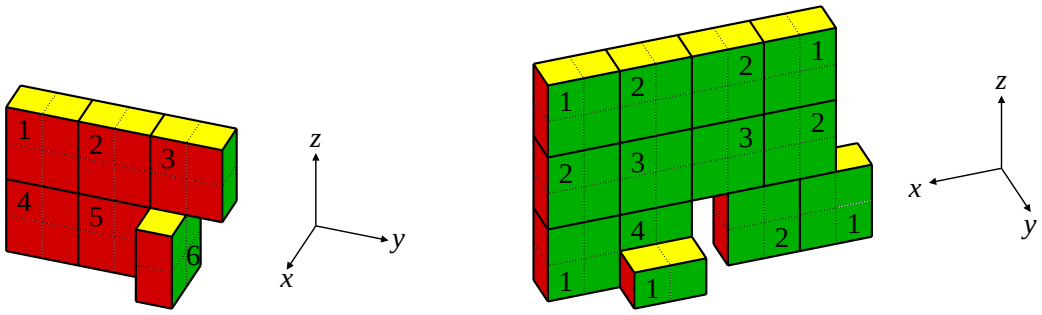

(a) Region X. (b) Region Y.

Figure 4.13: Regions used to modify the V-gadget.

ure 4.13a, that will fill the hole this loop makes. Indeed, let $X = \{-1\} \times [-5, 0] \times [0, 3] \cup \{(0, -1, 0), (0, -1, 1)\} \backslash \{(-1, 0, 0), (-1, 0, 1)\}$. The unique tiling is indicated in the figure; the labels will be used in the proof of Lemma 4.6.2. Similarly, the $\pm x$ wires are linked together to form a loop. Let us bend them towards the $+z$ direction when they hit 4 and -3, respectively, and bend towards each other when they hit $z = 5$. Define a region that will fill this hole, shown in Figure 4.13b: Take

$$[-3, 4] \times \{2\} \times [0, 5],$$

add the following six cubes

$$(-4, 2, 0), (-4, 2, 1), (1, 3, 0), (2, 3, 0), (1, 1, 1), (2, 1, 1),$$

and remove these two cubes

$$(0, 2, 0), (0, 2, 1).$$

Call this region Y. Note that the slab labeled 4 in the figure extends behind and is hidden from view. We will add regions X and Y to the V-gadget. This makes the V-gadget contractible.

Let $Z = [-10, 10n + 11] \times [0, 30(t + 1) + 1] \times \{-1\} \subset \mathbb{Z}^3$, where n and t are the number of variables and clauses, respectively. We then modify Z with a *hole* H*-gadget* around each V-gadget to allow its $\pm z$ wires to pass through. Indeed, Figure 4.14 shows the construction

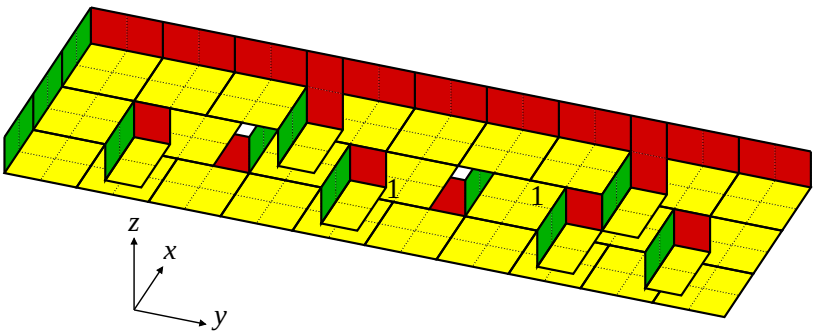

Figure 4.14: A hole H-gadget.

in the $z = -1$ plane viewed from below. The surrounding slabs on the boundary match that of the unique tiling of Z. The two cube pairs missing allow the $\pm z$ wires to pass through (spaced out according to the precise construction of the V-gadget in Figure 4.12). The cube pairs in $z = -2$ plane are necessarily tiled with its unique neighbor in the $z = -1$ plane. Let $X_k = \{10k - 1\} \times [0, 30(t + 1) + 1] \times [-9, -2]$ for each $k \in [n]$. Here we assume that the linking of the $\pm z$ wires (see Figure 4.9) are done at z-coordinates, say, -5 and -7, which are in $[-9, -2]$. Let Γ' be the disjoint union of the X and Y for each V-gadget, the region Z, and the X_k for each k. This finishes the construction.

4.6.2 Proof of correctness

It remains to check that that the construction works. The following two lemmas easily imply the result.

Lemma 4.6.1 *The region Γ constructed above is contractible.*

Proof. Notice that there are no holes in the $z = -1$ plane. In $z < -1$, we may deformation retract the wires onto the X_k plates, and then deformation retract these plates onto the $z = -1$ plane.

We now check that the modified V-gadget is contractible. The center of an original V-gadget was an example of a non-contractible region shown in Figure 4.1. Indeed, the interior will leave a point hole in the middle; however, it is filled by the slab labeled 4 in

Figure 4.13b. The loop formed by the $+z$ wire bending down is filled by X, while the loop formed by joining the $\pm x$ wires is filled by Y. Moreover, the $\pm y$ wires are all lying along Z so we may deformation retract everything to the $z = -1$ plane. We omit the (easy) details. □

Lemma 4.6.2 *The subregion $\Gamma' \subset \Gamma$ is frozen.*

Proof. Consider a cube $c \in \Gamma$. If it forms a $3 \times 1 \times 1$ region with a cube pair, then no slab containing this cube may contain its neighbor that is part of the cube pair. Not counting such cube pairs, if c only has two neighbors left, then c must be tiled by a slab covering both these neighbors. If this happens, we call c *isolated* and say that it *forces* the unique slab containing c. Just like in the proof of Theorem 4.1.4, we may inductively remove these forced slabs, which are obviously frozen.

Consider region X_k. Notice that the cube at the corner $(10k-1, 1, -9)$ is isolated. After removing the slab forced by it, we may consider the new corner next to it at $(10k-1, 3, -9)$. Inductively, we may remove the cubes with $z = -9$ or -8. Now when looking at $z = -7$, we may run into cubes that neighbor $\pm z$ wires. However, these wires are made of cube pairs that form $3 \times 1 \times 1$ regions with the cubes in question. As such, we may continue the removal process unhindered. It is clear that in this manner, we may remove all cubes from X_k.

Similarly, we remove most slabs from Z, starting from the boundary and working our way in. The ones sticking down out of the $z = -1$ plane can also be removed, leaving us with precisely two slabs around the hole for the $-z$ wire from the H-gadget (labeled with 1 in Figure 4.14). As for each V-gadget, we remove all the cubes from X and Y. In Figure 4.13, the forced slabs are labeled with a sample removal order, where each number is positioned on the isolated cube used at each step. Finally, we may remove the leftover slabs from Z. □

Now, given a 1-IN-3 SAT expression $\mathcal{C}$, we may take a region Γ_0 constructed in the proof of Theorem 4.1.1 and enlarge it to a contractible region Γ as described above. Since $\Gamma' = \Gamma \backslash \Gamma_0$ is frozen, Γ is tileable if and only if Γ_0 is tileable. These are tileable if and only if $\mathcal{C}$ is 1-in-3 satisfiable, thus Theorem 4.1.2 is proved. Moreover, since both reductions are parsimonious, we conclude the second counting result in Theorem 4.1.5 as well.

4.7 Generalized dominoes in higher dimensions

Let $\mathcal{D}_r^d \subset \mathbb{Z}^d$ be a $2 \times \ldots \times 2 \times 1 \times \ldots \times 1$ region with r number of 2's and $d-r$ number of 1's. We call this a *generalized domino* in d dimensions of rank r. Call the r coordinate directions that are 2 cubes wide *fat*. Previously we were concerned with tiling by dominoes $\mathcal{D}_1^3$ and slabs $\mathcal{D}_2^3$ in three dimensions.

Theorem 4.7.1 *For $2 \leq r < d$, tiling (contractible) d-dimensional regions with $\mathcal{D}_r^d$ is* NP*-complete. Similarly, for $1 \leq r < d$ and $d \geq 3$, tiling (contractible) d-dimensional regions with $\mathcal{D}_r^d$ is* #P*-complete.*

Note that in other cases of r and d, these problems are in P (see next section).

Proof. We reduce specific tiling problems in $\mathbb{Z}^3$ to higher dimensions. Let us first prove the statements without the contractibility constraint.

Suppose $2 \leq r < d$. Let $\Gamma \subset \mathbb{Z}^3$ be a region as afforded by the proof of Theorem 4.1.1. Let $\Gamma' = \Gamma \times \{0,1\}^{r-2} \times \{0\}^{d-r-1}$, that is, $\{(x_1, \ldots, x_d) \in \mathbb{Z}^d : (x_1, x_2, x_3) \in \Gamma,\ x_4, \ldots, x_{r+1} \in \{0,1\},\ x_{r+2} = \ldots = x_d = 0\}$. Consider a tiling of Γ' by $\mathcal{D}_r^d$. Notice that there are no $2 \times 2 \times 2$ subregion in Γ, thus each tile must be oriented with two of its fat directions in the first three coordinates, the remaining $r-2$ fat directions in the next $r-2$ coordinates. This means that any $\mathcal{D}_r^d$-tiling of Γ' induces a $\mathcal{D}_2^3$-tiling of Γ. It is easy to see that this correspondence is actually a bijection, finishing the proof of NP-completeness, and also #P-completeness when $r \geq 2$.

The case of $r = 1$ is straightforward. Take Γ from the proof of Theorem 4.1.3. Define $\Gamma' = \Gamma \times \{0\}^{d-3}$, and follow the argument above.

To prove the result for contractible regions, proceed in the same manner, and take the regions constructed in the proof of the corresponding theorems. For $2 \leq r < d$, take the region Γ from the proof of Theorem 4.1.2, and define Γ' in the same way as above. Notice, however, that the above strategy does not yield a reduction from $\mathcal{D}_2^3$-tilings to $\mathcal{D}_r^d$-tilings in general. Indeed, we used the fact that the specific $\Gamma \subset \mathbb{Z}^3$ did not contain $2 \times 2 \times 2$

subregions, which is no longer the case. The outlined argument actually still works, but more care must be taken. A tile might now be oriented with three of its fat directions in the first three coordinates. This means a $\mathcal{D}_r^d$-tiling of Γ' will, *a priori*, induce a tiling of Γ with slabs and the $[2 \times 2 \times 2]$ cube. However, in the proof of Theorem 4.1.2, we see that no tilings of Γ by slabs contain a $2 \times 2 \times 2$ subregion tiled by two slabs. As such, all $\mathcal{D}_r^d$ tiles in Γ' are still constrained to be oriented as before, with precisely two fat directions in the first three coordinates. This implies the result in this case.

The same approach works for the $r = 1$ case as well. Take Γ as in the proof of Theorem 4.1.4, and define Γ' as above. Now notice that in any tiling of Γ, there is no $2 \times 2 \times 1$ subregion of Γ that is tiled by two dominoes, which proves the result. □

4.8 Final remarks and open problems

4.8.1

Historically, the tiling problems played a crucial role in the developments of modern theoretical computer science. The tileability of the whole plane with a set of tiles was shown to be undecidable [Ber66, Rob71]. A version of the finite tileability problem was stated to be NP-complete in Levin's original paper [Lev73], where he (independently) defined NP-completeness. Finally, Theorem 4.1.3 is one of the first few applications of #P-completeness, developed by Valiant [Val79b].

4.8.2

In the context of statistical physics, the domino tiling problem is called the *dimer problem*, and has a long history. The classical results of Fisher [Fis61] and Kasteleyn [Kas61] express the number of domino tilings of finite regions in the plane as a certain Pfaffian, equal to a square root of a determinant. A closely related *monomer-dimer model* is #P-complete already in the plane [Jer87] (see also [Vad01]). Let us mention that both models can be

polynomially approximated (see [JSV04, KRS96]). We refer to [Tho06] for graph-theoretic reasons precluding the Pfaffian method in higher dimensions, and to [DG00, HK81] (see also [HN04]) for the general hardness results on *graph homomorphisms*, a concept generalizing perfect matchings.

4.8.3

In the *general tileability problem*, a set $\mathbf{T}$ of tiles is fixed, and one considers tilings with parallel translations of copies of tiles $T \in \mathbf{T}$. For a single tile T, the tileability problem is a special case, where $\mathbf{T}$ consists of all reflections and rotations of T. Let us briefly elaborate on the state of art of these tiling problems as they pertain to our results.

In the plane, when $|\mathbf{T}| = 1$, *i.e.*, when translates of a single tile are used, the tileability problem is linear in the area. However, already for $\mathbf{T} = \{2 \times 1, 1 \times 3\}$, the tileability is NP-complete [BNRR95]. It is not known whether the corresponding counting problem is #P-complete. The smallest set $\mathbf{T}$ for which #P-completeness is known is the set of four rotations of the L-tromino and a $[2 \times 2]$ square [MR01].

For simply connected regions in the plane, we recently found a set of 23 Wang tiles, which they showed to be NP-complete and #P-complete (see Chapter 2). This construction can be further decreased to 15 tiles (Lemma 3.1.1), and we conjecture that only three rectangles suffices (see Subsection 2.7.5). In contrast to the decision problem, it is still unclear how much the simple connectivity of regions helps counting the number of tilings, other than making the reductions harder and more technical.

4.8.4

In [Val79a], Valiant's goal is to show the hardness of the number of perfect matchings of grid graphs, defined as subgraphs (of the unit distance graph) of $\mathbb{Z}^3$. This is slightly weaker than the hardness of domino tilings of 3-dim regions, since the latter problem corresponds to *induced* subgraphs of $\mathbb{Z}^3$. However, Valiant's proof can be slightly modified, from subgraphs

of $[2 \times n \times n]$ to induced subgraphs of $[3 \times n \times n]$, to achieve the same goal. The proof we present in Section 4.3 is in fact a variation of the argument in [Val79a].

4.8.5

For tiling in three dimensions, we consider the domino and the slab. Here each tile has three distinct orientations. If we only allow two out of the three orientations in either case, each problem becomes equivalent to the ordinary domino tiling problem in two dimensions, and hence is in P. Of course, two orientations suffices for the tromino tile $I_3 = [3 \times 1 \times 1]$ (or the $[3 \times 3 \times 1]$ tile) to guarantee NP-completeness, since we have NP-completeness for the $[3 \times 1]$ tile.

Note that the *augmentation approach*, mentioned in the introduction, allows us to show the NP-completeness of the tileability problem with I_3 of contractible regions in $\mathbb{R}^3$. To see this, start with a flat region and color the holes in a checkerboard fashion. Now fill each unit cube with an up or down vertical tromino, depending on the color (see Figure 4.15). The contractible region thus obtained is tileable with I_3 if and only if the starting region is tileable by $[3 \times 1]$.

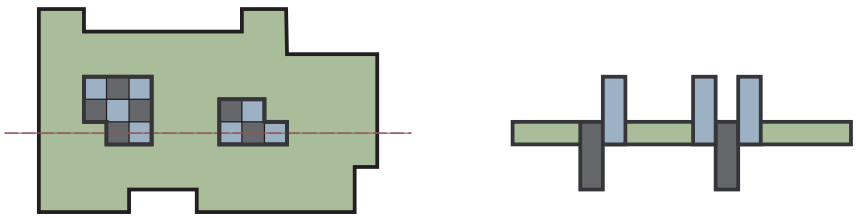

Figure 4.15: A construction of contractible 3-dim regions for tromino tilings.

4.8.6

The conditions in Theorem 4.7.1 are best possible. Indeed, if $r = 0$ or $r = d$, we are tiling with cubes of side length 1 or 2, respectively, both of which are linear in the volume. The

only remaining cases are the decision problem with $\mathcal{D}_1^d$, and the counting problem of ordinary dominoes in dimension $d = 2$, both of which are in P (see *e.g.* [LP09]).

4.8.7

The idea of graph embedding into a grid is quite standard. In this context of domino tilings it was used in [DKLM10, Val79a], and for other small sets of tiles in [BNRR95, MR01] and Chapter 2. Of course, the technical details are somewhat different in each case.

4.8.8

It would be interesting to see if Theorem 4.1.4 holds for contractible regions inside a $[2\times n\times n]$ brick, as they have a rather simple geometric structure. Our proof gives only a width 4 bound, but we believe that a width 3 modification can be made without difficulty. We should mention that for every fixed c, the counting problem is polynomial for regions inside a $[c \times c \times n]$ brick.

4.8.9

In the plane, there are several other generalizations of domino tilings. Notably, *ribbon tilings* was introduced and studied (see [Pak03]). Another interesting set of generalized dominoes $\mathbf{T}_n = \{2^k \times 2^{n-k}, 0 \le k \le n\}$ was studied in [Kor04]. Both sets satisfy the *local move* property: every two tilings of a s.c. region Γ can be obtained by a sequence of *flips*, each involving a fixed number of tiles (2 in both cases, see [Pak03]). For the (usual) domino tilings this is a classical property going back to Kasteleyn and famously proved by Thurston via the *height functions* [Thu90].

Of course, for the domino tilings of general regions there is no local move property, as large cycles can involve an unboundedly many tiles. However, for contractible regions, one would naturally assume that domino tilings and slab tilings are connected by flips corresponding to

different tilings of $[2 \times 2 \times 2]$. This is, in fact, false. As an early prequel to the constructions in the proofs of theorems 4.1.2 and 4.1.4, we state the following easy result.

Proposition 4.8.1 *Domino tilings of contractible regions in* $\mathbb{R}^3$ *does not have the local move property. The same result holds for slab tilings.*

The proof is apparent from Figure 4.16 (cf. Figure 4.15). In the first case, the middle dominoes alternate between up and down. In the second case, slabs are all vertical, with the middle slabs all one layer below.

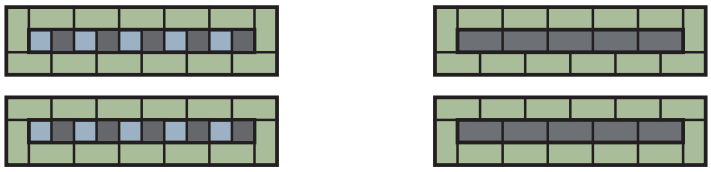

Figure 4.16: Cross sections of large regions in $\mathbb{R}^3$ with exactly two tilings, by dominoes and by slabs, respectively.

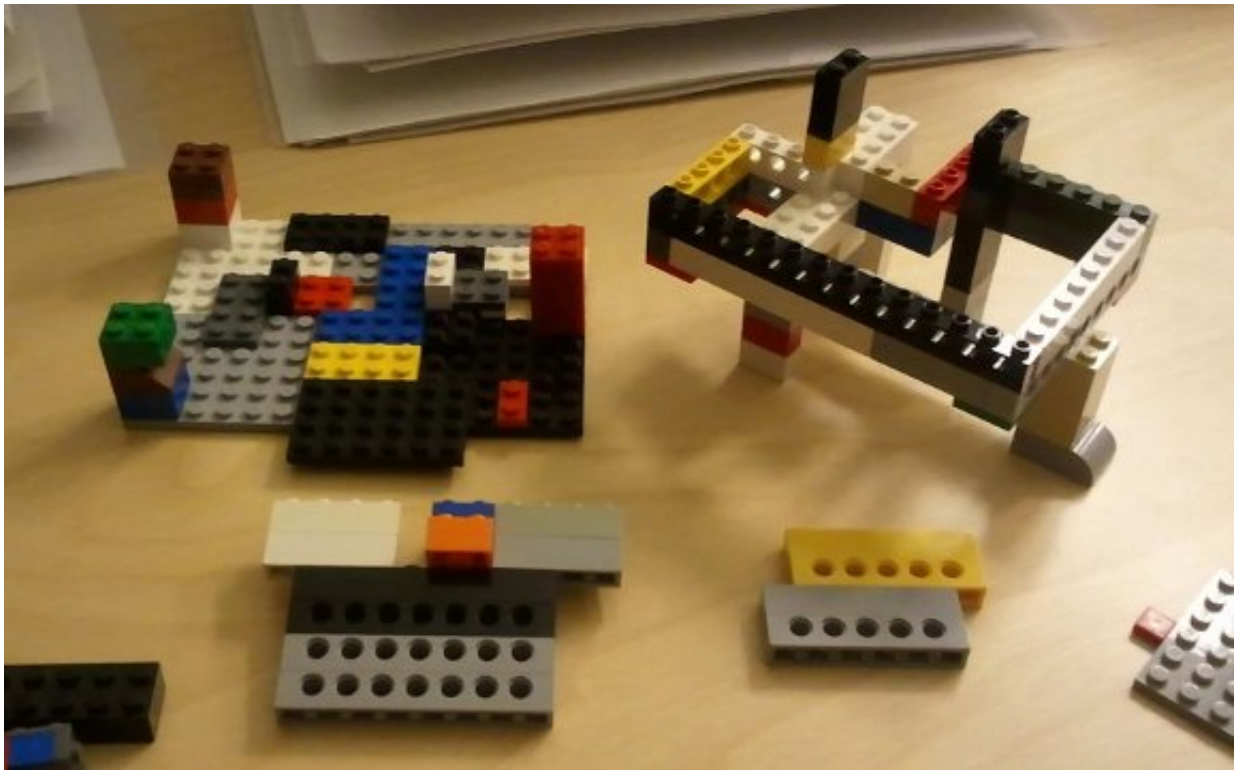

Figure 4.17: Using LEGO bricks to help with visualization.

CHAPTER 5

Rectangular tileability and complementary tileability are undecidable

Does a given set of polyominoes tile some rectangle? We show that this problem is undecidable. In a different direction, we also consider tiling a cofinite subset of the plane. The tileability is undecidable for many variants of this problem. However, we present an algorithm for testing whether the complement of a finite region is tileable by a set of rectangles.

5.1 Introduction

Tileability on the plane has been a subject of much study [GS87]. A lot of focus was in tilings on the square grid by polyominoes [Gol65], including establishing NP-completeness [Lew78, MR01] and finding efficient algorithms when possible [KK92, Rém05]. Aperiodicity in tilings of the entire plane has also been well studied [Moz97, Pen74], with connections to ergodic theory [Rad99, CR98] and quasicrystals [DS99]. Recently, a single (disconnected) tile that exhibits aperiodic behavior was found [ST11], partially settling a famous open problem.

Can the plane be tiled using translated copies of a given set of polyomino tiles? Berger showed that this decision problem is undecidable [Ber66], meaning that there is no general algorithm that can always answer this question from the input. This implies that there exists *aperiodic tilesets*, *i.e.*, tiles that can *only* tile the plane without translational symmetry. Indeed, Berger provided an aperiodic tileset of 20426 tiles, and Robinson reduces this number to 6 if rotations and reflections are allowed in addition to translations [Rob71]. This disproves a conjecture of Wang (see Subsection 5.7.4).

To have aperiodicity and undecidability, clearly the complexity of tiles and tilings must increase without bound. The following result shows that one can encode this complexity in a single tile alone.[1]

Theorem 5.1.1 (Complementary Tileability) *There is a tileset* $\mathbf{T}$ *such that it is undecidable whether the complement of a finite input region* Γ *is tileable by* $\mathbf{T}$*.*

Instead of tiling the entire plane or a cofinite subset, we also consider tiling finite regions. If a rectangle is tileable, then of course the plane is tileable. Thus the following is a variation of the result above.

Theorem 5.1.2 (Rectangular Tileability) *It is undecidable whether a given tileset* $\mathbf{T}$ *can tile* some *rectangle.*

This should be contrasted with tiling a given rectangle by a fixed tileset:

Theorem 5.1.3 ([LMP05]) *Tileability of an* $[n \times m]$ *rectangle by a fixed tileset can be determined in time* $O(\log n + \log m)$*.*

We discuss this connection and some curious consequences of Theorem 5.1.2 in Subsection 5.7.2. It is worth noting that if we are given a finite region to tile as opposed to the entire plane, the problem is decidable simply with exhaustive search (see Subsection 5.7.1 for results in this finite setting). However, although the region to be tiled in Rectangular Tileability is finite, the problem is (potentially) undecidable as the finite region is unspecified. That is, we are tiling a finite object from an infinite collection. Indeed, Theorem 5.1.2 shows that Rectangular Tileability is undecidable. We prove this in Section 5.3, where we moreover show that the problem remains undecidable when the size $|\mathbf{T}|$ of the tileset is fixed. Also, as a corollary, we see that tileability of a unit square by finitely many similar copies of tiles (where rotations, reflections, and dilations are allowed in addition to translations) is also undecidable.

[1] We require that this tile be used precisely once. To that end, we consider it as an input and tile its complement by a fixed tileset.

In Section 5.6, we prove undecidability for AUGMENTABILITY, where we are to *augment* a finite simply connected region Γ by tiles so that the union is tileable. Any augmentable region Γ by the (horizontal and vertical) dominoes must necessarily be *balanced*, *i.e.*, has the same number of black and white squares when the plane is colored as a checkerboard. Korn showed that this is not sufficient, and also proved that Γ is augmentable if it is *row-convex*, *i.e.*, each horizontal row forms a single contiguous region [Kor04, §11]. This should be compared with Theorem 5.1.4 below.

Usually once a result is established for a decision problem with several inputs, one may consider fixing some of these inputs and aim to obtain the same conclusion. To that end, we fix the tileset and instead let the region vary as the input of TILEABILITY. However, decidability makes sense only if the input is finite, yet the region is infinite. As such, in Section 5.4, we consider some variations of tiling cofinite regions. Though most of these problems are undecidable, in the positive direction, we provide an algorithm for TILEABILITY of cofinite regions by arbitrary sets of rectangular tiles.

Theorem 5.1.4 *It is decidable whether the complement of a given finite region* Γ *is tileable by a given tileset* $\mathbf{T}$ *consisting only of rectangles.*

In contrast, we show in Section 5.5 that TILEABILITY of *indented quadrants* by rectangles is undecidable.

5.2 Basic definitions

We call a subset of $\mathbb{Z}^2$ a *region*. By identifying $\mathbb{Z}^2$ as a union of closed unit squares in $\mathbb{R}^2$ centered at the integer lattice points, a region takes on a geometric *shape* in the obvious manner. We freely switch between viewpoints when convenient.[2] We say a finite region is an (*polyomino*) *tile* if its shape is simply connected (s.c.). A finite collection of tiles is called a *tileset*. Note that $\mathbb{Z}^2$ acts naturally on a tile by translation. Given a region Γ and a tileset

[2]For example, *finite* and *disjoint* refer to regions as subsets of $\mathbb{Z}^2$, so the shapes of disjoint regions (*e.g.*, tiles in a tiling) may intersect on their boundaries, but *simply connected* refers to the shapes of regions.

T, a **T**-*tiling* is a partition of Γ into translated copies of tiles in **T**. A region is **T**-*tileable* if it admits a **T**-tiling. When the tileset **T** is understood, we may suppress the prefix for notational convenience.

The *boundary* of (the shape of) a tile consists of unit-length horizontal and vertical *edges*. A (*generalized*) *Wang tile* is a tile whose edges are labeled with symbols that are referred to as *colors*. When tiling with Wang tiles, incident edges must be the same color. When a Wang tile is a single square, it is also called a *Wang square*.[3]

Consider the following decision problem:

TILEABILITY

Instance: A tileset **T** and a region Γ.

Decide: Does Γ admit a **T**-tiling?

Berger proved that TILEABILITY for Wang squares is undecidable when $\Gamma = \mathbb{Z}^2$ is the whole plane [Ber66]. By straight-forward reductions (see Lemma 2.3.1), most problems involving tileability of polyominoes, generalized Wang tiles, and Wang squares are equivalent. In this chapter we will consider a few other tileability problems that are undecidable. We will usually state theorems for polyominoes, but prove them (first) for Wang tiles, then appeal to the reductions in the appendix.

5.3 Rectangular tileability

Here we consider the decision problem RECTANGULAR TILEABILITY, where the input is a tileset and the region to be tiled is unspecified.

RECTANGULAR TILEABILITY

Instance: A tileset **T**.

Decide: Does there exist *some* rectangle that is tileable by **T**?

[3] In the literature, a *square Wang tile* is usually simply called a *Wang tile* and sometimes called a *domino* despite being a single square.

By an *alphabet* Σ we mean a set of symbols, whose elements could be juxtaposed to form *words*. Let Σ^* denote the set of all finite words in the alphabet Σ. The POST CORRESPONDENCE PROBLEM is a well-known undecidable decision problem:

PCP

Instance: An alphabet Σ, positive integer n, and words $j_t, k_t \in \Sigma^*$ for $t \in [n]$.

Decide: Does there exist a positive integer d and $e_i \in [n]$ for $i \in [d]$, such that the concatenated words $j_{e_1} j_{e_2} \dots j_{e_d}$ and $k_{e_1} k_{e_2} \dots k_{e_d}$ are the same?

Theorem 5.3.1 ([Pos46]) PCP *is undecidable.*

Given a PCP instance I, we will construct a tileset $\mathbf{T}$ such that $\mathbf{T}$ tiles some rectangle if and only if I admits a solution, and thus proving Theorem 5.1.2.

Lemma 5.3.2 *Given a* PCP *instance I, there is a computable*[4] *tileset $\mathbf{W}$ of generalized Wang tiles such that $\mathbf{W}$ tiles a white rectangle if and only if I admits a solution.*

Proof. For each $j_t = x_1 x_2 \dots x_r \in \Sigma^*$, create a $1 \times r$ tile J_t whose top boundary edges are all colored U, the bottom color sequence is $(x_1, t), x_2, \dots, x_r$, and the vertical sides are colored V. Similarly for $k_t = y_1 y_2 \dots y_s \in \Sigma^*$, create a $1 \times s$ tile K_t whose top boundary is $(y_1, t), y_2, \dots, y_s$, the bottom colored D, and the vertical sides are colored V (Figure 5.1). For each $x \in \Sigma$ and $t \in [n]$, create the following six *transmitter tiles* in Figure 5.2. Finally, add in the *border tiles* in Figure 5.3, which are the only ones with *white* (unlabeled) colors. This finishes the construction of the tileset $\mathbf{W}$.

If I has a solution $e_1, \dots, e_d$, we first put $\mathsf{J}_{e_1}, \mathsf{J}_{e_2}, \dots, \mathsf{J}_{e_d}$ in a row on top, $\mathsf{K}_{e_1}, \mathsf{K}_{e_2}, \dots, \mathsf{K}_{e_d}$ in a row on the bottom. If we view the color (x, t) as x, then the bottom of the top row and the top of the bottom row have the same color sequence. The transmitter tiles allow "shifting" the tag t to the left or right one step at a time until they match up as well. We

[4]The main proof technique of undecidability is by reducing a known undecidable problem to the current problem. This transformation must be done in a computable manner, *i.e.*, by a deterministic algorithm. Thus *computable* means that the existence of the object in question can be substantiated by an explicit construction.

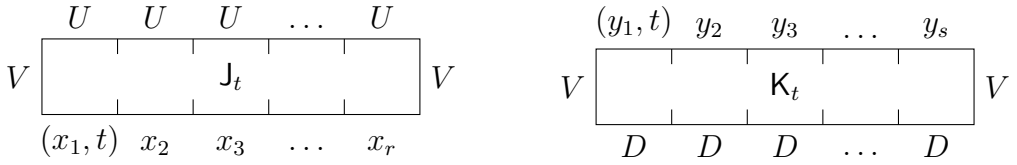

(a) Tile J_t. (b) Tile K_t.

Figure 5.1: PCP tiles.

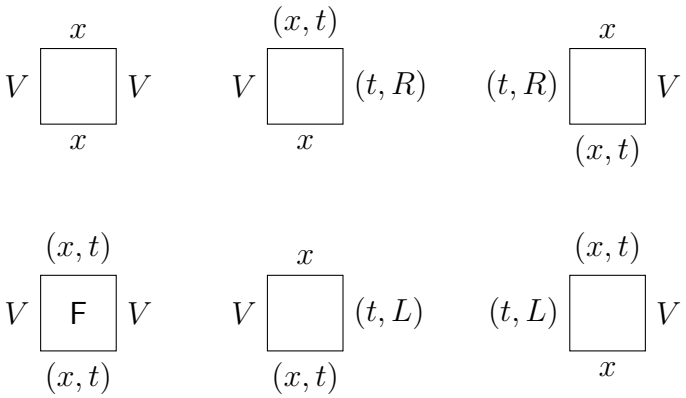

Figure 5.2: Transmitter tiles.

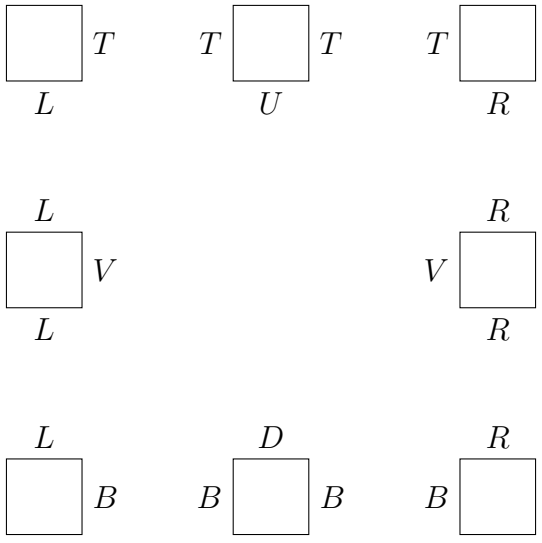

Figure 5.3: Border tiles.

thus have a rectangle with the top and bottom colored U and D, respectively, while the vertical sides are colored V. Notice that the border tiles can tile a rectangular border of any size, whose outside boundary is white, and the inside colors match exactly what we have.

Conversely, suppose $\mathbf{W}$ tiles a white rectangle. Consider the smallest white rectangle it can tile. The border tiles occur only on the boundary. Indeed, if there is any border tile in the interior, by construction, it must form a white rectangular frame with filled interior, a contradiction to the minimality. Now remove the border tiles on the boundary, the top (resp. bottom) row must be a sequence of J_t (resp. K_t) tiles. Let $e_1, \ldots, e_d$ be the indices of the top sequence. By construction of the transmitter tiles, the bottom sequence share the same indices. Furthermore, viewing the color (x, t) as x, the color sequences are the same. This means that the concatenated words coincide, and we indeed extracted a solution to I. □

Corollary 5.3.3 *Given a* PCP *instance I, there is a computable tileset $\mathbf{T}$ of polyominoes such that $\mathbf{T}$ tiles a rectangle if and only if I admits a solution.*

Proof. Take the set $\mathbf{W}$ of generalized Wang tiles afforded by Lemma 5.3.2, and transform it to a set $\mathbf{T}$ of polyomino tiles using Lemma 2.3.1 with a minor change. In the construction, we will replace the color white by a straight boundary, including the omission of the corner zig-zags.

If I admits a solution, then there is a tiling of a white rectangle by $\mathbf{W}$. Replace each Wang tile by its corresponding polyomino in $\mathbf{T}$. By construction, they fit together to form a tiling of a rectangle by $\mathbf{T}$.

Conversely, suppose $\mathbf{T}$ tiles some rectangle. Consider the smallest rectangle tileable by $\mathbf{T}$ and fix one such tiling. Note that the only tiles that can touch the boundary of the rectangle are the border tiles (*i.e.*, those tiles in $\mathbf{T}$ that correspond to the border tiles in $\mathbf{W}$), lest there be small holes that cannot be filled. Conversely, the border tiles cannot occur in the interior by minimality, since they always form rectangular frames. We have replicated the exact same situation as in the proof of Lemma 5.3.2, allowing us to extract a minimal Wang tiling of a white rectangle, and thus a solution to I, as desired. □

This concludes the proof of Theorem 5.1.2. Moreover, we can allow the pieces to be rotated, reflected, or even dilated.

Corollary 5.3.4 *It is undecidable whether a tileset* $\mathbf{T}$ *can tile a unit square with finitely*[5] *many similar copies of its tiles.*

Proof. We claim that the specific tiles $\mathbf{T}$ in the proof of Corollary 5.3.3 tile a rectangle by translation alone if and only if it admits a similar tiling of the unit square.

Suppose $\mathbf{T}$ tiles some $[a \times b]$ rectangle by translation. By repeating the rectangle ab times, we have a tiling of an $[ab \times ab]$ square. Dilating, we obtain a similar tiling of the unit square.

Conversely, suppose $\mathbf{T}$ admits a similar tiling of the unit square. Let S be the union of all tiles with the minimum scaling factor. All the corner zig-zag of tiles in S must be matched by other tiles of the same scaling factor. As such, all tiles that touch the boundary of S must be border tiles. In the proof of Lemma 2.3.1, we note that the interlocking corner zig-zags force all tiles to have the same orientation. This works even when we removed the corner zig-zags for the white edges. In this case, each border tile must be part of a rectangular frame with all its border tiles in the same orientation. Since there are finitely many rectangular frames, there exists one without border tiles within. This rectangular frame is fully tiled in its interior by tiles at this minimum scaling factor. Indeed, if there were any gaps, that would be a boundary of S, a contradiction. Finally, note that all tiles in this rectangular region has the same orientation. Thus $\mathbf{T}$ tile some rectangle by translation alone, as desired. □

Theorem 5.1.2 remains true even if the number of tiles is bounded.

Theorem 5.3.5 Rectangular Tileability *with* 19 *tiles is undecidable.*[6]

[5] If infinitely many similar copies are allowed, any tileset can tile a unit square greedily in a manner akin to that of an Apollonian gasket.

[6] Of course, the number of tiles can be incremented by splitting a tile in such a way that the pieces must reassemble to form the previous tile, or by adding tiles that *cannot* be used in any tiling of rectangles.

Proof. We first prove that some finite number suffices. This comes directly from the fact that PCP remains undecidable when the number of pairs n is fixed, for $n \geq 7$ [MS05]. Of course, by using a binary encoding of the alphabet, we may assume $m = |\Sigma| = 2$. By making sure that this encoding is of even length, we may omit the transmitter tile F that fixes (x, t), and let the labels oscillate back and forth. This means we need only $2n + m + 4nm + 8$ tiles. Taking $n = 7$ and $m = 2$, we see that 80 tiles suffices.

Now we briefly sketch a proof of the claimed 19 bound. In [Oll09], Ollinger constructs a tileset $\mathbf{T}$ of 11 polyominoes for an arbitrary Wang tileset $\mathbf{W}$, such that $\mathbf{T}$ tiles the plane if and only if $\mathbf{W}$ tiles the plane. By adding 8 (different) border tiles similar to the idea used above, we obtain a tileset $\mathbf{T}'$ of 19 polyominoes such that $\mathbf{T}'$ tile some rectangle if and only if $\mathbf{W}$ tile some white rectangle. It is worth noting that in [Oll09], the Wang squares are arranged on the square lattice grid as if they are (Aztec) diamonds. Thus we must create a new set of "diamond" Wang tiles to fit this setup, and create the border tiles to create a periodic border that fits Aztec diamonds. We omit the easy details. □

5.4 Complementary tileability

5.4.1 Tiling cofinite regions with a fixed tileset

Now we will consider a series of *complementary* tiling problems. First, as motivated in Section 5.2, we consider tiling a cofinite region, given by its finite complement in the plane.

Complementary Tileability

Instance: A tileset $\mathbf{T}$ and a finite region Γ.

Decide: Does the cofinite region $\mathbb{Z}^2 \backslash \Gamma$ admit a $\mathbf{T}$-tiling?

We will see that this is undecidable, by showing that the problem is undecidable even if the tileset $\mathbf{T}$ is fixed:

COMPLEMENTARY **T**-TILEABILITY

Instance: A finite region Γ.

Decide: Does the cofinite region $\mathbb{Z}^2 \backslash \Gamma$ admit a **T**-tiling?

Theorem 5.4.1 *There exists a tileset* **T** *such that* COMPLEMENTARY **T**-TILEABILITY *is undecidable.*

Proof. Fix a universal Turing machine $\mathfrak{M}$ on an alphabet Σ with blank symbol $0 \in \Sigma$. Treating the initial tape configuration as the input, it is undecidable whether $\mathfrak{M}$ halts. Let $\mathbf{x} = x_1 x_2 \dots x_r \in \Sigma^*$ be a word in Σ. Construct region $\Gamma_{\mathbf{x}}$ as shown in Figure 5.4a, where s is the starting state of $\mathfrak{M}$. Using the emulation of Turing machines by Wang tiles in Lemma 6.1.1, we obtain a Wang tileset $\mathbf{M}_{\mathfrak{M}}$ that emulates $\mathfrak{M}$. Add the additional tiles in Figure 5.4b, and pass to polyominoes by Lemma 2.3.1 along with input region $\Gamma_{\mathbf{x}}$.

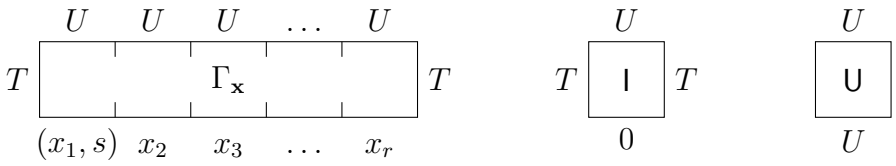

(a) Input region $\Gamma_{\mathbf{x}}$. (b) Additional tiles.

Figure 5.4: Initial tiles.

In a tiling, the left and right of the input region can only be tiled by (the polyomino associated with) I, thus initializing the tape with the blank symbol 0 bi-infinitely, and separating the plane into two halves. The upper half will be tiled by U. The lower half is tileable if and only if there is a non-halting computation of $\mathfrak{M}$. □

5.4.2 Tiling fixed cofinite regions

Obviously, for some tileset **T**, such as a single square, this problem is decidable. In contrast, we can fix the region Γ instead of the tileset **T**:

Γ-Complementary Tileability

Instance: A tileset $\mathbf{T}$.

Decide: Does the region $\mathbb{Z}^2 \backslash \Gamma$ admit a $\mathbf{T}$-tiling?

Theorem 5.4.2 Γ-Complementary Tileability *is undecidable for any finite simply connected*[7] *region* Γ.

In particular, even if we fix Γ as a single square, denoted $[1 \times 1]$, this problem is still undecidable.[8]

Sketch of proof. We modify Complementary Tileability to have a fixed starting region. Indeed, suppose we are given an instance consisting of a tileset $\mathbf{T}$ and a region Γ. Let $\mathbf{T}'$ be obtained by passing $\mathbf{T} \cup \{\Gamma\}$ to Wang tiles and back to polyominoes via Lemma 2.3.1. Scale all these tiles by a factor of 2, and then remove a single square from the tile Γ' corresponding to Γ. Note that $\mathbb{Z}^2 \backslash [1 \times 1]$ admits a $\mathbf{T}'$-tiling if and only if $\mathbb{Z}^2 \backslash \Gamma$ admits a $\mathbf{T}$-tiling. Indeed, by passing to Wang tiles and back, these tiles automatically align in a dilated integer lattice grid in any tiling. Since all tiles were dilated by a factor of 2, if Γ' is not used, there is no way to tile around the $[1 \times 1]$ unit square. On the other hand, every occurrence of Γ' will leave a $[1 \times 1]$ square uncovered. Thus Γ' will be used precisely once, matching the square at where it was removed. This transforms the original complementary tiling problem to one with fixed input region $[1 \times 1]$.

Fixing Γ as something else is similar. Indeed, let S be a large $[N \times N]$ square containing Γ, such that $S' = S \backslash \Gamma$ is connected. It is possible that S' is not simply connected, in which case we can break S' into two s.c. pieces that will interlock with each other only. Given an instance $\mathbf{T}$ of $[1 \times 1]$-Complementary Tileability, scale all tiles in $\mathbf{T}$ by a factor of N to obtain an equivalent $[N \times N]$-Complementary Tileability problem. Now add (the

[7] Simple connectivity is necessary. Indeed, if Γ has a missing unit square in its interior, then its complement is tileable if and only if the tileset contains a single unit square.

[8] This is not surprising, since tiling the entire plane ($\Gamma = \varnothing$) is undecidable [Ber66]. In fact, the main difficulty was the lack of a starting point. The case we consider is essentially the *origin-constrained* version of tileability, which is undecidable [Wan63]. We include a sketch for completeness.

two pieces of) S' to the scaled tileset, reducing to Γ-Complementary Tileability, as desired. □

5.4.3 Tiling cofinite regions with rectangles

On the positive side, somewhat surprisingly, when the tileset consists only of rectangles, the most general case (with neither the region nor the tileset fixed) is actually decidable.

Complementary Tileability with Rectangles

Instance: A region Γ and a tileset $\mathbf{R}$ of rectangles.

Decide: Does the region $\mathbb{Z}^2\backslash\Gamma$ admit a $\mathbf{R}$-tiling?

Proof of Theorem 5.1.4. We first describe the algorithm. Suppose we are given a region Γ and a tileset $\mathbf{T}$ consisting only of rectangles. Let A be the smallest rectangular region that contains Γ in its interior. Place tiles to cover A (where tiles are allowed to protrude outside of A), such that Γ is uncovered. Formally, find a region $B \supset A$ and a tiling of $B\backslash\Gamma$. Even though this may look like an infinite problem with B unspecified, note that it is really a finite problem, since we can exhaustively search all local tilings around Γ. Either there is no way to cover A while avoiding Γ, in which case there is no tiling of $\mathbb{Z}^2\backslash\Gamma$, or we find such a B and a tiling π of $B\backslash\Gamma$, in which case the complement of Γ is tileable.

Indeed, we may assume that π is minimal in the sense that removing any tile will leave parts of A uncovered. Consider the tiling π at the top boundary of A. It consists of some rectangles sticking out, and some that tile A just right. Regardless, simply use each of these rectangles to tile the infinite half-strip above each segment. Similarly, tile the three half-strips from the other three edges. Now we are left with four quadrants, which are obviously tileable. □

5.5 Tiling indented quadrants with rectangles

Lemma 2.3.1 lists several classes of TILEABILITY problems that are equivalent. Tiling with rectangles is equivalent with the others for finite regions, but Theorem 5.1.4 puts an end to the hope of extending the equivalence to cofinite regions. Here we present an equivalence for special infinite regions, and use it to exhibit yet another undecidable result.

Lemma 5.5.1 *Given a (Wang) tileset* $\mathbf{T}$*, it is undecidable whether the (white) fourth quadrant is* $\mathbf{T}$*-tileable.*

Proof. Take a Turing machine $\mathfrak{M}$ with blank symbol b and initial state q_0. Use Lemma 6.1.1 to get an associated tileset $\mathbf{M}_{\mathfrak{M}}$. Add the three initialization tiles from Figure 6.2, where $\varnothing$ signifies the white boundary of the fourth quadrant. Similar to the proof of Theorem 6.2.1, we see that the fourth quadrant is tileable if and only if the Turing machine has a non-halting computation when started on a 1-way infinite blank tape. Since that is undecidable (with $\mathfrak{M}$ varying as input), tileability of the quadrant is undecidable. □

As usual, this result holds for a tileset of polyominoes by Lemma 2.3.1, where edges with color $\varnothing$ are replaced by straight edges. Obviously, it makes no sense to ask the same question for rectangular tiles. However, if we replace the boundary of the quadrant by periodic rectilinear curves, then the problem becomes undecidable again. Call such a boundary a *periodically indented* fourth quadrant.

Theorem 5.5.2 *Given a periodically indented fourth quadrant* Γ *and a tileset* $\mathbf{R}$ *of rectangles, it is undecidable whether* Γ *admits a* $\mathbf{R}$*-tiling.*

Proof. Take a set of polyominoes $\mathbf{T}$. The reduction in Lemma 2.3.3 provides a set of rectangles $\mathbf{R}$, and a linear-time function f that transforms a finite region Γ to another finite region Γ', such that Γ is $\mathbf{T}$-tileable if and only if Γ' is $\mathbf{R}$-tileable. Explicitly, f takes each unit-length edge of Γ and replaces it with a rectilinear curve to get Γ'. By feeding a single vertical and a single horizontal edge to f, we get two rectilinear curves that can be used

to make the periodic boundary of an indented fourth quadrant. By *carefully* following the proof of the bijective correspondence of **T**-tilings of regions and **R**-tilings of the transformed regions, one can see that everything works for this specific infinite case as well. In particular, in Sublemma 2.5.1, the unique $\mathbf{R}_0$-tiling of $\Gamma_0(r, c)$ was proved by placing tiles in the order labeled in Figure 2.11. It is evident that this ordering extends to the infinite quadrant, and the proof works verbatim. □

We should note that the quadrant having a corner is essential when applying the *proof* of Lemma 2.3.3 to this context. For example, this reduction does not work for the half-plane. Indeed, for that case, the sketch of Lemma 5.5.1 does not work, but can be fixed with some additional ideas to prove the corresponding lemma. The theorem, however, cannot be salvaged, as the algorithm of Theorem 5.1.4 would apply with some minor alterations.

5.6 Augmentability

In the style of Rectangular Tileability, where we are interested if there is *some* finite (rectangular) region from an infinite collection that is tileable by a given tileset, we consider the following notion. A finite region Γ is *augmentable* if there is a finite s.c. region $\Gamma' \supset \Gamma$ such that both $\Gamma' \backslash \Gamma$ and Γ' are tileable.

Augmentability

Instance: A tileset **T** and a region Γ.

Decide: Is Γ augmentable by **T**?

As above, we can fix either **T** or Γ in the input (obviously not simultaneously). We have the following result:

Theorem 5.6.1 Augmentability *is undecidable. Moreover, it remains undecidable even when* Γ *is fixed. Similarly, there exists some tileset* **T** *such that* Augmentability *with* **T** *fixed is undecidable.*

Proof. We first prove undecidability in general, then briefly sketch how Γ or $\mathbf{T}$ may be fixed at the end of the proof. Recall that it is undecidable whether a Turing machine with a 1-way infinite tape halts. By convention, the machine head starts at the left end of the tape, where the input is written. Fix a Turing machine $\mathfrak{M}$ on an alphabet Σ, with blank symbol $0 \in \Sigma$, and starting state s. Let $\mathbf{M}_{\mathfrak{M}}$ denote the associated tileset of *machine tiles* afforded by Lemma 6.1.1. Let $\mathbf{B}_{\mathfrak{M}}$ be the tileset of *border tiles* defined in Figure 5.5, consisting of T, TR, L, R, BL, and BR, L_x, R_x, and $\mathsf{H}_{x,q}$ for $x \in \Sigma$ and q a halting state of $\mathfrak{M}$. The tileset $\mathbf{F}$ of *filler tiles* consists of those in Figure 5.6. Finally, replace unlabeled edges in $\mathbf{T}_{\mathfrak{M}} = \mathbf{M}_{\mathfrak{M}} \cup \mathbf{B}_{\mathfrak{M}} \cup \mathbf{F}$ with four new colors depending on which way each edge faces. By abuse of language, we will continue to refer to these four colors on the boundary as white, with the understanding that the white colors do not match, and thus the border tiles can only be used on the boundary of a tiling and not in its interior. This finishes the construction of the tileset $\mathbf{T} = \mathbf{T}_{\mathfrak{M}}$.

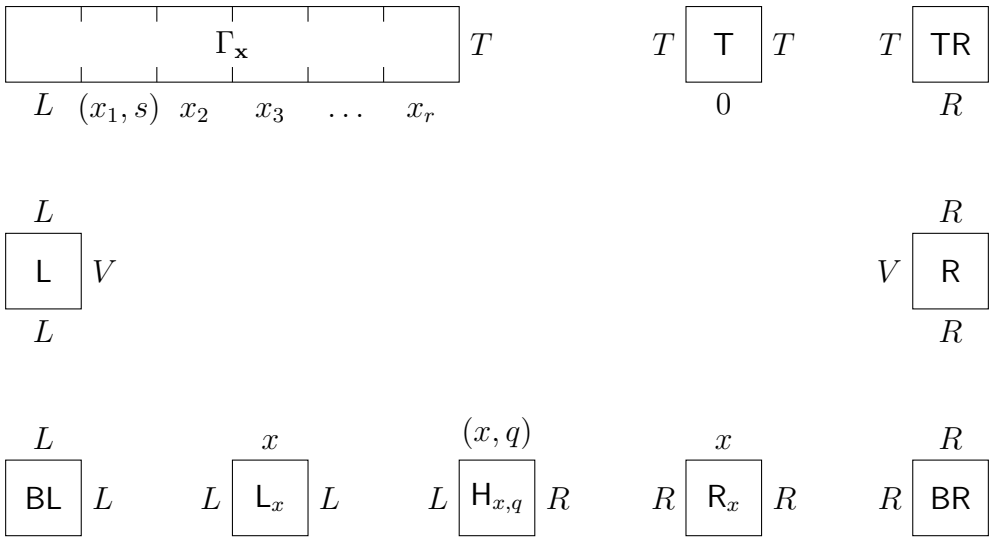

Figure 5.5: Border tiles $\mathbf{B}_{\mathfrak{M}}$.

Let $\mathbf{x} = x_1 x_2 \ldots x_r \in \Sigma^*$ be a word in Σ. Construct region $\Gamma = \Gamma_{\mathbf{x}}$ as shown in Figure 5.5, where s is the starting state of $\mathfrak{M}$, and the white colors are subject to the same aforementioned replacement treatment. It remains to show that $\Gamma_{\mathbf{x}}$ is augmentable by $\mathbf{T}_{\mathfrak{M}}$ if and only if $\mathfrak{M}$ halts on input $\mathbf{x}$.

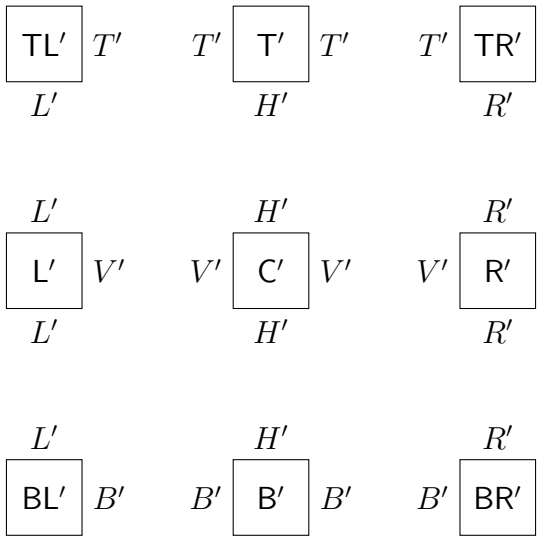

Figure 5.6: Filler tiles **F**.

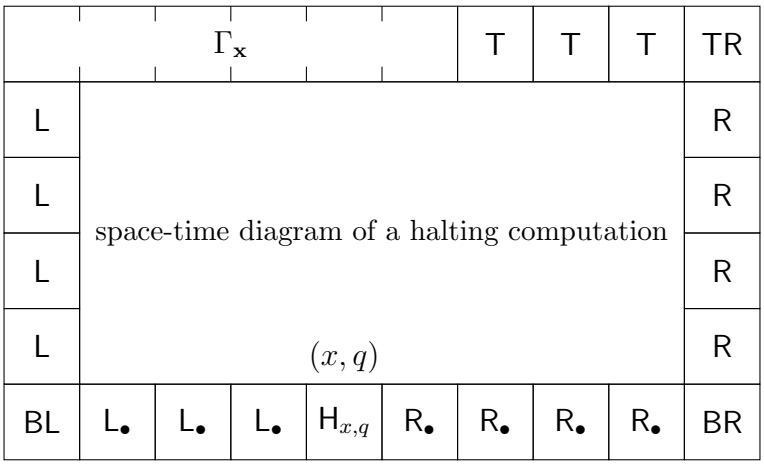

Figure 5.7: Tiling of $\Gamma'\backslash\Gamma$.

First, suppose $\mathfrak{M}$ halts on input $\mathbf{x}$. Take a tiling representing the space-time diagram of a halting computation. By definition, the top boundary color sequence of the tiling is $\mathbf{x}$, possibly with blank symbol 0 repeated on its right. We may therefore place Γ above the space-time diagram, with tiles T to its right (see Figure 5.7). Now we surround the region by the other border tiles to get a white rectangular region Γ'. Of course, the bottom is tiled by $\mathsf{H}_{x,q}$, which matches the state symbol in the last row of the space-time diagram, and with $\mathsf{L}_\bullet$ and $\mathsf{R}_\bullet$ tiles on the sides, where $\bullet$ denotes some unspecified symbol from Σ. We thus get a tiling of $\Gamma'\backslash\Gamma$ automatically. Notice that since Γ' is a white rectangle, it is tileable by the filler tiles $\mathbf{F} \subset \mathbf{T}_{\mathfrak{M}}$, as desired.

Conversely, suppose $\Gamma_{\mathbf{x}}$ is augmentable by $\mathbf{T}_{\mathfrak{M}}$. Since no tiles could be immediately above or to the left of Γ, Γ' matches the upper left corner of Γ. Thus in any tiling of Γ', the space currently occupied by Γ must be tiled by filler tiles. Note that as the filler tiles can only be adjacent to other filler tiles, and since Γ' is (simply) connected, Γ' is tileable by filler tiles alone. Of course, tilings of $\Gamma'\backslash\Gamma$ must not use filler tiles, as they cannot be adjacent to Γ. This means the boundary of Γ' must be colors common to both filler and non-filler tiles, meaning that Γ' is a white rectangle. The only way to tile $\Gamma'\backslash\Gamma$ is by using the border tiles as shown in Figure 5.7, with precisely one $\mathsf{H}_{x,q}$ somewhere. Since the interior cannot utilize border tiles, it must be tiled by the machine tiles $\mathbf{M}_{\mathfrak{M}}$ alone. Thus it emulates a computation starting from $\mathbf{x}$, potentially followed by finitely many blank symbols, and ending at a halting state (forced by the presence of a border tile $\mathsf{H}_{x,q}$ on the bottom boundary) after finitely many steps, as desired.

We may interchange the role of $\Gamma_{\mathbf{x}}$ and TL', adding $\Gamma_{\mathbf{x}}$ to the tileset and removing TL' to be used as the input region. This shows that AUGMENTABILITY remains undecidable even when Γ is fixed. On the other hand, by fixing $\mathfrak{M}$ as some Universal Turing machine, we see that there is some fixed $\mathbf{T}$ such that AUGMENTABILITY is undecidable. □

5.7 Final remarks and open problems

5.7.1

Tileability of a given finite region is decidable simply by exhaustive search. In this context, tileability of finite regions by a finite tileset is NP-complete [Lew78].[9] This is true even when the tileset is fixed as a horizontal bar h_n of n squares and a vertical bar v_m of m squares, $n \geq 2$ and $m \geq 3$ [BNRR95].[10] However, when the region is simply connected (s.c.), tileability by $\{h_n, v_m\}$ can be determined in linear time [KK92].[11] By comparing these results, it is apparent that simple connectivity makes a difference. This is in part due to Thurston's height function approach [Thu90] and techniques in combinatorial group theory developed by Conway and Lagarias [CL90]. Using these methods, Rémila showed that tileability of s.c. regions is quadratic for any two fixed rectangles [Rém05]. Perhaps surprisingly, there is a finite set of rectangular tiles such that tileability of s.c. regions is NP-complete (see Chapter 2). On the other hand, tileability of a rectangular region for a fixed set of tiles can be determined in linear time (see below). Of course, if the rectangular region is unspecified, undecidability returns. In a related direction, it is undecidable whether a tileset is a *code* [BN03], *i.e.*, every tileable finite region is uniquely tileable.

5.7.2

Theorem 5.1.2 leads to some curious consequences.

Theorem 5.7.1 ([DK75]) *Given a tileset* $\mathbf{T}$*, there is a tileset* $\mathbf{T}'$ *consisting only of rectangular tiles such that* $\mathbf{T}$ *and* $\mathbf{T}'$ *tile the same rectangular regions.*

[9] This was also indicated in an unpublished manuscript by Garey, Johnson, and Papadimitriou; see [GJ79, Pap94].

[10] Note that everything is tileable if $n = 1$; if $n = m = 2$, it is a matching problem and thus is solvable in polynomial time (see *e.g.* [LP09]).

[11] Whenever the tileset is fixed, the complexity of the running time is given in terms of the area of the input region.

Note that $\mathbf{T}$ can tile *some* rectangle if and only if $\mathbf{T}'$ is non-empty. As such, in light of our main theorem, it is undecidable if $\mathbf{T}'$ is non-empty and, *a fortiori*, $\mathbf{T}'$ is not computable from $\mathbf{T}$. Indeed, while the proof in [DK75] seems purely existential, now there is proof that it *cannot* be made constructive.

Theorem 5.7.2 ([LMP05]) *Tileability of an* $[n \times m]$ *rectangle by a fixed tileset of rectangles can be determined in time* $O(\log n + \log m)$.

Combining the two results, we see that there is a linear time algorithm for testing tileability of rectangles for any fixed tileset. Again, the main theorem proves that the linear time algorithm afforded by combining [DK75] with [LMP05] cannot be algorithmically determined if the tileset is not fixed in advance. In the next subsection, we outline another consequence regarding the growth of certain functions.

5.7.3

For a polyomino P that tiles some rectangle, Klarner defined the *order* $h(\mathsf{P})$ of P as the minimum number of copies it takes to tile some rectangle [Kla69], and conjectured that there is no polyomino of order 3, which has since been confirmed [SW92]. There are polyominoes of order $4s$ for each $s \in \mathbb{N}$ [Gol89], but no non-rectangular polyomino whose order is odd[12] is known, and their existence is an open question (see *e.g.* [GO04, §15]).

For convenience, let us set $h(\mathsf{P}) = 0$ if P does not tile any rectangle, and let

$$f(n) = \max\{h(\mathsf{P}) : |\mathsf{P}| = n\},$$

where $|\mathsf{P}|$ is the area of (the shape of) P. If it is computable or bounded above by a computable function, then Rectangular Tileability for a single polyomino would be decidable. Indeed, if there exists a computable function $g(n)$ such that $f(n) \leq g(n)$, then given P, simply try tiling all rectangles with areas up to $g(|\mathsf{P}|)$. This is a finite process that terminates. If no tilings are found, then P does not tile any rectangle. There are several

[12] One should not confuse this with the notion of *odd order*, also introduced in [Kla69].

claims that the problem is decidable (thus the function $f(n)$ is computable), but to our best knowledge (see *e.g.* [AS10]), no proofs are currently known.

Along the same vein, let $\widetilde{h}(\mathbf{T})$ denote the minimum area of a rectangle tileable by a tileset $\mathbf{T}$, and set $\widetilde{h}(\mathbf{T}) = 0$ if $\mathbf{T}$ does not tile any rectangle. Note that when $\mathbf{T} = \{\mathsf{P}\}$ is a single polyomino, we have $\widetilde{h}(\{\mathsf{P}\}) = h(\mathsf{P})/\left|\mathsf{P}\right|$. Similarly, define

$$\widetilde{f}(n) = \max\{\widetilde{h}(\mathbf{T}) : \mathbf{T} \text{ has } \textit{total} \text{ area } n\}.$$

Corollary 5.7.3 *The function $\widetilde{f}(n)$ grows faster than* any *computable function, e.g., the fast-growing Ackermann function.*

Proof. This follows immediately from the undecidability of Rectangular Tileability (Theorem 5.1.2). □

5.7.4

Wang conjectured that there is no aperiodic tileset of Wang squares [Wan61]. If this conjecture were true, Tileability for Wang squares would be decidable. Indeed, simply enumerate *all* tilings of $[N \times N]$ squares, $N = 1, 2, \ldots$. Either some square admits no tiling (and thus the plane is not tileable), or at some point a finite fundamental domain will be found that can be used to tile the whole plane periodically. Berger disproved the conjecture by showing the undecidability of this tileability problem [Ber66]. As a consequence, there is an aperiodic tileset of Wang squares. After a series of reductions in the number of Wang squares, the current record is 13 [Cul96].

5.7.5

Reducing the number of tiles in an aperiodic tileset has been the subject of much effort. The famous Penrose tilings derive aperiodicity from a pair of tiles [Pen74]. Here a tile is a geometric shape that can be rotated (and reflected) in addition to translation. These tilings inherit aperiodicity from quasicrystals and thus do not admit transformations onto

lattices. Socolar and Taylor constructed a single tile on the hexagonal lattice that exhibits aperiodic behavior when external matching rules are enforced [ST11]. Since the matching rules span non-adjacent tiles, encoding this as a geometric tile (with no external matching rules) necessarily resulted in a tile whose interior is disconnected. There seems to be no obvious way to circumvent this in the plane.

Returning to the square lattice, it is unknown whether there is a single polyomino that could force aperiodic behavior. Decidability of whether a polyomino admits a tiling (or a periodic tiling) of the plane is open. However, there is a polynomial-time algorithm for deciding whether a given polyomino admits an *isohedral tiling* [KV99], *i.e.*, a tiling where the group of isometries acts transitively on the tiles thereof. If only translations are allowed on a single polyomino, TILEABILITY of the plane is decidable [BN91], and an algorithm with running time quadratic in the boundary length is known [GV07].

5.7.6

Let us consider tilings of finite regions. Traditionally, the use of *coloring maps* is a main tool for proving non-tileability (see [Gol65]). It actually proves the non-existence of *signed tilings*, *i.e.*, a finite collection of tiles with ± 1 weights such that the weights of tiles covering each square sum to 1 inside the region and 0 outside (see [CL90]). Conversely, when there are no signed tilings, there is a coloring argument that certifies it (see [Pak00]). This is not true for ordinary tilings. Indeed, there are non-tileable regions that admit signed tilings, thus proving non-tileability using this method is impossible for those regions.

The notion of augmentability considered in Section 5.6 can be formulated in this language of signed tilings, by requiring tiles with equal weights to be pairwise disjoint. Augmentability is therefore a (proper) intermediate notion between tileability and signed tileability. That is, tileable regions are augmentable, and augmentable regions are signed tileable. Moreover, the implications are not bidirectional [Kor04].

5.7.7

There are instances where results of tilings in the plane do not extend to higher dimensions. For example, the number of tilings of a finite region by dominoes can be counted efficiently in the plane, but is #P-complete in higher dimensions (see Chapter 4). However, all of the results in this chapter extend easily to higher dimensions. Indeed, RECTANGULAR TILEABILITY extends by simply endowing each $2D$ tile with height 1 in the remaining directions. The results involving Turing machines can also be easily extended in the obvious manner. Extending COMPLEMENTARY TILEABILITY with rectangles to higher dimensions is only slightly trickier. A *brick* in $\mathbb{Z}^n$ is the Cartesian product of n intervals.

Theorem 5.7.4 *It is decidable whether the complement of a given finite region* Γ *in* $\mathbb{Z}^n$ *is tileable by a given tileset* $\mathbf{T}$ *consisting only of bricks.*

Proof. We follow the same proof as given in Subsection 5.4.3. Indeed, let A be the smallest brick region that contains Γ in its interior. Find a region $B \supset A$ and a tiling π of $B \backslash \Gamma$. This task is finite, and is possible if and only if $\mathbb{Z}^n \backslash \Gamma$ is tileable.

Indeed, assume that π is minimal. It remains to exhibit a tiling of $\mathbb{Z}^n \backslash B$. For a brick in π, call its facet *free* if it is entirely on the boundary of B. Suppose a brick centered at coordinates $\mathbf{x}$ has a free facet. Its *cone* is the set of copies of the brick centered at $\mathbf{x} + \mathbb{Z}_+ \mathbf{v}$, where $\mathbf{v}$ is the *width vector* from the opposite facet to the free facet, and $\mathbb{Z}_+ = \{0, 1, 2, \ldots\}$. More generally, if a brick centered at $\mathbf{x}$ has k free facets, with corresponding width vectors $\mathbf{v}_1, \ldots, \mathbf{v}_k$, define its cone as the set of copies of the brick centered at $\mathbf{x} + \mathbb{Z}_+ \mathbf{v}_1 + \ldots + \mathbb{Z}_+ \mathbf{v}_k$. (This works even if some pairs of free facets are opposite one another.) It is easy to see that the cones of the bricks partition $\mathbb{Z}^n \backslash \Gamma$. □

Another direction of generalization is to consider other infinite regions with reasonable finite descriptions. For example, consider a periodic perforated plane, where there are holes occurring throughout the region in some periodic manner. This may lead to interesting results like Theorem 5.5.2.

One could also ask for the running-time complexity of the algorithm described in the proof of Theorem 5.1.4. In particular, what happens if the tileset is the (horizontal and vertical) dominoes?

CHAPTER 6

Demonstrating the power of tiles by emulating Turing machines

In this short chapter, we outline the classical technique of emulating Turing machines with tiles, an idea mentioned in Subsection 2.7.2 and heavily used in Chapter 5. We then create a tileset that tiles a quadrant uniquely while performing prescribed calculations.

6.1 Emulating Turing machine with tiles

Consider a Turing machine $\mathfrak{M}$ on an alphabet Σ and let Q denote its set of states. We refer to the elements of $\Sigma \sqcup (\Sigma \times Q)$ as *colors*, where (x, q), $x \in \Sigma$ and $q \in Q$, are called *compound colors*. A configuration of $\mathfrak{M}$ is represented as a (possibly infinite) sequence of colors, where all but finitely many are the blank symbol $b \in \Sigma$. Moreover, there must be precisely one compound color (x, q). Reading (x, q) as x, this sequence represents the contents of the tape. The head of the machine is at the position of (x, q), and the current state is q. Such a sequence of colors (corresponding to a valid configuration) is called *valid*. A row of (possibly infinite) Wang squares is *valid* if their bottom colors form a valid sequence. We say a set of Wang squares $\mathbf{W}$ *emulates* $\mathfrak{M}$ if given a valid row of Wang squares, and a second row of Wang squares below it, the second row represents a configuration obtained from the previous one after one time step (and therefore is a valid row). Moreover, if $\mathfrak{M}$ is non-deterministic, all possible next configurations are realizable by such tilings. This way, a tiling with $\mathbf{W}$ is a space-time computation diagram of $\mathfrak{M}$, given that it starts with a valid row. Furthermore, all possible space-time diagrams are realizable as tilings.

Lemma 6.1.1 *There is a computable tileset* $\mathbf{M}_{\mathfrak{M}}$ *of Wang squares that emulates a given Turing machine* $\mathfrak{M}$.

Proof. This construction is classical and well known (see *e.g.* [LP97, §6]). For completeness and also to fix an explicit construction, we provide a proof here.

Let $\mathfrak{M} = (Q, q_0, \Sigma, b, \delta)$ be a deterministic Turing machine, with a finite set Q of states that contains a starting state $q_0 \in Q$, a finite alphabet Σ that contains a blank symbol $b \in \Sigma$, and a transition function $\delta : \Sigma \times Q \to \Sigma \times Q \times \{L, R\}$. There is a tape with a horizontal row of cells, each cell holds precisely one symbol from Σ. The tape has a left-most cell, but extends infinitely to the right. At the beginning, every cell contains the blank symbol b. The head of the Turing machine starts on the left-most cell, in starting state q_0. At each step, the head reads the symbol a from the cell at which it is located. Suppose the current state is q, and $\delta(a, q) = (a', q', D)$. The head replaces the content of the cell by a', and enters state q'. Moreover, it moves to the left or right on the tape depending on if D is L or R.

Let $\tau(w, \frac{n}{s}, e)$ denote a Wang tile whose north, east, south, and west colors are n, e, s, and w, respectively. To emulate $\mathfrak{M}$, we introduce the following tiles (see Figure 6.1). For each $a \in \Sigma$, add a Wang tile $\tau(V, \frac{a}{a}, V)$, where V is a new symbol. For each $a \in \Sigma$ and $q \in Q$, if $\delta(a, q) = (a', q', L)$, introduce $\tau((q', L), \frac{(a,q)}{a'}, V)$. Analogously, if $\delta(a, q) = (a', q', R)$, add $\tau(V, \frac{(a,q)}{a'}, (q', R))$. Finally, add $\tau((q, R), \frac{a}{(a,q)}, V)$ and $\tau(V, \frac{a}{(a,q)}, (q, L))$. To summarize,

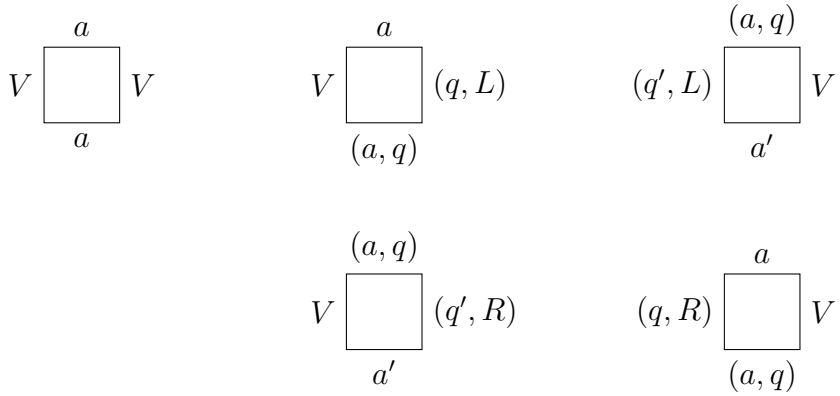

Figure 6.1: Machine tiles $\mathbf{M}_{\mathfrak{M}}$.

the horizontal colors are $\Sigma \sqcup (\Sigma \times Q)$, and the vertical colors are V and $Q \times \{L, R\}$. We refer to the colors involving Q as *compound colors*, and call these tiles the *machine tiles* $\mathbf{M}_{\mathfrak{M}}$.

Let us look at the top colors of a row of tiles. Suppose it has one compound color (a, q), and all others are not. The color sequence depicts contents of the tape, if we read (a, q) as a. The location of (a, q) indicates the position of the head, and q is the current state. In this manner, the color sequence encodes precisely the Turing machine at some time step. The bottom colors of this row of tiles will be the Turing machine at the next step. Indeed, suppose $\delta(a, q) = (a', q', L)$. By construction, there is precisely one tile that has top color (a, q). It has bottom color a', corresponding to replacing a with a' at the location of the head. The left color is (q', L), which causes the tile on the left to be precisely $\tau(V, \frac{c}{(c,q')}, (q', L))$, meaning now the head has moved left one tile. For all other tiles, if the top color is c, it must be the tile $\tau(V, \frac{c}{c}, V)$. Indeed, the other options would involve having a compound colors on a vertical side, forcing an adjacent tile to have a compound color on top, a contradiction.

Note that for a non-deterministic Turing machine, where the transition table is not necessarily a function, we simply add tiles corresponding to each possible transition. We omit the simple details. □

6.2 Tiles that do something specific, *e.g.*, calculate the digits of π

In this section, we illustrate the power of tiles by creating a set of tiles that encode the digits of π in some precise sense. Of course, there is nothing too special about π, and we can encode some other number that we know how to calculate well.

Theorem 6.2.1 *There exists a tileset* $\mathbf{T}$ *that admits a unique tiling of the fourth quadrant, such that the top row of this tiling uses tiles* $\tau_0, \tau_1 \in \mathbf{T}$*, and the sequence of* 0 *and* 1 *corresponding to the tiles used is the binary expansion of* π*.*

The idea is to encode a specific Turing machine $\mathfrak{M}$ using a set $\mathbf{W}$ of Wang tiles, and then pass to a set of tiles as usual.

Let $\mathfrak{M}$ be a Turing machine satisfying the following:

(i) when started on a blank tape, the head never moves left past the starting position,

(ii) its alphabet Σ contains *immutable* symbols 0 and 1, that is,

(iii) if it writes 0 or 1 on the tape, it never tries to change it at a later step, and

(iv) each cell on the tape is eventually marked with 0 or 1, which forms the binary expansion of $\pi - 2$ with the decimal point omitted.

The existence of $\mathfrak{M}$ can be proved by explicitly constructing such a Turing machine, and is essentially guaranteed by the Church–Turing thesis. Take such an $\mathfrak{M}$ and consider the machine tiles $\mathbf{M}_{\mathfrak{M}}$ afforded by Lemma 6.1.1.

Suppose we are to tile the fourth quadrant, whose boundary color is denoted $\varnothing$. Introduce three *initialization tiles* $\tau_{\varnothing} = \tau(\varnothing, \frac{\varnothing}{b}, \varnothing)$, $\tau_I = \tau(\varnothing, \frac{b}{L}, (q_0, R))$, and $\tau_L = \tau(\varnothing, \frac{L}{L}, V)$. Notice

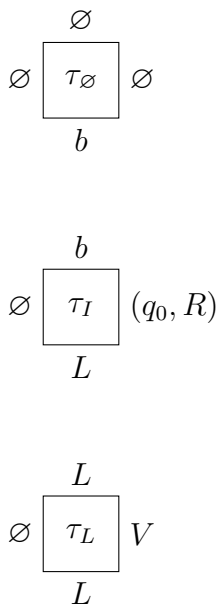

Figure 6.2: Initialization tiles for tiling the fourth quadrant.

that the top row is uniquely tiled by using only $\tau_{\varnothing}$, and the left column is uniquely tiled by $\tau_{\varnothing}$, τ_I, followed by τ_L repeatedly. Moreover, these three tiles cannot be used anywhere

else. Thus we have initialized a *decorated quadrant* with top color b, and left color sequence $(q_0, R), V, V, \ldots$. This exactly allows the machine tiles to start computation on a blank tape with initial state q_0, as desired.

After encoding the Turing machine $\mathfrak{M}$ as a set of Wang squares $\mathbf{M}_{\mathfrak{M}}$ and adding a few tiles to initialize, we are ready to employ one last trick to make the digits of π materialize at the top row. For each machine tile $\tau(w, \frac{n}{s}, e)$, replace it with two tiles $\tau(w, \frac{(n,i)}{(s,i)}, e)$, $i \in \{0, 1\}$, except when $s \in \{0, 1\}$, in which case we only add the tile with $s = i$. We call i the parity of the tile. By construction, each column of a tiling by these tiles must have consistent parity. This is possible since we will not have 0 or 1 occurring in the same cell in the Turing machine computation, as they are immutable. On the other hand, since each cell eventually is written with 0 or 1, the parities are forced. In other words, we have successfully lifted the output of the Turing machine computation all the way to the top!

It remains to make slight modifications to the initialization tiles as follows: replace $\tau_\varnothing$ with $\tau_i = \tau(\varnothing, \frac{\varnothing}{(b,i)}, \varnothing)$, $i \in \{0, 1\}$, change τ_I to $\tau(\varnothing, \frac{(b,1)}{L}, (q_0, R))$, and leave τ_L unchanged. Note that this hard codes the corner tile to be τ_1, which is why we chose a Turing machine that calculates the binary expansion of $\pi - 2$. The unique tiling of the quadrant is now restored, and the top row consists of τ_0 and τ_1, whose indices form the binary expansion of π, as desired.

CHAPTER 7

The interplay between tilings and cellular automata

The theory of cellular automata is rich and has attracted a lot of study (see *e.g.* [Kar05] for standard terminology and a survey of results), including the search for simple universal systems [Coo04, Oll02]. This is akin to the efforts in finding small universal Turing machines [NW09, Rog96]. In this chapter, we describe easy constructions to emulate cellular automata with tiles (Section 7.1) and *vice versa* (Section 7.3). In Section 7.2, we emulate the so-called `Rule 110` cellular automaton efficiently using this technology. A notion of *function-pair universality* is introduced in Section 7.4, which promises conjectural improvements of the number of rectangles needed in Theorem 2.1.1. Finally, we provide a brief reasoning as to the hope of such conjectural improvements being possible (Section 7.5). In this chapter, most proofs are merely sketches, and all cellular automata are 1-dimensional.

7.1 Emulating cellular automata with tiles

A cellular automaton $\mathcal{A}$ of rank n consists of a finite set of states Σ and a (local) update rule $f_{\mathcal{A}} : \Sigma^n \to \Sigma$. Let the global update function $\Phi_{\mathcal{A}} : \Sigma^{\mathbb{Z}} \to \Sigma^{\mathbb{Z}}$ be the action of applying $f_{\mathcal{A}}$ synchronously everywhere. Given a cellular automaton with neighborhood consisting of cells at most distance d away (*i.e.*, $n = 2d + 1$), we construct the following set of Wang squares.

For each $(x_{-d}, \ldots, x_0, \ldots, x_d) \in \Sigma^n$, we introduce a tile whose left and right colors are $(x_{-d}, \ldots, x_{d-1})$ and $(x_{-d+1}, \ldots, x_d)$, respectively, the top color is x_0, and the bottom color is $f(x_{-d}, \ldots, x_d)$. This construction yields s^n Wang squares.

To start the computation on configuration $C : \mathbb{Z} \to \Sigma$, take the lower half-plane with top-border colors

$$\ldots, c(-1), c(0), c(1), c(2), \ldots.$$

The sequence of horizontal colors in each subsequent row is the configuration after one synchronous update by the cellular automaton. The validity of this construction is straightforward and thus omitted. As we have obtained the space-time diagram of the cellular automaton as a tiling, we say that the tileset *emulate* the given cellular automaton. We have proved the following theorem.

Theorem 7.1.1 *A 1-dimensional cellular automaton with neighborhood consisting of cells at most distance d away can be emulated by a tileset of at most s^{2d+1} Wang squares.*

7.2 `Rule 110`, an example

A 1-dimensional nearest-neighbor cellular automaton on the binary symbols $\mathbb{Z}_2 = \{0, 1\}$ is called *elementary*. Of the 2^8 elementary ones, `Rule 110` is especially famous, whose update function $f(x, y, z) : \mathbb{Z}_2^3 \to \mathbb{Z}_2$ is given by

$$\sum_{(x,y,z)\in\mathbb{Z}_2^3} 2^{4x+2y+z} f(x, y, z) = 110,$$

where calculations are done in $\mathbb{Z} \supset \mathbb{Z}_2$. By Theorem 7.1.1, there exists $2^3 = 8$ Wang squares that emulate `Rule 110`, shown in Figure 7.1.

However, notice that $f(x, y, z) = f(\min(x, y), y, z)$, *i.e.*, the following diagram commutes:

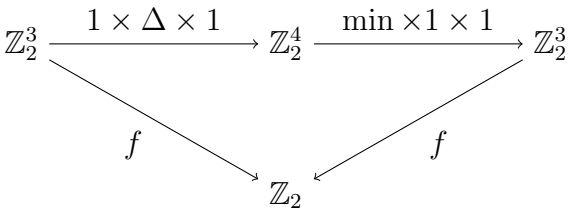

where $\Delta(y) = (y, y)$ is the diagonal map. Indeed, if $y = 1$ then $\min(x, y) = x$. Otherwise, notice $f(x, 0, z)$ does not depend on x. Thus we may change each vertical color (a, b) to

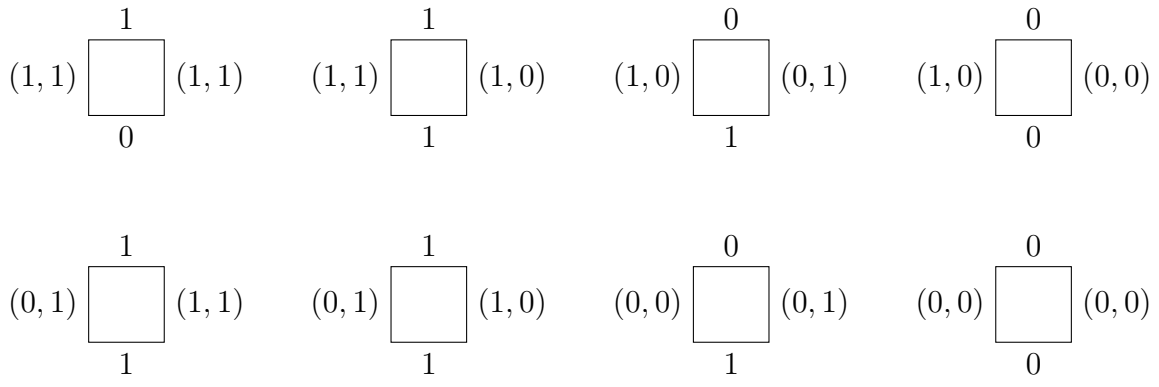

Figure 7.1: Emulating `Rule 110` with 8 tiles.

$(\min(a,b),b)$ in the construction (see Figure 7.2, changes are underlined). This yields the general tile

$$\tau((\min(x,y),y),\frac{y}{f(\min(x,y),y,z)},(\min(y,z),z)).$$

Thus we get six tiles, one for each $x,y,z\in\{0,1\}$ with $x\leq y$.

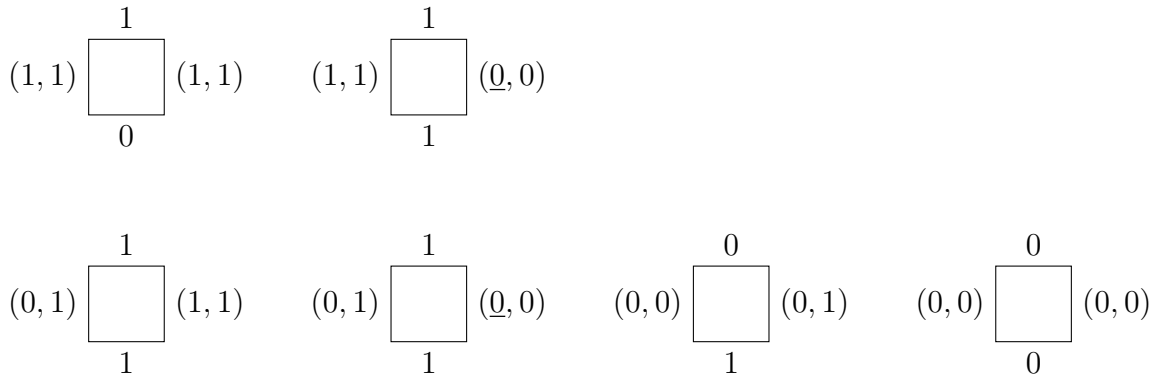

Figure 7.2: Emulating `Rule 110` with 6 tiles $\mathbf{W}_6$.

Corollary 7.2.1 *There is a set* $\mathbf{W}_6$ *of* 6 *Wang squares that emulate* `Rule 110`.

We can use these tiles in various ways. For example, by adding the initialization tiles in Figure 7.3, the (white) third quadrant will admit a unique tiling showcasing the famous picture of `Rule 110` started with a single 1. In Figure 7.4, each tile with bottom color 0 (resp. 1) is drawn as a white (resp. black) pixel.

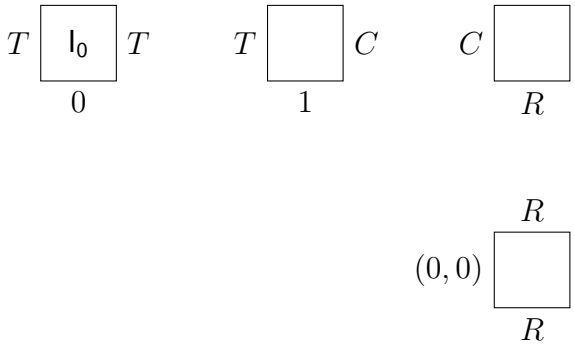

Figure 7.3: Tiles to initialize `Rule 110` to fill the third quadrant.

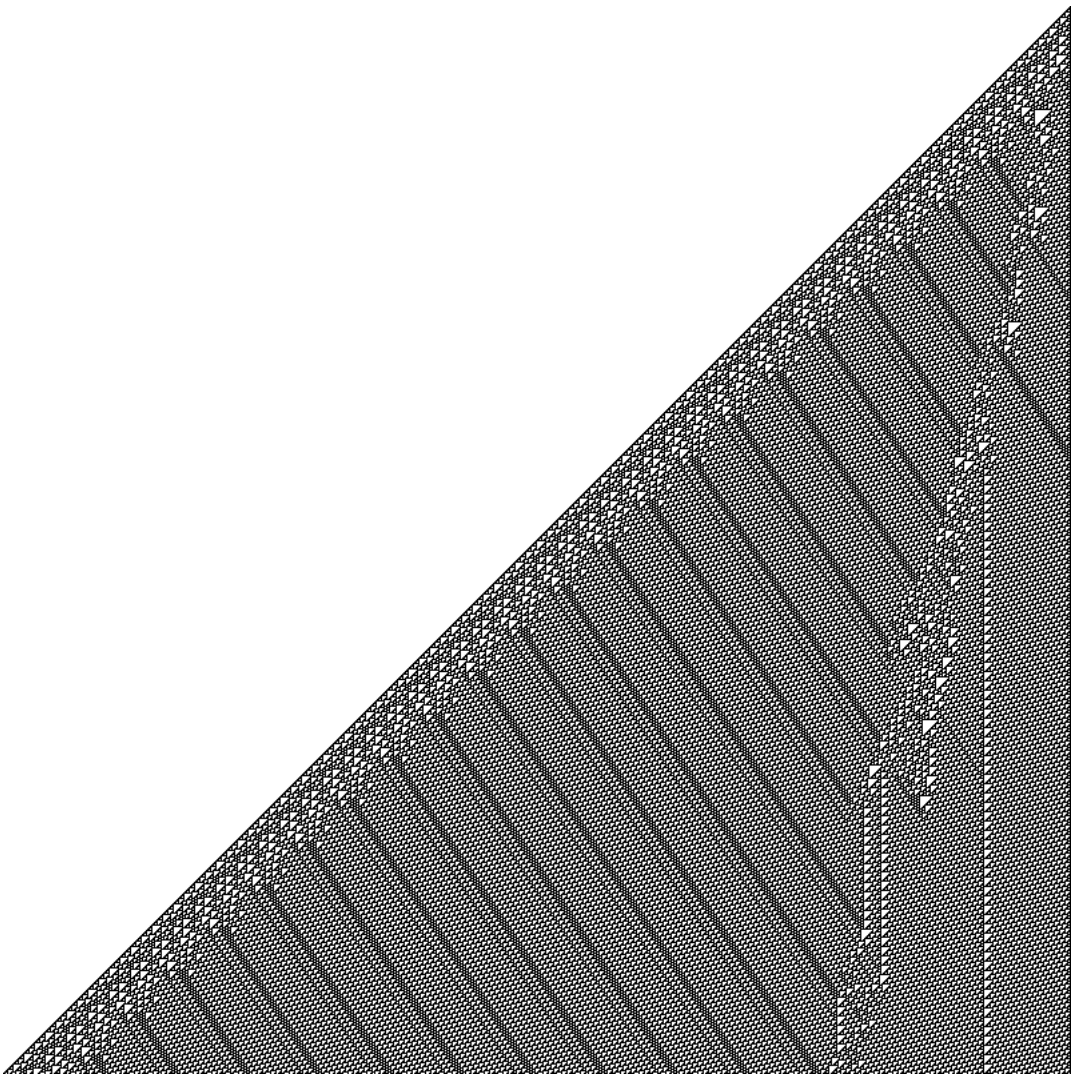

Figure 7.4: `Rule 110` filling the third quadrant started with a single 1.

Alternatively, we can add the tiles in Figure 7.5 to allow random initial configurations for `Rule 110` for the lower half-plane, say.

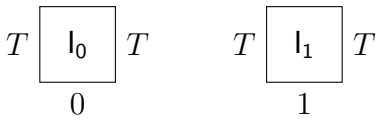

Figure 7.5: Tiles to introduce random initial configuration for `Rule 110`.

7.3 Emulating tiles with cellular automata

Since we can emulate cellular automata with tiles, we could emulate a specific universal cellular automaton, in the hopes of reducing the size of our tilesets. For simplicity, we avoid repeatedly defining "emulate" in various settings, implicitly appealing to standard literature when the meaning is not clear from context.

A tileset of Wang squares is *NW-deterministic* if there are no two Wang squares that have the same colors on their north and west edges as each other.

Lemma 7.3.1 *A tileset of NW-deterministic Wang squares can be emulated by a cellular automaton.*

Proof. Denote the vertical and horizontal colors of the tileset V and H, respectively, and let $\Sigma = V \sqcup H$. Define a nearest-neighbor cellular automaton on Σ with the following update rule: for $w \in V$, let $f(z, w, n) = s$, where s is the south color of the unique tile[1] with west and north colors w and n, respectively; similarly, for $n \in H$, let $f(w, n, z) = e$, where e is the east color of the same tile. This finishes the construction. Each tiling appears as a subset of some space-time diagram of this cellular automaton (rotated by $\pi/4$). □

There are several notions of universality in the theory of cellular automata. If a cellular automaton can emulate any other cellular automata (of the same dimension), it is

[1]If no such tile exists, the update rule can be arbitrary, as that case will not be used in the emulation.

intrinsically universal. Intrinsic universality is strictly stronger than Turing computational universality.

Corollary 7.3.2 *There is a tileset of Wang squares that emulate any NW-deterministic Wang squares.*

Proof. Fix an intrinsically universal 1-dimensional cellular automaton $\mathcal{A}$. For example, [OR11] presents one with only 4 states (see also [Oll02]). Any tileset of NW-deterministic Wang squares can be emulated by a cellular automaton (Lemma 7.3.1), which in turn can be emulated by $\mathcal{A}$, and is finally emulated with Wang squares (Theorem 7.1.1). Since $\mathcal{A}$ is fixed, so is the resulting tileset. □

Unfortunately, known examples of intrinsically universal cellular automata all lead to too many Wang squares when emulating, thus foiling our plan. In the previous section, we saw that, as an example, `Rule 110` can be emulated with 6 Wang squares. However, though Turing universal [Coo04], it is unknown whether `Rule 110` is intrinsically universal. In the following section, we outline a weaker form of universality that is sufficient for our purposes.

7.4 Function-pair universality of cellular automata

Let $\oplus$ denote string concatenation. A cellular automaton on alphabet Σ with global update function Φ is *function-pair universal* if for all pairs $f, g : \Omega^2 \to \Omega$, where Ω is an arbitrary alphabet, we have injective "encoding function" $h : \Omega \to \Sigma^t$ for some $t \in \mathbb{N}$, "time dilation factor" $N \in \mathbb{N}$, and "program" words $a, b, c, d \in \Sigma^*$, such that

$$\Phi^N(a \oplus h(x) \oplus b \oplus c \oplus h(y) \oplus d) = c \oplus h \circ f(x, y) \oplus d \oplus a \oplus h \circ g(x, y) \oplus b \qquad (*)$$

for all $x, y \in \Omega$, regardless of the states of the rest of the cellular automaton. The following theorem is important, albeit obvious.

Theorem 7.4.1 *Every intrinsically universal cellular automaton is function-pair universal.*

This demonstrates the existence of function-pair universal cellular automata. We now show that they are sufficiently powerful for our needs.

Theorem 7.4.2 *Any tileset* $\mathbf{W}$ *of NW-deterministic Wang squares can be emulated by any function-pair universal cellular automaton* $\mathcal{A}$*.*

Proof. Fix some $\mathbf{W}$ and $\mathcal{A}$ as in the statement. Let Ω be the set of colors used in $\mathbf{W}$, and let $f(w, n)$ and $g(w, n)$ be the south and east colors, respectively, of the unique tile with west and north colors w and n, respectively. By function-pair universality, there are programs $a, b, c, d \in \Sigma^*$, encoding function h, and time dilation factor N such that (*) is satisfied. We may now represent an NW-staircase boundary by encoding the colors by h, punctuated by the programs a, b, c, and d. The output of running $\mathcal{A}$ for N steps would be (an encoding of) the colors on the next diagonal of the unique tiling by $\mathbf{W}$. Moreover, the programs c and d would trade places with the programs a and b, allowing the computation of the next row using the new boundary. □

We say that function-pair universality is *tight* if for $\Omega = \Sigma^t$, (*) is satisfied with the identity map as h. Now we aim to emulate a tileset whose tiling problem is known to be NP-complete.

Lemma 7.4.3 *There exists a NW-deterministic Wang tileset* $\mathbf{W}$ *and tiles* τ_0, τ_1*, appearing only on the boundary, such that* Simply Connected $\mathbf{W} \cup \{\tau_0, \tau_1\}$-Tileability *is* NP*-complete.*

Proof. Consider the set $\mathbf{W}_{15}$ constructed in the proof of Lemma 3.1.1. It is not NW-deterministic for several reasons, including the tile R_i that transmit information to the left, the tile X_{ij} that transmit information upwards, and V_i that initiates the computation. Besides the last one (which is needed for the tiling to have computational power), the others are easily fixed.

Indeed, we modify $\mathbf{W}_{15}$ to obtain $\mathbf{W}_d$. The tiles are drawn in Figure 7.6, where the symbols i, j, and k, which appear in the subscripts of the tiles can be replaced by 0 or 1, and

the other symbols are distinct colors. First, we trade the roles of L and R so L propagates signal to the southeast while R goes due south. We make the X tiles appear when L^2 would have intersected with an R^2 tile. To solve the X problem, we shift *everything* down by one on a column with R. That is, after starting with R^1, the signal of the current row will be propagated downward (coupled with r). This signal will be exhibited on the next row by R^2, which also shifts a signal down, and similarly onwards with many R^2 tiles. Then X^1 will do the same, but summons X^2, which allows the signal in this row to pass through without change. Then X^3 displays the signal from two rows above (thus effectively crossing two signals over), and continue the chain of moving the signals down one row by repeated use of X^3 tiles. Finally, the X^4 tile is used for the last tile, which has west boundary $\varnothing$. If there are n variables, the old region for $\mathbf{W}_{15}$ is a trapezoid of height $3n$. Now the region starts with $3n$ rows, becomes $3n+1$ rows in a column whose top color is r, and is followed by $3n$ rows shifted one row down. This is repeated as many times as the color r is used on the top boundary. The extra vertical edges resulting from the shifted boundary will be colored by $\varnothing$.

It is pretty easy to break V and C tiles into Wang squares. Finally, we add in F_i from $\mathbf{W}_{15}$ without modification. This completes the construction. Removing $\tau_i = \mathsf{V}_i^1$ from $\mathbf{W}_d$ yields a NW-deterministic tileset of Wang squares, as desired. □

Theorem 7.4.4 *Suppose there is a tight function-pair universal cellular automaton $\mathcal{A}$ that can be emulated by a tileset $\mathbf{W}$ of n Wang squares. The tileset $\mathbf{W}_d$ constructed in Lemma 7.4.3 can be emulated by adding two extra tiles to $\mathbf{W}$.*

Proof. Recall that the $\mathbf{W}_d$ is not NW-deterministic because of τ_i. We change tile τ_i to have color i' instead of $\varnothing$ on the west edge. Represent all the colors as different strings of $\Omega = \Sigma^t$, where $0'$ and $1'$ are the same string except for one bit. Apply the construction in Theorem 7.4.2. Finally, add a special pair of tiles (cf. Figure 7.5) that can be used on the boundary to change a bit, representing either τ_0 or τ_1 as the starting tile for computation. □

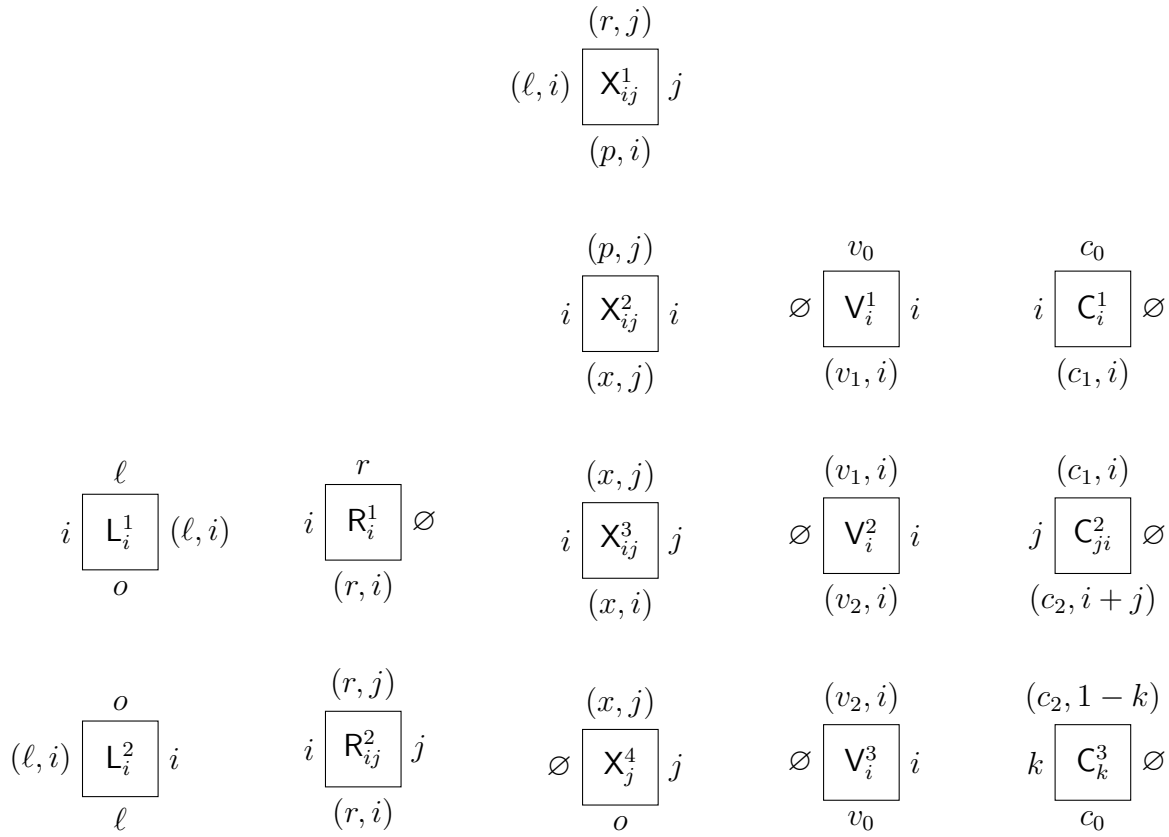

(a) L tiles. (b) R tiles. (c) X tiles. (d) V tiles. (e) C tiles.

Figure 7.6: Tiles for constructing $\mathbf{W}_d$.

Recall that `Rule 110` can be emulated by 6 tiles (Corollary 7.2.1). Combining with the series of results in this section, we get the following conjectural result.

Corollary 7.4.5 *If* `Rule 110` *is tight function-pair universal (or intrinsically universal), then it can emulate* $\mathbf{W}_d$ *with* 8 *Wang squares* $\mathbf{W}_8$*. As such,* Simply Connected $\mathbf{W}_8$-Tileability *is* NP*-complete.*

Finally, this leads to another conjectural improvement on the number of rectangles needed in Theorem 2.1.1.

Corollary 7.4.6 *If* `Rule 110` *is tight function-pair universal, then there exists a set* $\mathbf{R}_{51}$ *of* 51 *rectangles such that* Simply Connected $\mathbf{R}_{51}$-Tileability *is* NP*-complete.*

Proof. Apply Lemma 3.2.1 to the tileset $\mathbf{W}_6$ in Figure 7.2 that emulates `Rule 110`. By adding two tiles with the width of the h tiles but a height too tall to fit in anywhere else (one needs to trace through the uniqueness proof in Sublemma 2.5.1 to verify this), we can make it possible for colors 0 and 1 to appear on the boundary without being specified. This removes the need for emulating $\mathbf{W}_8$. By counting carefully the number of resulting tiles (as in Theorem 3.3.2), we see that $\mathbf{W}_6$ yields 23 tiles before doubling, thus giving a total of $23 \cdot 2 + 3 + 2 = 51$ tiles. □

7.5 Using Turing computation universality of cellular automata

Let $\mathfrak{M}$ be a Turing machine defining a partial recursive function $\Psi : T \to T$, where T is some countable set of Turing machine tapes. A cellular automaton $\mathcal{A}$ on alphabet Σ with global update function Φ *emulates* $\mathfrak{M}$ if there exists mappings $h : T \to \Sigma^{\mathbb{Z}}$ and $g : \Sigma^{\mathbb{Z}} \to T$, a finite "program" word $p \in \Sigma^*$, and a "time dilation factor" $N \in \mathbb{N}$, so that

$$\Psi(x) = g \circ \Phi^N(h(x) \oplus p) \qquad (\dagger)$$

whenever $\Psi(x)$ is defined. If this can be done for all $\mathfrak{M}$, then $\mathcal{A}$ is *Turing (computation) universal.*

Towards evidence of function-pair universality, we consider this following simplification. Fix a Turing universal cellular automaton $\mathcal{A}$. Let $f : \Sigma^t \to \Sigma^t$ be some total function. Find p and N such that

$$\Phi^N(x \oplus p) = f(x) \oplus p.$$

We sketch an argument below to show how this may be accomplished by using Turing universality.

For each string q, there is a Turing machine $\mathfrak{M}_q$ calculating $\Psi_q : \Sigma^t \to \Sigma^{t+|q|}$ given by

$$\Psi_q(x) = f(x) \oplus q,$$

where $|\cdot|$ denotes the length of a string. By universality of $\mathcal{A}$, there exists (h, g, p, N) for each q satisfying (†). For simplicity, suppose that h and g are identity (so $T = \Sigma^{\mathbb{Z}}$), $N = N(t)$ does not depend on f, and denote the p obtained by each q as $p(q)$. We thus obtain

$$\Phi^N(x \oplus p(q)) = \Psi_q(x) = f(x) \oplus q.$$

We wish to find a fixed point e such that $p(e) = e$. We cannot do this, but we can use results from logic to do something that is sufficient for our purpose:

Theorem 7.5.1 (Second Recursion Theorem) *If F is a total computable function then there is an index e such that $\varphi_e = \varphi_{F(e)}$, where φ_e is the partial recursive function with Gödel number e.*

For each program p, associate a function

$$\varphi_p(x) = \Phi^{N(|x|)}(x \oplus p).$$

Note that by universality, φ_p enumerates all partial recursive functions. Thus we may apply the Second Recursion Theorem with $F = p$ to obtain an index e such that $\varphi_e = \varphi_{p(e)}$. Therefore we get

$$\Phi^{N(|x|)}(x \oplus e) = \varphi_e(x) = \varphi_{p(e)}(x) = \Phi^{N(|x|)}(x \oplus p(e)) = \Psi_e(x) = f(x) \oplus e,$$

as desired. In other words, there is a way to select a program e such that running the cellular automaton $\mathcal{A}$ for $N = N(t)$ steps transforms a string of length t to an arbitrary target string of the same length. Moreover, the program e will appear in the right place for us to run the computation again.

CHAPTER 8

Conjectural improvements on the number of rectangles

Lemma 2.3.3 establishes a bound of $2n^2 + 4n + 2$ rectangles, where $n = 2k$ is double the size of the input Wang tileset. The state of the art for this bound given in Lemma 3.2.1 is $5n + 3$. This improvement is made by fixing the h and the v tiles and varying the w tile instead (see Table 8.1). In the first section, we go back to the original setup and outline a conjecture that would reduce the number of h and v tiles to constants without increasing the number of w tiles. In the second section, we tackle the $4n$ bottleneck for the s tiles with another conjecture, which is a strengthening of the first.

8.1 Alternate number theory component

A *digraph* G on $[n]$ is a subset of $[n]^2$. For this chapter, digraphs are loopless, *i.e.*, $(i, i) \notin G$ for any $i \in [n]$. Let $\mathbf{a} = (a_1, \ldots, a_n) \in \mathbb{N}^n$, $N \in \mathbb{N}$, and $D \subset \mathbb{N}$. We say $(\mathbf{a}, N, D)$ *emulates* a digraph G if

(i) $N > 1000 \max_i a_i$, and

	h and v	w	s	f	Sum
Lemma 2.3.3	$2 \cdot n^2$	1	$4n$	1	$2n^2 + 4n + 2$
Lemma 3.2.1	$2 \cdot 1$	n	$4n$	1	$5n + 3$
Conjecture 8.1.1	$2 \cdot 3$	1	$4n$	1	$4n + 8$
Conjecture 8.2.1	$2 \cdot 3$	1	3	1	11

Table 8.1: Summary of the bounds on the number of rectangles obtained.

(ii) $N + (a_i - a_j) \in D^*$ if and only if $(i, j) \in G$,

where D^* is the additive closure of D in $\mathbb{N}$.

Conjecture 8.1.1 *Every digragh G can be emulated by some $(\mathbf{a}, N, D)$ with $|D| \leq 3$.*

Theorem 8.1.2 *If every digraph G can be emulated by some $(\mathbf{a}, N, D)$ with $|D| \leq \ell$, then the bound in Lemma 2.3.3 can be reduced to $2\ell + 8k + 2$.*

Proof. Let $\mathbf{W}$ be a set of k Wang squares. We consider the set $\{\tau_1, \ldots, \tau_n\}$, $n = 2k$, of irreflexive Wang squares obtained by the usual doubling argument. Define a digraph G_1 on $V = [n]$ such that $ij \in G_1$ if and only if τ_i can be placed on the right of τ_j. Similarly, define G_2 such that $ij \in G_2$ if and only if τ_i can be below τ_j. Suppose G_t is emulated by $(\mathbf{a}_t, N_t, D_t)$, $\mathbf{a}_t = (a_t^1, \ldots, a_t^n)$.

Let $\mathbf{R}_0 = \{h, v, s, f, w\}$ be the tiles constructed in the proof of Lemma 2.3.3. Consider an (M, e)-expansion such that h has width N_1 and v has height N_2. Replace s with $4n$ tiles that stretch $(\pm a_1^i, \pm a_2^i)$. Use D_1 as the widths of the h tiles and D_2 as the heights of the v tiles. This gives $|D_1| + |D_2| + 4n + 2$ rectangles in the expansion $\mathbf{R}$ of $\mathbf{R}_0$, as desired.

It remains to check that no non-standard tilings occur, *e.g.*, where pieces of h fit into other slots. To do that, dilate everything by a factor of 4 and then adjust as follows: increase the widths of s and w tiles by 1, v by 3, and decrease the width of f by 2. By modular arithmetic considerations, no combination of h pieces can fit in the other places. Similarly for the height, dilate every tile by a factor of 4 and adjust heights: increase heights of s and h tiles by 1, f by 2, and w by 3. □

Note that we need not prove the conjecture for all digraphs, but very specific digraphs obtained from the Wang tiles we constructed. Furthermore, any bound we get on the size of D will yield some theorem. For example, we can recover Lemma 2.3.3 in this framework. Indeed, take $a_t^i = 5^i$, $N_1 = 31M$, $N_2 = 14M$, where $M = 100 \cdot 5^n$. Then we may take $D_k = \{N_k + a_k^i - a_k^j \mid ij \in G_k\}$. By the choice of N_k, D_k is an initial segment of D_k^*, thus the conditions for emulation are satisfied.

8.2 Another alternate number theory component

In this section, we provide a strengthening of Conjecture 8.1.1, where we prescribe some structure to the $\mathbf{a}$, N, and D that emulate a digraph G. We follow the notations from the previous section.

Conjecture 8.2.1 *Given digraphs G_1 and G_2, there exist*

(i) *an odd prime p,*

(ii) $a \equiv a' \equiv b \equiv b' \equiv 0 \pmod 2$, $ab \equiv 2 \pmod 3$, $a, b, b' \equiv 0 \pmod p$, $a' \equiv 1 \pmod p$,

(iii) $D_1 \subset \mathbb{N}$ *consisting of multiples of* $2p$,

(iv) $D_2 \subset \mathbb{N}$ *consisting of odd multiples of* $3p$,

(v) $\ell > 0$ *and* $g : [n] \to \mathbb{N}$ *such that* $\min g > \ell$,

(vi) $(p-2)a' > \mathbf{wd}\, f$,

(vii) $\mathbf{ht}\, f$ *odd multiple of* $3p$, $\mathbf{wd}\, f$ *even and* $-2 \pmod p$,

(viii) $s_k = R(ka + (k+1)b, a' + (k+1)b')$,

(ix) $N_1 = 2\mathbf{wd}\, s_\ell + \mathbf{wd}\, f$ *is a multiple of* $2p$, *and* $N_2 = \mathbf{ht}\, f - 2\mathbf{ht}\, s_\ell$ *is* $1 \pmod 6$, *and*

(x) $a_1^i = \mathbf{wd}\, s_{g(i)} - \mathbf{wd}\, s_\ell$ *and* $a_2^i = \mathbf{ht}\, s_{g(i)} - \mathbf{ht}\, s_\ell$,

such that $(\mathbf{a}_t, N_t, D_t)$ emulates G_t. Moreover, this can be done with $|D_1|, |D_2| \leq 3$.

The conditions in the statement of the conjecture may seem daunting, but that is because we recorded exactly the modular arithmetic constraints needed to prove the claim below. It seems reasonable to think that methods of proving this conjecture would apply in such a generality as to allow much of $\mathbf{a}$, N, and D to be prescribed when emulating a general digraph G.

For the conjecture to be useful, we need a corresponding theorem like the one immediately following Conjecture 8.1.1.

Claim 8.2.2 *If Conjecture 8.2.1 holds for all digraphs, then the bound in Lemma 2.3.3 can be reduced to* 11*.*

Unfortunately, this one is much more complicated, with a lot of details to be checked while carefully following the proof of Sublemma 2.5.1 to prove uniqueness of a base tiling. For simplicity, we call this a claim and omit the details. We say a few words on how the claim can be proved.

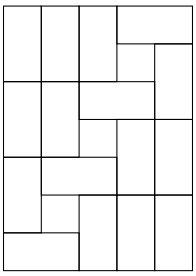

Figure 8.1: Tiling s_k by s tiles, $k = 3$ shown.

Add rectangles $R(a, a')$, $R(a+b, b')$, and $R(b, a'+b')$ for s. Note that s_k is constructable with these three s rectangles (Figure 8.1). The tiles corresponding to h will have the same height $\mathbf{ht}\, h \equiv 1 \pmod{p}$, and numbers in D_1 as widths. Similarly, the tiles corresponding to v have the same width $\mathbf{wd}\, v$, and numbers in D_2 as heights. When choosing the remaining parameters, we further stipulate that $(p+1)\mathbf{ht}\, h > \mathbf{ht}\, w$ and $\mathbf{ht}\, h > \mathbf{ht}\, f$, which are both easy to satisfy. Some of the inequalities imply $pa' + 2(\ell+1)b' > N_1 > 1000b'(\max g - \ell)$, which of course gives $pa' > b'[1000(\max g - \ell) - 2(\ell+1)]$. We summarize the modular arithmetic requirements in Table 8.2. An asterisk (*) means that there is no constraint. A set is listed if each element in the set appears as some tile. The ones marked "big" have inequalities (from below) that need to be satisfied. The table also reiterates that the widths of the h tiles and the heights of the v tiles come from D_1 and D_2, respectively.

For instance, when tiling the (v, s) pair at the location labeled 6 in Figure 2.11, there is a bounded segment of height $\mathbf{ht}\, f - \mathbf{ht}\, s$, which is obviously too short for f to fit. Furthermore, since $\mathbf{ht}\, w > \mathbf{ht}\, h > \mathbf{ht}\, f$ by construction, they are also too tall. Thus we must fill this gap

tile	$\mathbf{ht} \to \mathbb{Z}_2 \times \mathbb{Z}_3 \times \mathbb{Z}_p$	$\mathbf{wd} \to \mathbb{Z}_2 \times \mathbb{Z}_p$
s	0, $\mathbb{Z}_3$, 0	0, $\{0, 1\}$
f	1, 0, 0	0, -2
w	*, 2, 1; big	1, *; big
h	*, 0, 1; big	0, 0; D_1
v	1, 0, 0; D_2	1, *; big

Table 8.2: Summary of modular arithmetic constraints of tiles.

with v and s tiles. Since $\mathbf{ht}\, f - \mathbf{ht}\, s$ is odd, we must have an odd number of v tiles. Since $\mathbf{ht}\, v \equiv 0 \pmod 3$ but the gap is not, we also must use s tiles, thus we will have a (v, s) pair.

If v is on top, it is wide enough to overhang and create the next bounded segment, allowing us to continue with the argument for placing the adjacent (h, s) pair at label 7. On the other hand, if only s tiles are on top, overhang still occurs as s tiles have even widths while $\mathbf{wd}\, w$ is odd.

Similar arguments must be carefully made for the placement and orientation of each pair. We omit the details. Indeed, if more modular arithmetic restrictions are needed to make the argument work, we can simply add those requirements to the setup. Presumably the only way to prove the conjecture would be robust enough to take into account any non-contradictory modular arithmetic restrictions.

References

[AS10] F. Ardila and R. P. Stanley, Tilings, *Math. Intelligencer* **32** (2010), 32–43.

[Bar82a] F. W. Barnes, Algebraic theory of brick packing, I, *Discrete Math.* **42** (1982), 7–26.

[Bar82b] ———, Algebraic theory of brick packing, II, *Discrete Math.* **42** (1982), 129–144.

[Ber66] R. Berger, The undecidability of the domino problem, *Mem. Amer. Math. Soc.* **66** (1966), 72 pp.

[BG82] A. Blass and Y. Gurevich, On the unique satisfiability problem, *Inform. and Control* **55** (1982), 80–88.

[BN91] D. Beauquier and M. Nivat, On translating one polyomino to tile the plane, *Discrete Comput. Geom.* **6** (1991), 575–592.

[BN03] ———, A codicity undecidable problem in the plane, *Theoret. Comput. Sci.* **303** (2003), 417–430.

[BNRR95] D. Beauquier, M. Nivat, É. Rémila, and M. Robson, Tiling figures of the plane with two bars, *Comput. Geom.* **5** (1995), 1–25.

[BSST40] R. L. Brooks, C. A. B. Smith, A. H. Stone, and W. T. Tutte, The dissection of rectangles into squares, *Duke Math. J.* **7** (1940), 312–340.

[CGG+82] F. R. K. Chung, E. N. Gilbert, R. L. Graham, J. B. Shearer, and J. H. van Lint, Tiling rectangles with rectangles, *Math. Mag.* **55** (1982), 286–291.

[CH96] N. Creignou and M. Hermann, Complexity of generalized satisfiability counting problems, *Inform. and Comput.* **125** (1996), 1–12.

[Cha96] T. Chaboud, Domino tiling in planar graphs with regular and bipartite dual, *Theoret. Comput. Sci.* **159** (1996), 137–142.

[CL90] J. H. Conway and J. C. Lagarias, Tiling with polyominoes and combinatorial group theory, *J. Combin. Theory Ser. A* **53** (1990), 183–208.

[Coo04] M. Cook, Universality in elementary cellular automata, *Complex Systems* **15** (2004), 1–40.

[CR98] J. H. Conway and C. Radin, Quaquaversal tilings and rotations, *Invent. Math.* **132** (1998), 179–188.

[Cul96] K. Culik II, An aperiodic set of 13 Wang tiles, *Discrete Math.* **160** (1996), 245–251.

[DG00] M. Dyer and C. Greenhill, The complexity of counting graph homomorphisms, *Random Structures Algorithms* **17** (2000), 260–289.

[DK75] N. G. de Bruijn and D. A. Klarner, A finite basis theorem for packing boxes with bricks, *Philips Res. Rep.* **30** (1975), 337*–343*, available at `http://tinyurl.com/65g8kvr`

[DKLM10] S. Datta, R. Kulkarni, N. Limaye, and M. Mahajan, Planarity, determinants, permanents, and (unique) matchings, *ACM Trans. Comput. Theory* **1** (2010), 10.

[DL92] P. Dagum and M. Luby, Approximating the permanent of graphs with large factors, *Theoret. Comput. Sci.* **102** (1992), 283–305.

[DS99] D. P. DiVincenzo and P. J. Steinhardt, *Quasicrystals: The State of the Art*, World Scientific, Singapore, 1999.

[dT08] B. de Tilière, The dimer model in statistical mechanics, Lecture notes at Swiss Doctoral Program in Mathematics and the EPFL doctoral school, University of Neuchâtel, 2008, available at `http://proba.jussieu.fr/~detiliere/Cours/polycop_Dimeres.pdf`

[Fis61] M. E. Fisher, Statistical mechanics of dimers on a plane lattice, *Phys. Rev. (2)* **124** (1961), 1664–1672.

[GJ79] M. R. Garey and D. S. Johnson, *Computers and intractability: A guide to the theory of* NP*-completeness*, Freeman, San Francisco, CA, 1979.

[GO04] J. E. Goodman and J. O'Rourke (eds.), *Handbook of discrete and computational geometry*, 2nd ed., CRC, Boca Raton, FL, 2004.

[Gol65] S. W. Golomb, *Polyominoes*, Scribners, New York, 1965.

[Gol70] ———, Tiling with sets of polyominoes, *J. Combinatorial Theory* **9** (1970), 60–71.

[Gol89] ———, Polyominoes which tile rectangles, *J. Combin. Theory Ser. A* **51** (1989), 117–124.

[Gon85] T. F. Gonzalez, Clustering to minimize the maximum intercluster distance, *Theoret. Comput. Sci.* **38** (1985), 293–306.

[GS87] B. Grünbaum and G. C. Shephard, *Tilings and patterns*, Freeman, New York, 1987.

[GV07] I. Gambini and L. Vuillon, An algorithm for deciding if a polyomino tiles the plane, *Theor. Inform. Appl.* **41** (2007), 147–155.

[HK81] P. Hell and D. G. Kirkpatrick, On generalized matching problems, *Inform. Process. Lett.* **12** (1981), 33–35.

[HN04] P. Hell and J. Nešetřil, Counting list homomorphisms for graphs with bounded degrees, in *Graphs, morphisms and statistical physics*, DIMACS Ser. Discrete Math. Theoret. Comput. Sci., vol. 63, Amer. Math. Soc., Providence, RI, 2004, pp. 105–112.

[Jer87] M. Jerrum, Two-dimensional monomer-dimer systems are computationally intractable, *J. Statist. Phys.* **48** (1987), 121–134, Erratum in **59** (1990), 1087–1088.

[Jer03] ———, *Counting, sampling and integrating: algorithms and complexity*, Lectures in Mathematics ETH Zürich, Birkhäuser Verlag, Basel, 2003.

[JSV04] M. Jerrum, A. Sinclair, and E. Vigoda, A polynomial-time approximation algorithm for the permanent of a matrix with nonnegative entries, *J. ACM* **51** (2004), 671–697.

[Kar05] J. Kari, Theory of cellular automata: a survey, *Theoret. Comput. Sci.* **334** (2005), 3–33.

[Kas61] P. W. Kasteleyn, The statistics of dimers on a lattice, I, *Physica* **27** (1961), 1209–1225.

[Ken96] R. Kenyon, A note on tiling with integer-sided rectangles, *J. Combin. Theory Ser. A* **74** (1996), 321–332.

[Ken04] ———, An introduction to the dimer model, in *School and Conference on Probability Theory*, ICTP Lect. Notes, XVII, Abdus Salam Int. Cent. Theoret. Phys., Trieste, 2004, pp. 267–304.

[KK92] C. Kenyon and R. Kenyon, Tiling a polygon with rectangles, in *Proc. 33rd FOCS* (1992), 610–619.

[Kla69] D. A. Klarner, Packing a rectangle with congruent n-ominoes, *J. Combinatorial Theory* **7** (1969), 107–115.

[Kor04] M. R. Korn, *Geometric and algebraic properties of polyomino tilings*, Ph.D. thesis, Massachusetts Institute of Technology, 2004, available at `http://dspace.mit.edu/handle/1721.1/16628`

[KP04] M. Korn and I. Pak, Tilings of rectangles with T-tetrominoes, *Theoret. Comput. Sci.* **319** (2004), 3–27.

[KRS96] C. Kenyon, D. Randall, and A. Sinclair, Approximating the number of monomer-dimer coverings of a lattice, *J. Statist. Phys.* **83** (1996), 637–659.

[KV99] K. Keating and A. Vince, Isohedral polyomino tiling of the plane, *Discrete Comput. Geom.* **21** (1999), 615–630.

[Lar93] P. Laroche, Satisfiabilité de 1-parmi-3 planaire est NP-complet, *C. R. Acad. Sci. Paris Sér. I Math.* **316** (1993), 389–392.

[Lev73] L. A. Levin, Universal sorting problems, *Problems of Information Transmission* **9** (1973), 265–266.

[Lew78] H. R. Lewis, Complexity of solvable cases of the decision problem for the predicate calculus, in *Proc. 19th FOCS* (1978), 35–47.

[LMP05] T. Lam, E. Miller, and I. Pak, Tiling rectangles with rectangles, unpublished manuscript, 2005.

[LP97] H. R. Lewis and C. H. Papadimitriou, *Elements of the Theory of Computation*, Prentice Hall, Upper Saddle River, NJ, 1997.

[LP09] L. Lovász and M. D. Plummer, *Matching theory*, AMS, Providence, RI, 2009, Corrected reprint of the 1986 original.

[LRS01] M. Luby, D. Randall, and A. Sinclair, Markov chain algorithms for planar lattice structures, *SIAM J. Comput.* **31** (2001), 167–192.

[Moz97] S. Mozes, Aperiodic tilings, *Invent. Math.* **128** (1997), 603–611.

[MP02] C. Moore and I. Pak, Ribbon tile invariants from the signed area, *J. Combin. Theory Ser. A* **98** (2002), 1–16.

[MR01] C. Moore and J. M. Robson, Hard tiling problems with simple tiles, *Discrete Comput. Geom.* **26** (2001), 573–590.

[MR08] W. Mulzer and G. Rote, Minimum-weight triangulation is NP-hard, *J. ACM* **55** (2008), Art. 11, 29 pp.

[MS05] Y. Matiyasevich and G. Sénizergues, Decision problems for semi-Thue systems with a few rules, *Theoret. Comput. Sci.* **330** (2005), 145–169.

[NW09] T. Neary and D. Woods, Four small universal Turing machines, *Fund. Inform.* **91** (2009), 123–144.

[Oll02] N. Ollinger, The quest for small universal cellular automata, in *Automata, languages and programming*, Lecture Notes in Comput. Sci., vol. 2380, Springer, Berlin, 2002, pp. 318–329.

[Oll09] ———, Tiling the plane with a fixed number of polyominoes, in *Proc. 3rd LATA* (2009), 638–647.

[OR11] N. Ollinger and G. Richard, Four states are enough!, *Theoret. Comput. Sci.* **412** (2011), 22–32.

[Pak00] I. Pak, Ribbon tile invariants, *Trans. Amer. Math. Soc.* **352** (2000), 5525–5561.

[Pak03] ———, Tile invariants: New horizons, *Theoret. Comput. Sci.* **303** (2003), 303–331.

[Pap94] C. H. Papadimitriou, *Computational complexity*, Addison-Wesley, Reading, MA, 1994.

[Pen74] R. Penrose, The role of aesthetics in pure and applied mathematical research, *Bull. Inst. of Math. and its Appl.* **10** (1974), 266–271.

[Pos46] E. L. Post, A variant of a recursively unsolvable problem, *Bull. Amer. Math. Soc.* **52** (1946), 264–268.

[PY11] I. Pak and J. Yang, Tiling simply connected regions with rectangles, preprint, 2011, `arXiv:1305.2796`

[PY12] ———, The complexity of generalized domino tilings, preprint, 2012, `arXiv:1305.2154`

[Rad99] C. Radin, *Miles of tiles*, Student Mathematical Library, vol. 1, AMS, Providence, RI, 1999.

[Rei03] M. Reid, Tile homotopy groups, *Enseign. Math. (2)* **49** (2003), 123–155.

[Rei05] ———, Klarner systems and tiling boxes with polyominoes, *J. Combin. Theory Ser. A* **111** (2005), 89–105.

[Rém98] É. Rémila, Tiling groups: new applications in the triangular lattice, *Discrete Comput. Geom.* **20** (1998), 189–204.

[Rém05] ———, Tiling a polygon with two kinds of rectangles, *Discrete Comput. Geom.* **34** (2005), 313–330.

[Rob71] R. M. Robinson, Undecidability and nonperiodicity for tilings of the plane, *Invent. Math.* **12** (1971), 177–209.

[Rob82] P. J. Robinson, Fault-free rectangles tiled with rectangular polyominoes, in *Combinatorial mathematics, IX (Brisbane, 1981)*, Lecture Notes in Math., vol. 952, Springer, Berlin, 1982, pp. 372–377.

[Rog96] Y. Rogozhin, Small universal Turing machines, *Theoret. Comput. Sci.* **168** (1996), 215–240.

[Sch78] T. J. Schaefer, The complexity of satisfiability problems, in *Proc. 10th STOC* (1978), 216–226.

[She02] S. Sheffield, Ribbon tilings and multidimensional height functions, *Trans. Amer. Math. Soc.* **354** (2002), 4789–4813.

[ST11] J. E. S. Socolar and J. M. Taylor, An aperiodic hexagonal tile, *J. Combin. Theory Ser. A* **118** (2011), 2207–2231.

[Sta97] R. P. Stanley, *Enumerative combinatorics*, vol. 1, Cambridge University Press, Cambridge, 1997, Corrected reprint of the 1986 original.

[SW92] I. N. Stewart and A. Wormstein, Polyominoes of order 3 do not exist, *J. Combin. Theory Ser. A* **61** (1992), 130–136.

[Tho06] R. Thomas, A survey of Pfaffian orientations of graphs, in *Proc. ICM, Vol. III* (2006), 963–984.

[Thu90] W. P. Thurston, Conway's tiling groups, *Amer. Math. Monthly* **97** (1990), 757–773.

[Vad01] S. P. Vadhan, The complexity of counting in sparse, regular, and planar graphs, *SIAM J. Comput.* **31** (2001), 398–427.

[Val79a] L. G. Valiant, Completeness classes in algebra, in *Proc. 11th STOC* (1979), 249–261.

[Val79b] ———, The complexity of enumeration and reliability problems, *SIAM J. Comput.* **8** (1979), 410–421.

[VV86] L. G. Valiant and V. V. Vazirani, NP is as easy as detecting unique solutions, *Theoret. Comput. Sci.* **47** (1986), 85–93.

[Wan61] H. Wang, Proving theorems by pattern recognition, II, *Bell System Tech. J.* **40** (1961), 1–41.

[Wan63] ———, Dominoes and the AEA case of the decision problem, in *Proc. Sympos. Math. Theory of Automata* (1963), 23–55.

[Wan65] ———, Games, logic and computers, *Scientific American* **213** (Nov. 1965), 98–106.

[Yan10] J. Yang, Vertex-pancyclicity of hypertournaments, *J. Graph Theory* **63** (2010), 338–348.

[Yan12] ———, Rectangular tileability and complementary tileability are undecidable, preprint, 2012, `arXiv:1212.3380`